University of Alberta

Design and Construction of Haul Roads Using Fly Ash

by

Vivek Kumar ©

A thesis submitted to the Faculty of Graduate Studies and Research in partial fulfillment of the requirements for the degree of Master of Science

in

Mining Engineering

Department of Civil and Environmental Engineering

Edmonton, Alberta

Fall 2000

0-612-59826-8

University of Alberta

Library Release Form

Name of Author: Vivek Kumar

Title of Thesis: Design and construction of haul roads using fly ash

Degree: Master of Science

Year this Degree Granted: Fall 2000

Vivek Kumar

Vivekashram,
Mohanpur Punaichak,
Patna – 800023
India.

15st of August, 2000

ABSTRACT

Large haul trucks are used at surface mines in Canada thus requiring better haul roads. The mines use empirical design methods, which may not result in optimum road design.

A road design method based on resilient modulus gives better results than the CBR based method. Numerical modeling done to analyze the effect of material modulus, layer thickness and tire interaction on strain bulbs in a haul road, showed that putting the stiffest layer at the top results in least vertical strain and the interaction tires on a rear axle of a truck results in a 20% to 80% increase in the vertical strain.

Coal mines located adjacent to coal-fired electrical power plants produce fly ash as a waste by-product. Test of fly ash, kiln dust and aggregate mixes proved that fly ash significantly improves the strength and bearing capacity of aggregates thus enabling use of thinner layers for road construction.

University of Alberta

Faculty of Graduate Studies and Research

The undersigned certify that they have read, and recommend to the Faculty of Graduate Studies and Research for acceptance, a thesis entitled Design and construction of haul road using fly ash submitted by Vivek Kumar in partial fulfillment of the requirements for the degree of Master of Science in Mining Engineering.

Dwayne Tannant

Dr. Dwayne D. Tannant

Dr. Jozef Szymanski

D S Chanasyk

Dr. David Chanasyk

August 18, 2000

ACKNOWLEDGEMENT

The research reported in this thesis was carried out at the University of Alberta under the auspices of the School of Mining & Petroleum Engineering, Department of Civil & Environmental Engineering. Late Professor Ian Muirhead and Dr. Dwayne D. Tannant supervised the research, and provided invaluable inspiration and direction.

Many professors in the Department of Civil & Environmental Engineering contributed to this thesis with advice and moral support. I would particularly like to thank Dr. D. C. Sego, Dr. J. Szymanski, and Mr. B. Regensberg.

Faculty Service officer, Mr. D. Booth enthusiastically helped with software required for computation and numerical modeling. The laboratory testing could not have been done without able help and guidance from Mr. G. Cyre and Mr. S. Gamble.

I specially thank all those mines that participated in the questionnaire survey and provided invaluable information. Transalta and Lafarge donated materials required for the laboratory testing.

Transalta, Lafarge, Alberta Power Limited (ATCO), Finning and NSERC provided necessary funding for the research. Bursaries and partial teaching assistantships were provided by the University of Alberta and Department of Civil & Environmental Engineering.

The writer wishes to express his sincere appreciation for all of the help received throughout his work at the University of Alberta.

TABLE OF CONTENTS

LIST OF TABLES

LIST OF FIGURES

1 INTRODUCTION

Economics of scale and expansion of surface mining, especially oil sand and coal mining, in Canada has led to use of ultra large mining trucks with payload capacity of more than 300tonnes. Gross Vehicular Weight (GVW) of these trucks may reach 600tonnes. The introduction of large haul trucks demands well-designed haul roads. Presently the design of haul roads in most mines in Canada is based on empirical methods and past experience. The design of a new road is based on past experience that whether the past design was adequate or not. This practice may be sufficient for smaller haul trucks, as the cost of these trucks is not very high. The ultra large haul trucks can cost up to six million dollars. So maximum and efficient utilization of these machines is desired to recover the cost. This is possible only with sturdy haul roads, which provide a smooth ride without any major failure of the road. A good haul road ensures low vehicle operating and maintenance cost. Moreover, a well-designed road has a lower maintenance cost than a road with inadequate cover thickness.

A haul road design has two main aspects, structural and geometric designs. The structural design of haul roads is basically the determination of the thickness of various layers of a haul road for a particular combination of construction materials and load configuration. The geometrical design of haul road deals with physical dimensions such as width, cross-slope, ditch height and safety berm height. The objective of both designs is to provide a safe, efficient, smooth and vehicle friendly ride to the haul trucks and other vehicle without excessive maintenance through its designed life.

1.1 Research Objectives

The objectives of this research were as follows:

- To review the current practices followed in surface mines in Canada for the design and construction of haul roads and to assess the impact of introduction of larger trucks (+200 tonnes) on these practices. Secondly, to tabulate specifications of some of the larger trucks and their tires, which affect haul road design.
- To review 'CBR' and 'Resilient Modulus' based methods for haul road design, illustrate the methods, and discuss their merits and disadvantages. Based on the review and subsequent numerical modeling, to provide a recommended design procedure for mine haul roads.

- To use a numerical model to understand strain bulbs generated in a haul road cross-section due to tire load(s) and to assess the adequacy of the designed cross-section using bearing capacity and strain model analyses. Secondly, to study the effect of material modulus, layer thickness and interaction of tires on strain bulbs.
- To analyze potential benefits of fly ash as a cementing agent for haul road construction materials.

1.2 Thesis Structure

Chapter 2 presents the state of the art of haul road design as practiced by various mines in Canada. It primarily consists of a summary of the questionnaire responses from various mines about haul road design, construction, maintenance and operating conditions. The chapter also includes information about large haul trucks (+200tonnes) and their tires, which was received from manufacturers and vendors.

Chapter 3 discusses various haul road design procedures. Two of the most important methods for haul road design are CBR and resilient modulus based design methods. The two methods are discussed in detail with illustrations and analyses of their advantages and disadvantages.

For designing any haul road, it is imperative to understand the stress and strain distribution in the haul road cross-section induced by the haul truck tires. Chapter 4 first presents a theoretical analysis of stress with respect to the bearing capacity of the soil. The vertical strain distribution is then analyzed using Phase^2 software, which is a two-dimensional finite element program for calculating stresses and displacements. The objective of the modeling is to analyze vertical strain distributions for various combinations of layer rigidity, different thickness of haul road layers and effect of interaction of tires.

Chapter 5 investigates potential use of fly ash as a cementing agent to improve properties such as bearing capacity and rigidity of haul road construction materials. The chapter presents findings of a literature review done to assess suitability of fly ash as a cementing agent for road construction materials. Finally the method and the results of a series of unconfined compression test done to measure compressive strength and Young's modulus of a variety mixes of fly ash with haul road construction materials is presented.

The final chapter summarizes the findings of the previous chapters and states the recommended design procedure for large haul trucks.

2 STATE OF THE ART: HAUL TRUCKS AND ROADS FOR SURFACE MINES

2.1 Introduction

To assess current haul road design and construction procedures, a questionnaire was sent to 37 surface mines in the western Canada, out of which 13 replied. The questionnaire asked for information about:

- Equipment used – haul trucks, haul road construction and maintenance equipment.
- Method of haul road construction and maintenance – haul road geometry, construction materials, symptoms of haul road deterioration and maintenance procedures.
- Procedure(s) for haul road design.

Information was also gathered from haul truck manufacturers and suppliers about the specifications of present and future large haul trucks. This information included gross vehicle weight (GVW), turning radius, truck dimensions, etc. that were deemed to affect the haul road design and construction procedures.

Another factor affecting the design of haul roads is the type of tire used on haul trucks. Inflation pressure and size of the tire determines the size, shape and magnitude of the stress bulb in the layers of a haul road (especially in the upper layers). Tire specifications such as size, footprint area, shape of footprint and designed inflation pressure, were gathered from Michelin and other tire manufacturers. Currently, Michelin appears to be the sole producer of tires used on the largest haul trucks, e.g., CAT 797.

2.2 Summary of Questionnaire Responses

The questionnaire was sent out in December 1998 and responses were received as late as July 1999. Out of the 13 responding mines, eight were coal mines, three were metal mines, one was an oil sand operation and one was a graphite mine. Some mines had very large yearly production (e.g., Syncrude mines 260 million metric tonnes (mt) of oil sands and waste per year) whereas others were relatively smaller operations (e.g., Mount Polley handles only 14 million mt (ore and waste) per year). Most of the coal mines handled materials in the order of 25 million mt per year. The average stripping ratio varied from 0.8:1 (Syncrude oil sand operation) to 18.9:1 (Bullmoose mine) but most of the coal mines had a stripping ratio less than 10:1.

A similar survey was done by Wade (1989), in which 13 mines participated. In fact, six operations are common between these two surveys, but they have grown significantly in size over the past decade. In this section, questionnaire responses are summarized and compared to those gathered by Wade (1989).

The details of questionnaire responses are provided in Appendix 8.1.

2.2.1 Equipment Used

Nearly all mines used graders, dozers, and dump trucks for haul road construction. Graders, dozers and water trucks were also used for haul road repair and maintenance work. Dump trucks played a dual role in haul road construction. Besides transporting construction materials, they were used for compacting various layers during haul road construction. One mine used a sheep-foot compactor for clayey materials and a smooth vibratory drum roller for granular material. Water sprinkling trucks were used at all mines for dust suppression. Except for the compactors, Wade (1989) reported similar haul road construction and maintenance equipment.

Different mines use a variety of haul trucks for ore and waste transportation. As expected, the oil sand operation being the largest handler of materials used the largest trucks. Their fleet included CAT 797 and Haulpak 930E (September 1999), the two largest haul trucks available as of 1999 (payload capacity – 300 mt). Most of the coal mines used trucks with payload capacities around 200 mt, while some of the smaller operations used trucks with payload capacities less than 100 mt. Table 1 gives the truck models operating in these mines as of January 1999.

2.2.2 Haul Road Length

The 13 mines surveyed had a total of 50km of in-pit road with an average life expectancy of 1.4 years and a total of 100km of ex-pit roads with an average life expectancy of 8 years. The haul road length varies widely from mine to mine. Temporary haul roads were 0.5km to 10km long whereas length of permanent haul roads varied from 1.3km to 14km. Wade (1989) reports a total of 50km in-pit and 180km of ex-pit roads for the 13 mines surveyed. But it can not be said that haul road lengths in surface mines has decreased in the past ten years because different mines were involved in the two surveys.

Table 1 Haul trucks used at Canadian mines (as of January 1999).

Make	Model No.	No. of Trucks	GVW (mt)	Payload (mt)
Caterpillar	CAT 769 C	4	68	32
Caterpillar	DJB 25 C	1	42	23
Caterpillar	CAT 777 B	6	161	80
Caterpillar	CAT 776 A	1	250	120
Caterpillar	CAT 776 D	4	250	150
Caterpillar	CAT 785	8	250	136
Caterpillar	CAT 789	11, 43*	317.5	180, 172*
Caterpillar	CAT 793	34	415	218
Dresser Haulpak	630 E	11	286	170
Dresser Haulpak	830 E	53	399	231
Haulpak	930 E	8	480	290
Euclid	R 170	12	-	-
Titan	3315(B/C)	33	285	170
Unit Rig	MT 4400	5	392.3	236
Unit Rig	M 36	7	-	-
Wabco	120	8	204	109
Wabco	170	27	268	154
Wabco	630 E	3	-	-

* Different mines used the same models with different pay loads, number used and payloads are given in order.

- Data not available.

2.2.3 Haul Road Geometry

Haul road geometry is comprised of many factors including maximum grade, cross slopes of road, running width, etc. The maximum haul road gradient was limited to 10% but generally gradients more than 8% were avoided. Maximum curve super-elevation was generally limited to 4% and speed limits were imposed at tighter curves to reduce the required super-elevation. Maximum road cross slope varied widely from mine to mine (1.5% to 4%) depending upon the precipitation and nature of soil but a 2% cross slope was considered optimum for most mines.

Ditch sizes varied widely depending on precipitation. Average ditch widths and depths were 3m and 1m respectively. The height of safety berms was generally calculated as 1/2 to 3/4 of the largest tire diameter in use and thus varied from 1.2m to 3.5m.

The breaking distance limitation was not considered at some mines, but in others it was limited by statute (e.g., Section 4.36 Art. 4921 H,S,R code for mines in British Columbia). The geometry of run-away lanes is a function of final velocity, road grade, acceleration due to gravity, and rolling resistance, and thus varied from mine to mine. On average, run-away lanes had a length of 100m with a gradient of 25%.

Wade (1989) reported similar slopes or gradients for the road running surface. One notable change over the past ten years is that running width has increased from 25m average in 1989 to 30m average in 1999 and height of safety berms has grown from an average of 1.5m in 1989 to 2.5m in 1999. The increased dimensions can be attributed to increases in average size of haul trucks used.

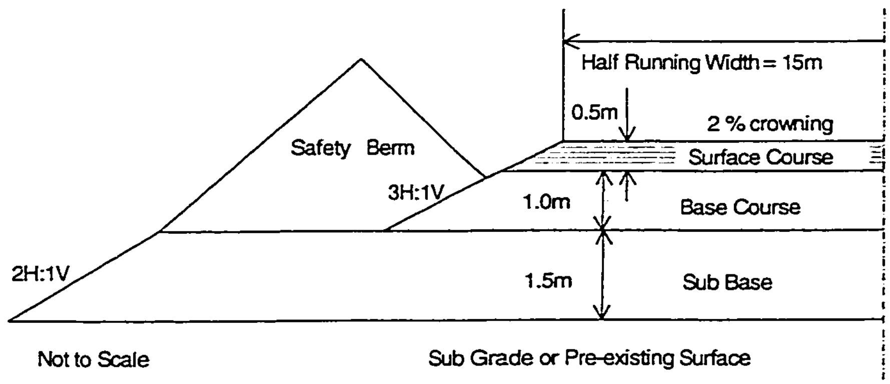

Figure 1 Typical haul road cross-section.

2.2.4 Haul Road Construction Materials

A haul road cross-section can be broadly divided into four layers as shown in Figure 1. The sub-grade is the naturally occurring surface on which the haul road is built. It may be leveled by excavation or back-filled in some cases to provide a suitable surface. Generally, the sub-base thickness was about 1m and base course was 2m thick. However, sub-base thickness can be much larger (up to 10m) when a higher road elevation was required. Most mines used run of mine (waste) as road construction material for layers other than the surface coarse while some mines used sandstone with maximum particle size less than 100 mm for base layers. In some cases, the sub-base was constructed from materials containing rocks larger than 100mm. The surface course was generally laid 0.3m to 0.5m thick. The most common material used for the road surface was crushed run of mine (waste), while some mines used pit run gravel crushed to -19mm.

Rock drains and culverts were the most popular provisions for water crossing, while one of the mines used 0.61m diameter pipes for this purpose.

Most of the mines used no imported material for haul road construction, thus minimizing the haul road construction cost, however, geotextile was used by one of the mines while another mine constructed a test pad of sulfur, tailing sand and lean oil sand. Roller compacted concrete was tested for the surface layer of one haul road.

Comparison with the report by Wade (1989) shows that haul road construction materials have not changed over the last decade although the thickness of different layers have increased marginally with use of larger haul trucks.

2.2.5 Symptoms and Causes of Haul Road Deterioration

Potholes, rutting, and settlement were major symptoms observed by almost all the mines. Frost heave and wash-boarding were also experienced. The running surface of the road suffered mostly due to precipitation/runoff, heavy traffic volume, spring breakup and vehicle spillage. Main causes of deterioration to the base course were spring breakup, precipitation/runoff, heavy traffic volume and poor compaction. Poor compaction, high ground water level and precipitation were major causes of deterioration to other layers. Wade (1989) reports similar symptoms and causes for haul road deterioration.

2.2.6 Haul Road Maintenance

Grading, resurfacing and plowing-scarifying-sanding were practiced at most mines to improve the haul road trafficability. Some mines resorted to excavation and then backfilling up to sub-grade level for major haul road failures while others found raising the haul road grade a better solution. For dust suppression, most of the mines depended on water sprinkling while some mines sprayed calcium chloride or oil on the running surface. Wade (1989) confirms the use of similar haul road maintenance methods but for dust suppression also documents the use of saline ground water, potash and chemical additives such as calcium lignosulfate, Bio-Cat 300-1.

Different mines followed widely varying maintenance schedules depending upon needs and past experience. The frequency of haul road cleaning/regrading and repairing was mostly mine specific. Cleaning and regrading at some mines was done daily and major repair work was performed after haul road failure. The frequency of measures taken for dust suppression, as expected, increased during summer and in some cases was as high as once per shift. Mines surveyed by Wade (1989) also removed snow from haul roads in winter to improve traction. Three mines surveyed by Wade (1989) and one mine surveyed in this study reported use of preventive maintenance for haul roads.

2.2.7 Haul Road Design

Kaufman and Ault (1977) did pioneering work on haul road design and construction for surface mines. The design procedure followed in this work was based on the CBR (California Bearing Ratio) analysis of the haul road construction material and the applied loads. Wade (1989), Wieren and Anderson (1990) and many other authors repeated the design procedure with modifications needed to suit changes in parameters such as weight of the haul trucks and nature of the construction materials.

As truck size increased, the CBR-based design procedure failed to deliver optimum design criteria for haul roads. The method was denounced by the authors such as Thomson and Visser (1997) on the basis that this method assumes uniform elastic modulus for different materials in different layers of haul roads. Moreover this method was originally designed for a paved road. Morgan et al. (1994) and Thompson and Visser (1997) proposed a design method based on elastic deformation of each layer in a haul road taking into account different moduli of elasticity for different layers. They suggest a maximum strain limit for each layer between 1500 – 2000 micro-strain. Cameron (per. comm. 1999) confirmed that design of haul roads based on this new method gave better results than the CBR-based designs. Still, the CBR method remains a popular design method in the industry because the method is simple and has been used for a long time to design haul roads as well as commercial roads.

Design of haul roads, apart from geometry considerations, mainly deals with analysis of the bearing capacity and stiffness of roadbed materials. Syncrude oil sands operation has reported a detailed procedure for haul road construction, and it may be inferred that they have adopted a rigorous design procedure, especially for the CAT 797 trucks (which they introduced in 1999). The current design procedure followed by Syncrude is based on strain analysis of haul road layers. In past they have also designed their haul roads based on CBR but for the larger trucks, strain-limit design gave better results (Cameron, 1999). No other mine has reported such a detailed haul road construction procedure. It may be possible that they do not face severe haul road bearing capacity failure problems and/or the locally available construction materials are sufficient to withstand the loads from the trucks they use. But as larger trucks are introduced, the design of haul roads will gain significance. The survey done by Wade (1989) does not report the design procedures followed by mines in the 1980's.

2.3 Large Haul Trucks

Haul trucks used in surface mines have grown significantly in terms of size and capacity (Table 2). In 1989, the largest trucks available had less than 200 mt payload capacity, but by 1999 the payload capacity has risen to more than 300 mt. Considering the fact that increases in the size of haul trucks were virtually at a stand still during the early half of this decade, (due to limitations of tire technology for larger trucks), this recent increase in haul truck size is significant. Larger haul trucks are being designed, produced, and accepted by the industry for one important reason: economy of scale.

Table 2 Specifications of larger haul trucks (+200mt).

Model No.		CAT 793	CAT 797	T 262	TI 272	T 282	MT 4400	MT 5500	830 E	930 E
Make		Caterpillar	Caterpillar	Liebherr	Liebherr	Liebherr	Unit Rig	Unit Rig	Komatsu	Komatsu
Capacity	mt	232	326	218	270	308-327	236	308	218-255	272-290
	m^3	129	220	119	164	173.6	139	181	147	184
Operating Weight (mt)		377	558	370	411	529	392	510	386	480
Tires		40.00R57	55/80R63	40.00R57	44/80R57	55/80R63	10.00-57*	55/80R63	40.00-57*	50/90R57
Pressure (kPa)		690	590**	690	690	590**	690	590**	690	690
Loading Height Empty (m)		5.21	7.0	5.9	6.2	6.5	6.6	6.7	6.71	6.68
Width (m)		7.67	9.15	7.4	7.9	8.7	7.4	9.05	7.32	8.43
Length (m)		12.18	14.5	13.3	13.7	14.5	13.9	14.77	13.51	15.24
Steering Diameter (m)		30.2	31.9	28.5	32.6	32.7	30.4	-	28.4	-
Axial Weights (mt)										
Empty	Front	70	-	68.5	64	99	74.1	96.9	76.5	92.7
	Rear	78	-	83.5	74.4	102	82.2	104.9	77.8	97.6
Loaded	Front	124	-	122	127.3	188.3	130.8	170.1	128.0	160.1
	Rear	253	-	248	283.2	340.3	261.5	340.1	257.8	320.2
Maximum Speed (km/hr)		55	64	51	68	64	59	-	56.9	64.5

* both radial and bias ply tire can be used.
** low pressure, low profile tire.
- data not available.

Almost all of the large haul trucks in current use have two axles (with four tires on the rear axle). The use of two axles provides better maneuverability and smaller steering radius. The limiting factor in the design of larger haul trucks is the design of tires to match the trucks.

Haul trucks with gross weights of more than 500 mt (payload of more than 300 mt) have been recently introduced at some mines. Correspondingly, the load per tire has increased to more than 85 mt.

Apart from haul road construction materials, the geometry of haul roads also requires modifications to accommodate the new larger trucks. The haul road width depends upon the width the largest truck in use. The maximum truck width has gone up from 7m in 1989 to 9m in 1999. Moreover, the turning radius of the trucks, on average, has increased by 10% over that of a generation earlier. For example CAT 793C has a turning radius of 15m but CAT 797 has a turning radius of 16m. The increase in turning radius becomes significant as the length of the truck increased from 12.9m for CAT 793C to 14.5m for CAT 797. So, a larger turning radius and width of road is required to accommodate these trucks. More importantly, the maximum speed of these trucks has increased in most cases by 8 to 10km/h. For example, TI 252 and T 262 trucks by Liebherr have a maximum speed of 51km/hr whereas next generation trucks from same company, namely the TI 272 and T 282 have a maximum speed of 68 and 64km/h respectively. This also impacts the haul road geometry in terms of stopping distance. Other haul road dimensions would also have to increase to fit these larger, faster trucks.

2.4 Haul Truck Tires

Haul truck tires have grown with the size and capacity of trucks thus becoming a very costly piece of equipment (Table 2). A single tire can cost more than $33,000 (55/80R63 Michelin tire) (Doyle, 1999). Given the constraints due to the tires on the size of haul trucks and the high cost of tires, it is important to understand the construction of tires.

2.4.1 Tire Components and Composition

Tires are made from rubber (both synthetic and natural), carbon black, sulfur, and other chemical agents. A common ratio of rubber to other materials is 80:20. For large haul truck tires, 80% of the rubber comes from natural sources. A higher proportion of natural rubber means a greater capacity to dissipate heat, but lower wear resistance. A higher proportion of carbon black leads to greater wear resistance of tires, but carbon tends to retain heat, thus the tire heats more easily.

As such, the selection of proper composition depends on the intended use for the tire. If the haul road has an abrasive surface, a tire with a greater percentage of carbon black would be desired. But, if the haul road is smooth and free of abrasive materials, a tire with higher percentage of natural rubber gives better service in terms of tons per kilometer per hour (TKPH).

2.4.2 Types of Tires

There are two major types of tire: bias ply and radial. Bias ply tires use nylon casing plies to form the carcass, and have several bead bundles. Radial tires generally use a steel carcass ply positioned radially about the tire (Appendix 8.2). The bead may typically be formed by only one bundle of wires. Compared to bias ply tires, radial tires have greater stability, better grip, more even ground pressure, and lower rolling resistance. Large haul trucks tend to use radial tires (Table 2).

2.4.3 Tire Foot Print Area and Pressure

Two important elements of tires that affect haul road design are foot print area and tire pressure. Tire pressure has gone up to 690kPa (100psi) from 551kPa (80psi) during last five years, although the new low profile truck tires (55/80 R63) have an inflation pressure of 586kPa (85psi). The increase in tire pressure has placed greater stresses on the road surface. The bearing capacity of materials used for the surface coarse should be greater than the tire pressure. So, any material having a bearing capacity less than roughly 1MPa (equivalent to compressive strength of soft rock) cannot be used for the surface coarse. Due to the large tire foot print areas, the stress bulb below a tire can extend quite deep, resulting in the need for well designed sub-base and base layers with sufficient bearing capacities and stiffness. The shape of tire footprint can be approximated as either a circular or rounded rectangle. The conventional tire (e.g., 40.00R57) can better be assumed to have circular footprint but newer tires, such as 55/80 R63, which is a low profile, low pressure tire, has an elongated footprint. Thus the shape of the footprint can be approximated by a rounded rectangle. The pressure distribution beneath a tire is non-uniform, especially for bias ply tires. However, an assumption of uniform pressure distribution across the tire foot print area for the purpose of stress analysis in haul road layers gives reasonably satisfactory results.

For the surface course the pressure bulbs caused by individual tires can be assumed to be non-interfering and stress analysis for the surface course can be done using a single tire. In contrast, at depths about 0.5m below the road surface, the stress bulbs from individual tires on rear axles begin to interact and the vertical stresses in the road layers also become a function of tire spacing on the truck (see Section.4.6).

Table 3 Tire specifications (after Doyle, 1999).

Tire	Truck Payload	Footprint Area (m^2)	Load Per Tire	Tire Pressure kPa (psi)	Free Radius (mm)
Standard Tire 40.00R57	218 mt	1.11	63 mt	689 (100)	1776
Retrofit Tire 44/80R57	218 mt	1.13	63 mt	586 (85)	1705
Low Profile 55/80R63	327 mt	1.68	93 mt	586 (85)	1946

2.5 Summary

There has been a marked increase in the size of the trucks used over the last decade. Some mines use trucks of payload capacity as high as 360 mt. Consequentially, geometrical elements of haul roads, such as width, have been enlarged to accommodate larger trucks. But larger trucks also mean greater load on the road but little design work has been done by various mines (except Syncrude) to account for larger truck sizes. Haul road construction and maintenance procedures followed by various mines are based on past experience and trial and error methods.

Developing tires suitable for large trucks was a real challenge. Michelin has developed a 'low pressure, low profile' tire that can satisfactorily carry high loads at higher speed while also imposing lower stress to the haul road.

3 DESIGN OF HAUL ROAD CROSS-SECTION

3.1 Introduction

In this chapter, structural aspects of haul road design will be discussed. A haul road cross-section can be divided into four distinct layers, namely sub-grade, sub-base, base course and surface or wearing course (Figure 1).

Sub-grade: Sub-grade refers to the in-situ soil bed after vegetation is cleared and ground is leveled for road construction. If the roadbed surface lacks the required bearing capacity, then it needs to be altered through suitable measures such as compaction, use of geotextile, or addition of binders.

Sub-base: Sub-base is the layer of a haul road between sub-grade and base course of the road. It usually consists of compacted granular material, either cemented or untreated. Run of mine and course rocks are the general components of this layer. Apart from providing structural strength to the road, it serves many other purposes such as preventing intrusion of sub-grade soil into the base course and vice-versa, minimizing effect of frost, accumulation of water in the road structure, and providing working platform for the construction equipment.

Base Course: The layer of haul road directly beneath the surface course of the road is called the base course. If there is no sub-base, then the base course is directly laid over the sub-grade or roadbed. Usually high quality treated or untreated material with suitable particle size distribution is used for construction of this layer. Specifications for base course materials are generally considerably more stringent for strength, plasticity, and gradation than those for sub-grade. It is the main source of the structural strength of the road.

Surface Course: The uppermost layer of the haul road that comes directly in contact with tires is known as the surface course. A haul road surface is generally constructed with fine gravel with closely controlled grading to avoid dust problems while maintaining proper binding characteristic of the material. Apart from providing a smooth riding surface, it also distributes the load over a larger area thus reducing stresses experienced by the base course.

Various methods exist for road design as summarized in Figure 2. These methods are used to calculate the appropriate thickness of each layer in the road by considering material properties such as plasticity index, California Bearing Ratio (CBR) or resilient modulus. The design method based on use of plasticity index has been limited mostly to the design of flexible pavement design for the commercial roads (Australian Asphalt Pavement Association, 1983). A popular method of road design uses the CBR of the construction materials as a design criterion. This method originated in 1928-29 for the design of commercial roads but found major application to construction of airfields after 1949.

Recent research on design of haul roads has highlighted a shift towards the use of a resilient modulus based design method. In this case, the road layers are designed on the basis of the design stresses and each layer's resilient modulus. A critical strain limit is used to establish the required moduli (and hence material and compaction properties) of each layer.

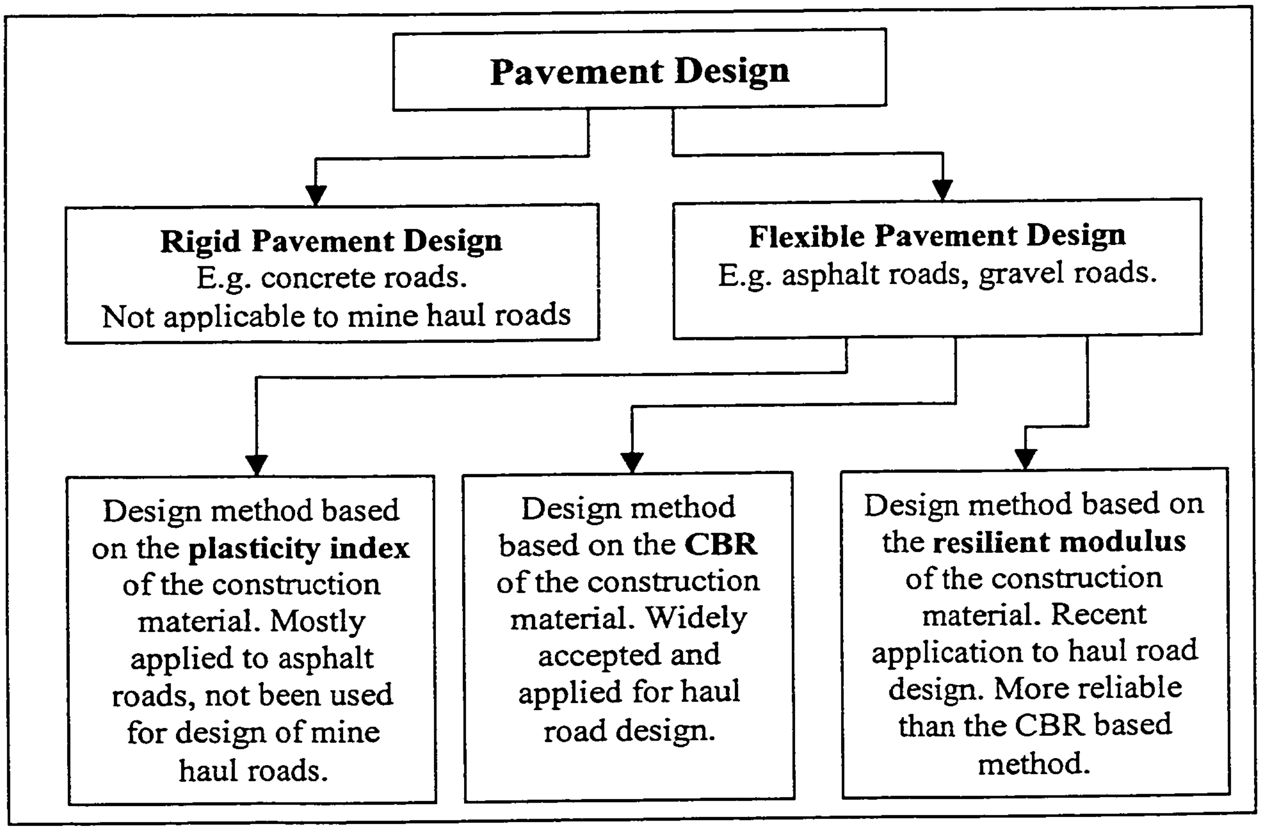

Figure 2 Types of pavement design.

3.2 Haul Road Design Based on California Bearing Ratio

One of the most widely used methods of computing required fill thickness for road construction is the California Bearing Ratio (CBR) method. This approach characterizes the bearing capacity of a given soil as a percentage of the bearing capacity of a standard-crushed rock, the ratio of capacities being referred to as the CBR for the given soil. Empirical curves, known as CBR curves, relate the required fill thickness and applied wheel load to the CBR value. The first use of CBR (%) values to determine the cover thickness over the in-situ material was reported by California Division of Highways during 1928-1929 (American Society of Civil Engineers, 1950). The standard test to determine the CBR was established during 1930s at the laboratory of the Materials Research Department of the California Division of Highways, USA, and was reported by Porter (1938). Porter (1949) further developed the procedure for airfield pavement design. Boyd & Foster (1949) addressed the dual wheel assembly problem through consideration of Equivalent Single Wheel Load (ESWL). Traffic volume and its effect on the structural design of pavements was considered by Ahlvin et al. (1971) in which a repetition factor was determined according to the load repetitions and the total number of wheels used to determine the ESWL. Kaufman & Ault (1977) were among the first who recommended the use of the CBR method for the design of haul roads in surface mines.

The CBR value, expressed as a percentage, is a comparative measure of the resistance offered by a soil to the penetration of a standard size cylindrical plunger, forced into the soil at a specified rate to a designated depth, to the resistance required to force the plunger into a standard crushed stone under the same conditions. The end area of the plunger is $1935mm^2$, the specified penetration rate is 1mm per minute and the depth of penetration is 75mm. The test is conducted on the -20mm fraction of a soil, which is compacted by prescribed procedures into a 152mm diameter mould. A 2.27kg annular disk surcharge weight, which is intended to simulate the load of the pavement on the soil, is placed on the soil surface and the plunger is forced into the soil through the hole in the disk. The detailed procedure and apparatus used for conducting the test are described in the "Standard Test Method for Bearing Ratio of Laboratory-Compacted Soils", ASTM D1883. The test may also be carried out on undisturbed soil samples taken in the field by the CBR mould, or on soaked or swelling samples. To minimize soil disturbance, the test can be conducted in the field on in-situ deposits by jacking the plunger into the ground, using for jack reaction the rear bumper or undercarriage of a truck, and measuring penetration by appropriately placed deformation gauges.

Design charts have been developed that relate pavement, base and sub-base thickness to vehicle wheel load and CBR values. A typical CBR chart is shown in Figure 3. The curves in Figure 3 depict cover thickness requirements for various wheel loads corresponding to wide CBR value of a construction material. The ranges of bearing ratios for the typical soils included at the bottom of the graph should be regarded as approximate and should be used for preliminary planning purposes only. For final design, CBR values obtained from testing the actual sub-grade and fill materials designated for road construction should be used in the CBR charts for determining fill thickness requirements.

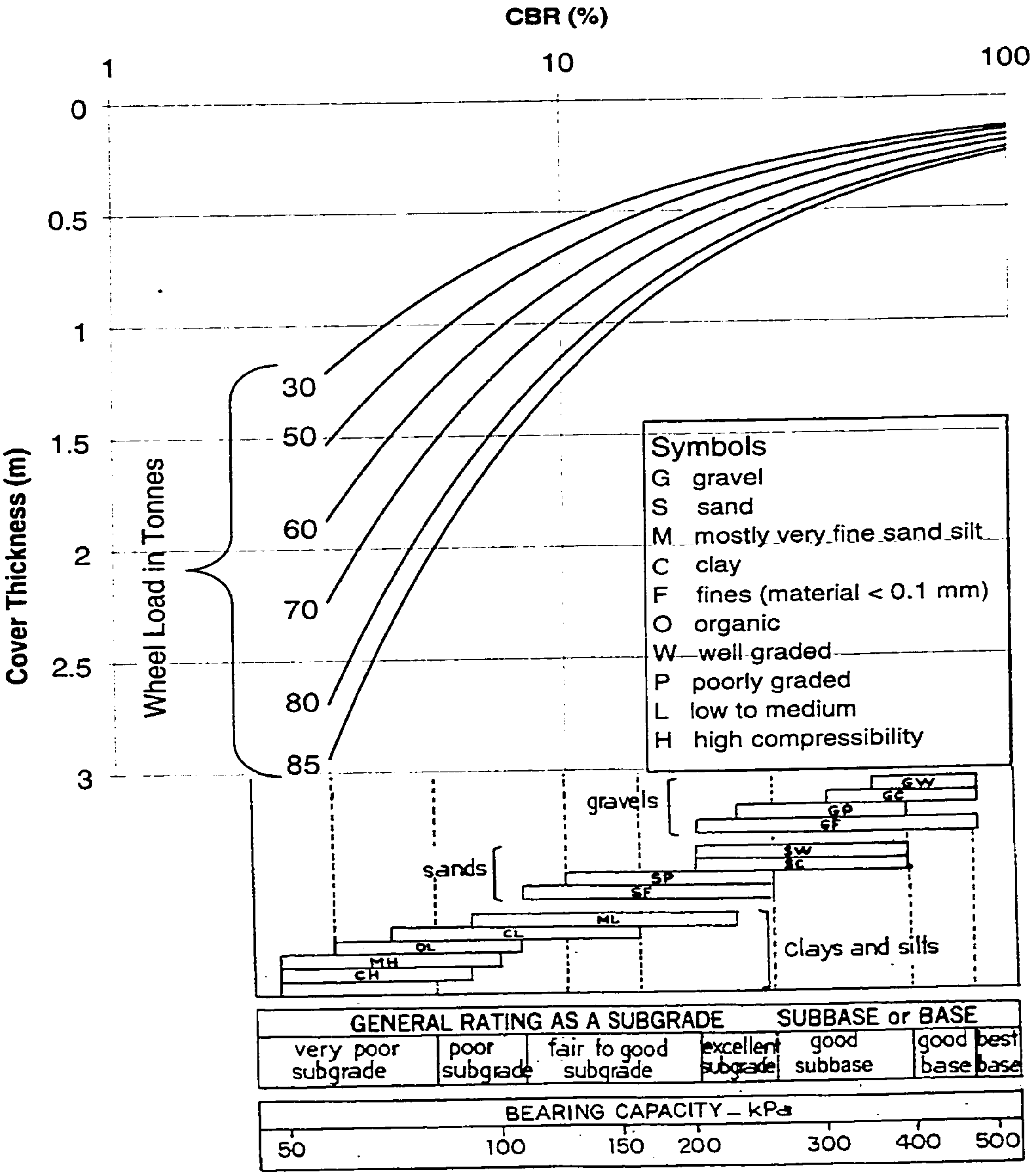

Figure 3 CBR curves (after Atkinson, 1992).

Wheel loads for any haul truck can readily be computed from the manufacturer's specifications. By dividing the loaded vehicle weight over each axle by the number of tires on that axle, the maximum load for any wheel of the vehicle can be established. In every case, the highest wheel load should be used in the design computations. When a wheel is mounted on a tandem axle, the wheel load should be increased by 20% (Kaufman & Ault, 1977).

Table 4 gives the calculated fill thickness using the CBR chart for a wheel load of 80mt (800kN). The required cover thickness for any material can be read from curves on Figure 3 corresponding to the CBR value of the material. For example, a sub-base material having CBR of 25 will require a cover thickness of 0.6m for a 80mt wheel load (Komatsu 930 E). The layer thickness can be calculated by subtracting the cover thickness required by that layer from the cover thickness required by the immediate lower layer.

Table 4 Haul road cross-section based on the CBR chart for a wheel load of 80 mt.

Layer	Typical Material	CBR (%)	Total Fill Cover (m)	Layer Thickness (m)
Surface Course	Crushed Rock	95	-	0.30
Base Course	Pitrun Sand & Gravel	60	0.30	0.30
Sub-Base	Till, Mine Spoil	25	0.60	1.60
Sub-Grade	Firm Clay	4	2.20	-

3.2.1 Modifications to CBR Design Method

The method discussed above can be improved upon by using equivalent single wheel load (ESWL) instead of single wheel load, as the road not only faces one wheel load but a combination of wheel loads thus increasing the stress level in various layers of the haul roads.

ESWL is calculated under the following conditions:

- The ESWL should have same contact area as that of the other wheel loads.
- The maximum deflection generated by ESWL should be equal to that generated by the group of wheels it represents.

Foster & Ahlivin (1954) gave the following method for calculation of ESWL for various depths of a road cross-section:

Deflection under a single wheel (D_s) = $r_s \, P_s \, F_s \, / \, E$

Where: r_s = contact radius for single wheel (m)

E = Young's modulus of the pavement (MPa)

P_s = tire pressure for a single wheel (MPa)

F_s = deflection factor for a single wheel

Deflection under a group of wheels (D_d) = $r_d \, P_d \, F_d / E$

Where: r_d = contact radius for a group of wheels (m)

P_d = tire pressure for a group of wheels (MPa)

F_d = deflection factor for a group of wheels

Following the assumptions for calculation of ESWL and the above equations:

$$D_s = D_d \quad \text{and} \quad r_s = r_d$$

Tire loads (L_s and L_d) are related to tire pressure and contact radius as follows:

$$L_s = \pi \, r_s^2 \, P_s \quad \text{and} \quad L_d = \pi \, r_d^2 \, P_d$$

$$\therefore \quad L_s / L_d = F_d / F_s$$

The above equation gives the relationship between tire load and the deflection factor. The deflection factor for various depth and horizontal locations are given in Figure 4, which can be utilized to calculate ESWL at various pavement depth for a given set of wheel geometry.

Yoder & Witczak (1975) reported four critical points for stress level under a truck as shown in Figure 5. The ESWL is calculated at a range of pavement depths from which the required cover thickness can be calculated using the CBR curve. The specific wheel grouping of a haul truck is reduced to four wheels by means of an equivalent single wheel load representing dual assemblies or axles and the deflections under four characteristics points are recorded. These characteristic points are derived from consideration of the stresses generated in a uniform homogenous pavement under the action of two sets of the two wheels, specifically the increase in stress (and thus deflection), where stress fields overlap.

The CBR method of haul road design has been very popular and been used by many authors such as Kaufman & Ault (1977), Atkinson (1992) and Thompson (1996). The method is simple, well understood and gives fairly good design guidelines for most haul roads. But, the method has many inherent shortcomings, which will be discussed in Section 3.3.

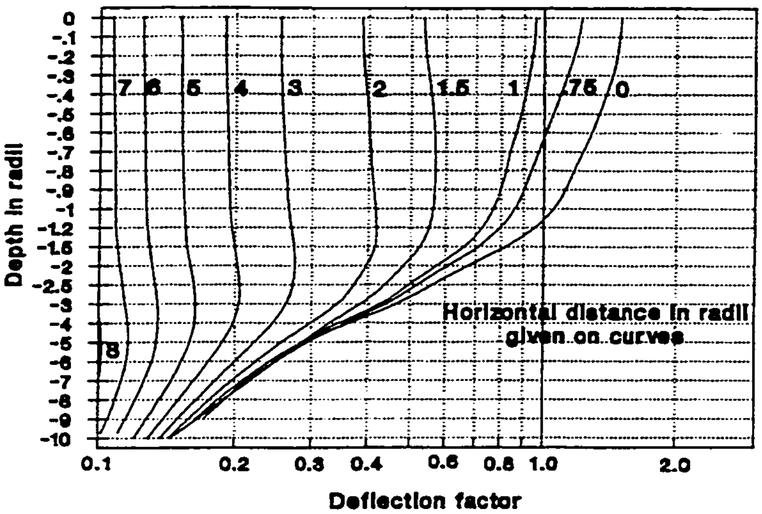

Figure 4 Deflection factor for ESWL determination (after Foster & Ahlvin, 1954).

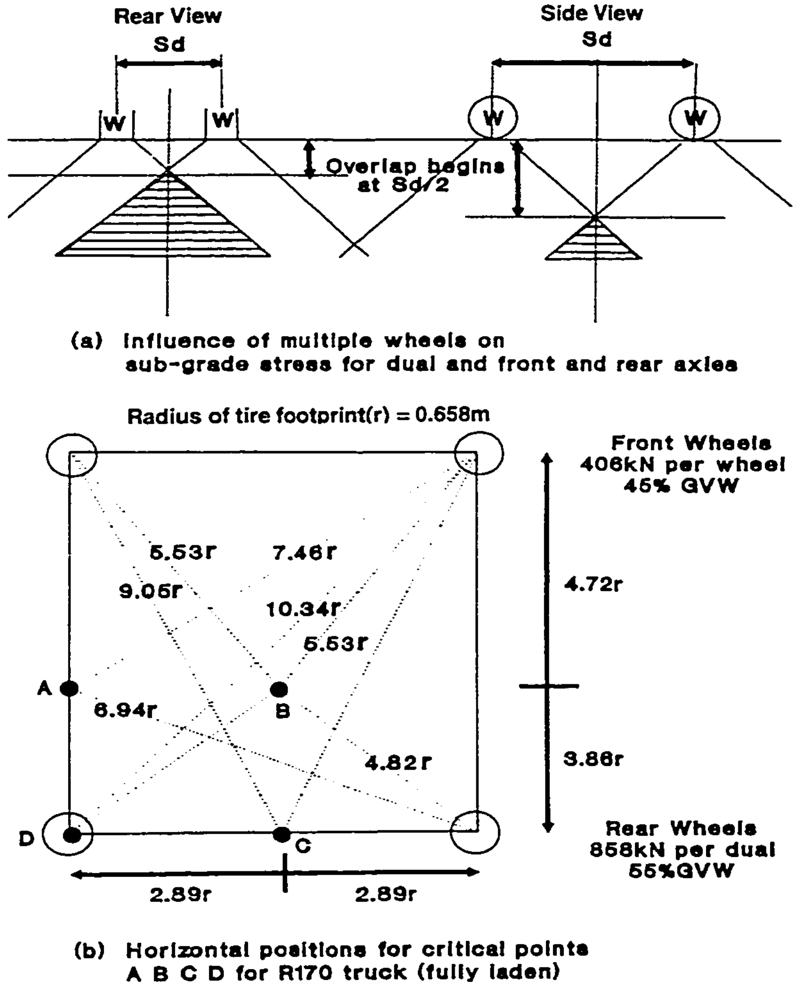

Figure 5 Critical points for a fully laden truck (after Thompson, 1996).

3.3 Haul Road Design Based on Resilient Modulus

Morgan et al. (1994) and Thompson & Visser (1997) criticized the CBR method of haul road design due to the following factors:

- The CBR method is based on the Boussinesq's semi-infinite single layer theory, which assumes a constant elastic modulus for different materials in the pavement. Various layers of a mine haul road consist of different materials each with its own specific elastic and other properties.
- The CBR method does not take into account the properties of the surface course material.
- The CBR method was originally designed for paved roads and surfaces for airfields. Therefore the method is less applicable for unpaved roads, especially haul roads which experience much different wheel geometry and construction materials.

Morgan et al. (1994) and Thompson & Visser (1997) provide a haul road design method based on the strain caused in different layers of the haul road. Based on field observations, maximum vertical strain limits have been established to be 1500 - 2000micro-strains for typical haul roads. Moreover, the stress level in any layer of a haul road cross-section should not exceed the bearing capacity of the material used in that layer.

For a given stress in a layer, the induced strain is a function of the modulus or the stiffness of the material. The stiffness of the material depends upon the grain shape, grain size distribution, compaction achieved and other parameters. The proponents of this design method (Morgan et al., 1994 and Thompson & Visser, 1997) suggest the use of resilient modulus for describing the material properties of the layer. Resilient modulus is the ratio of the amplitude of the repeated axial stress to the resultant recoverable axial strain. Hence, the nature of the test required to determine the resilient modulus is similar to the cyclic loading experienced in a road (Figure 6). AASHTO (1993[b]) T294 gives the laboratory test method to determine the resilient modulus of unbound soil by repetitive loading of a soil sample in a triaxial chamber.

Thompson (1996) estimated the resilient modulus by the falling weight deflectometer test. Alternatively, Young's modulus of elasticity for a material can be determined by an unconfined compression test in laboratory. The resilient modulus can be assumed greater than Young's modulus. Figure 6 shows the method to obtain resilient modulus by repeated triaxial loading of a soil sample. As evident from the Figure 6, Young's modulus can be assumed a conservative estimate of the resilient modulus. The author determined Young's modulus by performing unconfined compression tests on compacted -19mm fraction of construction materials. The test is simple and very well understood and gives a fairly good estimate of the modulus, albeit on the conservative side as there is no confining pressure and stiffening of soil due to repeated loading. Mohammad et al. (1998) describes yet another method for calculation of resilient modulus using a cone penetration test with continuous measurement of tip resistance and sleeve friction.

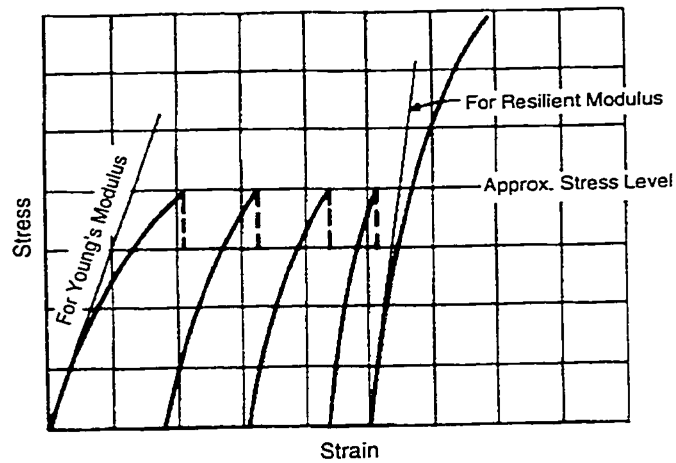

Figure 6 Method to obtain resilient modulus (after Bowles, 1984).

The strains in a layer are a function of applied stress (tire pressure/size) and the resilient modulus of the layer.

The wheel load of the haul truck can be obtained as described in the CBR method. The stresses in layers below the surface course can be calculated using stress models or application of elastic theory. For example, the simplest assumption is that a tire creates a uniform circular load over an isotropic, homogeneous elastic half space. Although, the assumption of homogeneity of the haul road cross-section results in some error in estimation of the stress level in various layers, the assumption simplifies the problem for preliminary examination (detailed modeling discussed in Chapter 4 considers layers with different moduli). The fore-mentioned assumptions combined with the theory of elasticity can be used to examine the stresses beneath a typical tire (Figure 7) with an inflation pressure, p. A typical haul truck tire has a foot print area of about $1.13m^2$ giving an equivalent diameter, w of 1.2m.

Figure 7 shows that the stresses in the base layer, which typically starts at 0.3 to 0.6m below the road surface will be about 0.65 to 0.9 times the tire pressure or about 0.3 to 0.65MPa. Similarly, a typical sub-base begins at a depth of roughly 1.5m. Therefore, the sub-base experiences about 0.2 times the tire pressure or about 0.1 to 0.2MPa. Based on a strength criterion, appropriate construction materials for the base and sub-base need to have bearing capacities that exceed the expected stresses as shown in Table 5.

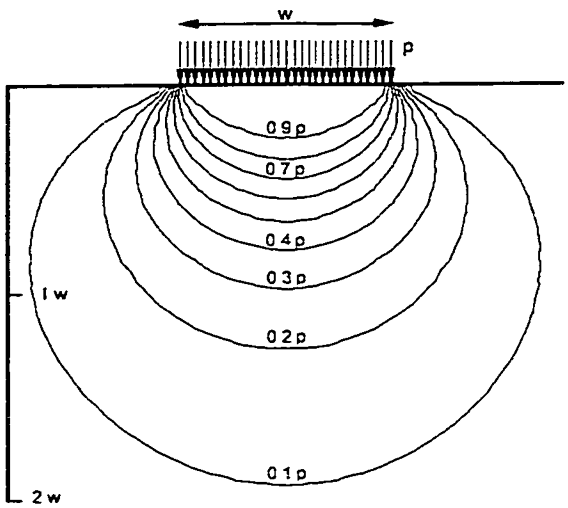

Figure 7 Stress bulbs below a circular pressure distribution.

Table 5 Minimum bearing capacity and Young's modulus of haul road construction materials.

	Thickness (m)	Bearing capacity (MPa)	Young's modulus (Mpa)
Surface Course	0.3 to 0.6	0.7 to 0.9	-
Base Course	1.0	0.3 to 0.65	150 to 350
Sub-base	1.5	0.1 to 0.2	100 to 150

3.3.1 Critical Strain Limit

The important criterion for haul road design is a critical strain limit for each layer. A road can not adequately support haul trucks when vertical strain exceeds a critical strain limit as the road ceases to act as a beam. Morgan et al. (1994) found that the critical strain limit was about 1500micro-strain while Thompson and Visser (1997) noted that the limit was around 2000micro-strains. Possible reasons for difference in the critical strain limits suggested by the two authors could be different design life of the road and traffic density. The strain limit depends on the anticipated number of haul trucks using the road over its working life as given by Knapton (1988) through an empirical relation. Thus, the critical strain limit depends on the design life of the road and the traffic density.

$E = 21600 / N^{0.28}$

Where: E = allowable strain limit (micro-strain)

N = number of load repetitions.

Using the above equation, critical strain limit for a haul road can be calculated. An example of such calculation for a haul road at Bullmoose Mine with a yearly ore and waste production of 3.15and 35.07 million metric tons respectively. The haul trucks used had a payload capacity of 180 metric tons.

Various operating factors such as required design life (period after construction of the road before any major reconstruction is done) and total number of loaded trucks travelling over the road in the designed life, depends upon the operation and following assumptions were made:

- Design life of in-pit road and ex-pit roads are **3** and **12** months, respectively.
- An in-pit road carries **one-tenth** of the total **ore** and **waste** tonnage handled by the mine in a year.
- An ex-pit road carries **half** of the yearly **ore** production by the mine.
- The haul roads are single lane each way.

For in-pit road:

Total load carried by the road in its life = (3.15 + 35.07) * 3 / (12 * 10)

= 0.955 million metric tons

∴ Number of loaded trucks (N) = 0.955 * 1000000 / 180 = 5305

∴ From the equation given above critical strain limit =

$$E = 21600 / (5305)^{0.28} = 1957 \approx 1960 \text{ micro-strain}$$

For ex-pit road:

Total load carried by the road in its life = 3.15 / 2

= 1.575 million metric tons

∴ Number of loaded trucks (N) = 1.575 * 1000000 / 180 = 8750

∴ From the equation given above critical strain limit =

$$E = 21600 / (8750)^{0.28} = 1700 \text{ micro-strain}$$

The critical strain is based on the argument that a haul road acts as a beam if strain is below the limit, which is essential for it to support the load of the haul truck.

The estimated stresses in each layer (noted above) can be used to estimate the minimum Young's modulus that will ensure strains are less than the critical strain limit. For example, a 1m thick base course subjected to vertical stresses of 0.3 to 0.65MPa requires a Young's modulus greater than 150 to 350MPa.

The above method considers stress generated by only one tire, i.e. assumes no interaction between stress bulbs generated by different tires of a truck. This limitation can be overcome by calculating stress numerically and superimposing stress generated by adjacent tires of the rear axle of a truck on a vertical plane parallel to the rear axle of the truck. Stresses below tires can also be calculated using Table 35, which gives influence factors for a circular load at various depths and lateral positions. This method of calculating stress, illustrated by a hypothetical example in section 3.3.2, assumes haul road construction material as isotropic, homogenous and elastic.

3.3.2 Sample Calculation for the Method

The following is a sample calculation for a hypothetical back axle of a loaded truck.

Assumptions:

Shape of tire footprint = circular

Width of truck = 9.0m

Gross vehicular weight = 500mt

No. of tires = 6

Pressure distribution over footprint = uniform

Tire width (w) = 1.2m = Diameter of area of contact

Distance between adjacent wheels = 1.8m

Load equally distributed over the six tires.

$\therefore$ Pressure (q) = load/ (no. of tires * footprint area) = $(500*9.81/6) / (\pi*(1.2/2)^2) \approx 700$kPa

Using the above information and Table 35 (Appendix 8.3), stress level at various points in haul road cross-section can be calculated by adding stresses due to all four tires at a particular point. The result of the calculation is given in Table 36. Required resilient modulus of the material can be calculated by using the critical strain limit and the maximum stress value at the depth of the material. For example, choosing critical strain limit of 2000micro-strains, the resilient modulus of material 0.5m below the surface should more than 270MPa as the maximum stress at that depth is 532kPa. A further improvement to the design method described above involves calculating stress levels at various depths taking into consideration all the tires of the trucks, instead of rear axle only but this would make the analysis 3 dimensional instead of 2 dimensional as discussed above. Interaction between the front and rear axle stress bulbs can be neglected. The analyses in the next chapter show that compared to the tire pressure, the stress level below the center of the rear axle becomes significant only after depth of 6m, a depth at which the magnitude of the stress, itself becomes insignificant.

3.4 Comparison of the Two Methods

As discussed in the previous sections, there are two different methods of haul road design. The first method is based on the CBR value of the construction materials, whereas the second method takes the resilient modulus and the unconfined compressive strength as the design criteria.

The CBR method estimates the bearing capacity of a construction material by measuring the resistance offered by it to a standard plunger whereas the second method relies on the measurement of the resilient modulus and the unconfined compressive strength (either in-situ or in the laboratory) of the construction material.

The CBR method assumes that failure will occur when the cover thickness above a certain material is less than that required, according to a standard CBR chart. The failure criterion for the second method is based on the vertical strain in each layer of the haul road cross-section. It assumes that failure will occur when the strain at any point exceeds the critical strain limit. The critical strain limit is determined for a particular road depending on the number of loaded trucks expected to travel over it during the designed life of the road as discussed in section 3.3. The number of loads passing a particular section of a road depends on the designed life of the road as well as the traffic density. These factors, which are highly variable (e.g. designed life for a haul road can vary from few months to tens of years), are not directly taken into account in CBR method. Also, the CBR method does not take into account the bearing capacity of the surface course, thus the selection of construction material for the surface course becomes arbitrary in this method.

Moreover, failure by the CBR method is assumed to occur when the tire penetrates a haul road layer or an upper layer's material penetrates into the lower one, thus causing failure of the structure (as the method estimates the bearing capacity by measuring the resistance offered by a penetrating plunger) but failure can occur much before such a condition arises. The haul road cross-section acts as a layered beam structure and under excessive strain this structure can cease to act as a beam thus loosing strength and failure becomes imminent. Consequently, it can be expected that a design using CBR method would result in under-design in most cases. But in case of haul roads with very short designed life, CBR method can be over-conservative.

Illustration of the Comparison

A hypothetical but realistic case of haul road design will be solved in this section using both the methods and the results obtained will be analyzed.

Problem: To determine the thickness of various layers of a haul road for a given set of construction materials for 80mt single wheel load (Komatsu 930E).

Assumptions:

Assumed material properties used for various layers are given in Table 6.

Table 6 Properties of the materials constituting different layers.

Layer	CBR (%)	Bearing capacity (kPa)	Resilient Modulus (MPa)
Sub-Grade	3	80	40
Sub-Base	10	150	80
Base Course	50	400	200
Surface Course	100	700	350

Critical strain limit = 2000micro-strains

Tire diameter (w or 2a) = 1.2m

Type of pressure distribution = circular and uniform

Construction materials are homogenous, isotropic and elastic.

CBR Method: Using Figure 3 and the CBR values of the material given above the cover thickness for each type of material was determined. The thickness of any layer is equal to the difference of the cover thickness required for that layer and that for the previous layer. Table 7 shows the layer thickness obtained by the method.

Table 7 Course thickness based on the CBR method.

Layer	CBR	Cover Thickness (m)	Thickness of Layer (m)
Sub-Grade	3	2.70	-
Sub- Base	10	1.20	1.50
Base Course	50	0.45	0.75
Surface Course	100	-	0.45

Method Based on the Resilient Modulus and Bearing Capacity:

Foot print area of the tire = $\pi (w/2)^2 = \pi (1.2/2)^2 = 1.13\ m^2$

Stress exerted by the tire (q) = load/area = 80*9.81/1.13 = 690kPa

The stress can be estimated from Figure 7 using the tire width (w or 2a) and the surface pressure (q).

The thickness of various layers should be such that the maximum stress level faced by any layer should be less than the bearing capacity of that layer and the strain induced should be less than 2000micro-strains. The detailed calculation of thickness of various layers is given in Appendix 8.3. The results are shown in Table 8.

Table 8 Course thickness based on the resilient modulus method.

Layer	Bearing capacity (kPa)	Resilient Modulus (MPa)	Cover Thickness (m)	Thickness of Layer (m)
Sub-Grade	80	40	2.04	-
Sub- Base	150	80	1.44	0.60
Base Course	400	200	0.58	0.86
Surface Course	700	350	-	0.58

This is a preliminary calculation of cover thickness, only. The result should be checked with a stress-strain model, which considers variable resilient modulus of different layers. The stress and strain induced in each layer should be below the accepted limits.

Table 9 Thickness of haul road courses by the two methods.

Layer	CBR Method		Method based on the Resilient Modulus	
	Depth of Cover (m)	Layer Thickness (m)	Depth of Cover (m)	Layer Thickness (m)
Sub-Grade	2.70	-	2.04	-
Sub-Base	1.20	1.50	1.44	0.60
Base Course	0.45	0.75	0.58	0.86
Surface Course	-	0.45	-	0.58

The cover thickness required for the sub-grade obtained by CBR method is more than that by the method based on the resilient modulus (Table 9), but for other layers, the required cover thickness by CBR method is much less. So, the base course and sub base, if designed by the CBR method, may face excessive strain or structural failure. Thus CBR method has resulted in under-design although total cover thickness required by CBR method is greater than that required by the other method. This under-design will be more pronounced for a haul road with a longer design life as the strain limit would be lower than 2000micro-strains, say 1500micro-strains, thus increasing the cover thickness by the second method.

3.5 Design of the Surface Course

Surface course design is slightly different from that of the other layers due to the fact that apart from meeting the general requirements as for the other layers, the design should take care of operational requirements such as dust control, smoothness of ride etc.

Generally the surface course is constructed using high quality gravel crushed to –19mm size. Thompson (1996) reports use of a 200mm thick layer of material having resilient modulus in the range of 150-200MPa compacted to 98% modified AASHTO for a 170mt haul truck. For larger trucks, thicker layers with material having higher modulus of elasticity should be used as the surface course.

The American Association of State Highway and Transportation Officials (AASHTO): M147 (1993[a]) gives the following guidelines for surface course aggregates:

- Coarse aggregate retained on the 2.00mm (No. 10) sieve shall consist of hard, durable particles or fragments of stone, gravel or slag. Materials that break up when alternately frozen and thawed or wetted and dried shall not be used.
- Coarse aggregate shall have a percentage of wear, by the Los Angeles Abrasion test, AASHTO T96, of not more than 50.
- Fine aggregate passing the 2.00mm (No. 10) sieve shall consist of natural or crushed sand, and fine mineral particles passing the 0.075mm (No. 200) sieve.
- The fraction passing the 0.075mm sieve shall not be greater than two-thirds of the fraction passing the 0.425mm (No. 40) sieve. The fraction passing the 0.425mm sieve shall have a liquid limit not greater that 25 and a plasticity index not greater than 6.
- All the materials should be free from vegetable matter and lumps or balls of clay. The soil-aggregate material shall confirm to the grading requirements (four different grading, grading C to grading F can be used) of Table 10.

Table 10 Grading requirements for soil-aggregate materials for surface course (after AASHTO, 1993).

Sieve Designation		Mass Percent Passing			
Standard (mm)	Alternate	Grading C	Grading D	Grading E	Grading F
25.0	1 in.	100	100	100	100
9.5	3/8 in.	50-85	60-100	-	-
4.75	No. 4	35-65	50-85	55-100	70-100
2.00	No. 10	25-50	40-70	40-100	55-100
0.425	No. 40	15-30	25-45	20-50	30-70
0.075	No. 200	5-15	5-20	6-20	8-25

3.6 Summary

There are many methods of road design out of which the CBR and resilient modulus methods are particularly applicable to the design of haul roads. Although the CBR method is a commonly accepted and applied method of haul road design in surface mines, it has many inherited shortcomings, which may lead to under or over design. In case of mines that use ultra-large trucks (GVW > 400 mt), it becomes imperative to use a haul road design method based on the resilient modulus of the construction materials, which requires more complex analysis than the CBR method.

4 BEARING CAPACITY AND STRAIN IN A HAUL ROAD CROSS-SECTION

4.1 Introduction

For designing any haul road, it is imperative to understand the stress and strain distribution in the haul road cross-section induced by the haul truck tires. Theoretical analysis of stress with respect to the bearing capacity of the soil was done to show that the vertical strain, not the bearing capacity, is the limiting factor in most haul road designs. The vertical strain distribution was analyzed using Phase^2 software, which is a two-dimensional finite element program for calculating stresses and displacements. The objective of the modeling is to analyze vertical strain distributions for various combinations material rigidity and different thickness of haul road layers. As discussed in section 3.3, the haul road cross-section is adequate if the stress at any point is less than the bearing capacity of the material and the vertical strain is less than the critical strain limit (generally assumed to be between 1500 to 2000micro-strains). The adequacy of the haul road cross-section for the given wheel load(s) is examined using this stress and strain criteria for various models discussed.

Different cases listed in Figure 8 were analyzed. The load distribution on the road surface beneath a tire was assumed to be uniform over a circular area for all analyses. Bearing capacity analysis (case A of Figure 8) was done using a circular footing to represent a tire. Phase^2 was used for case B, C and D analyses. An axisymmetric model was used to analyze the effect of different combinations of layer moduli (case B of Figure 8) on strain bulbs below a single tire. Various combinations of moduli were analyzed including uniform moduli (B1), surface course stiffest (B2), base course stiffest (B3), and sub-base stiffest (B4). The combination which gave the best result (least strain), namely case B2, was used to study the effect of layer thickness on the strain bulbs (case C). The thinnest layer, which satisfied the critical strain limit, namely case C3, was used to study the effect of interaction of vertical strain bulbs generated by a set of two and four tires along the back axle of a truck (Case D).

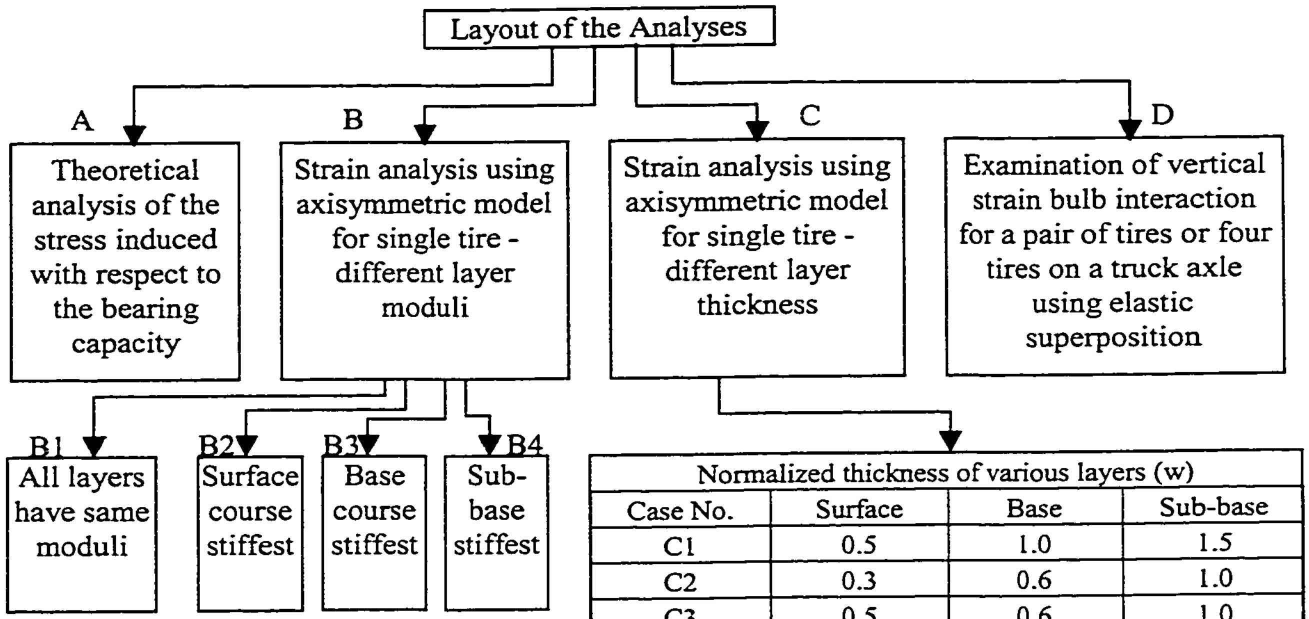

Normalized thickness of various layers (w)			
Case No.	Surface	Base	Sub-base
C1	0.5	1.0	1.5
C2	0.3	0.6	1.0
C3	0.5	0.6	1.0
C4	0.3	1.0	1.0
C5	0.3	0.6	1.5
w = width of the tire			

Figure 8 Layout of the models discussed in the chapter.

4.2 Bearing Capacity Analysis

The bearing capacity of a soil depends on its shear strength, which in turn depends on the soil's cohesion (c) and angle of friction (ϕ). Most of the bearing capacity theories are based on the plasticity theory. Prandtl developed the following expression for ultimate bearing capacity (q_{ult}) for footings by assuming failure conditions shown in the Figure 9 and undrained ($\phi = 0$) conditions (Bowles, 1984).

$$q_{ult} = (\pi + 2)c = 5.14c$$

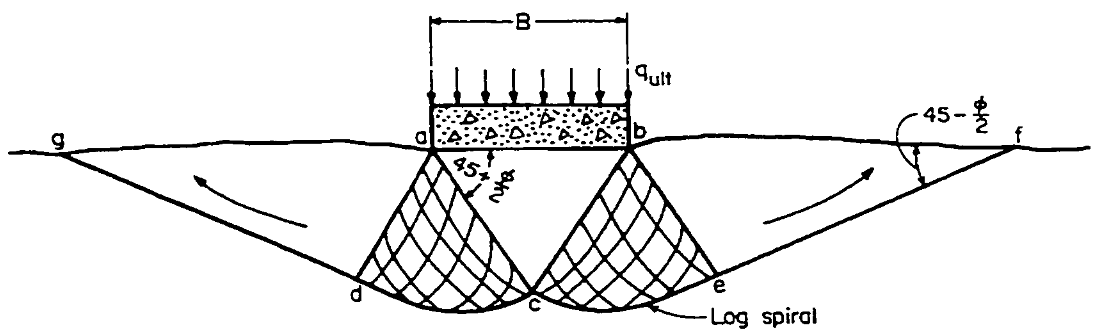

Figure 9 Bearing capacity failure under a surface footing or tire (after Bowles, 1984).

Terzaghi (1943) modified the expression for circular footings as follows:

$$q_{ult} = 1.3cN_c + \gamma DN_q \ +0.6\gamma RN_\gamma$$

where: D = footing depth (m)

R = footing radius (m)

γ = unit weight of the soil (kN/m^3)

N_i = bearing capacity factors (ϕ dependent) as shown in Figure 10

The load exerted by a tire can be approximated by a circular footing. For a tire, the footing depth (D) is zero and footing radius is equal to half of the tire width.

Apart from footing (tire) geometry and unit weight of soil, the bearing capacity of a soil depends on the cohesion and the angle friction of the soil. Figure 11 shows a plot of normalized bearing capacity versus angle of friction and cohesion. The ultimate bearing capacity was calculated using Terzaghi's equation, using R = 0.7m (for tire 55/80R63), $\gamma = 20kN/m^3$ and reading N_i from Figure 10 for various values of ϕ. The dashed line in Figure 10 is for undrained conditions but haul road construction materials are mostly granular so solid lines representing drained conditions were used for reading N_i values. The factor of safety was calculated by dividing the ultimate bearing capacity by the applied stress, which was assumed equal to the tire pressure (700kPa). Bowles (1984) recommends using 2.0 as factor of safety for cohesionless soil and 3.0 for cohesive soils for footings. The material used for road construction are mostly cohesionless (or low cohesion), especially for the surface course. Moreover, some local failure (rutting) is allowable for haul roads, which is not the case for footings. So, a factor of safety of 2.0 can be taken as safe. The surface course of a haul road is generally built with compacted gravel. The cohesion of compacted gravel can be assumed to be zero and the angle of friction ranges between 35° and 50° depending on the degree compaction and gravel characteristics. For well-compacted good quality gravel, ϕ can be taken as 45°, thus from Figure 11, the factor of safety is about 6. Thus, bearing capacity should not be a concern in most haul road designs. It is the vertical strain or the settlement, which is the limiting factor.

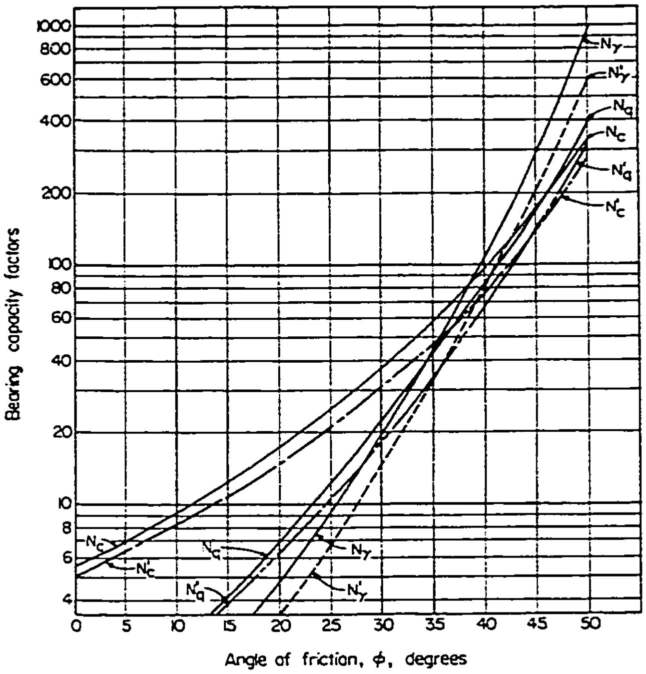

Figure 10 Bearing capacity factors for Terzaghi equations (after Bowles, 1984).

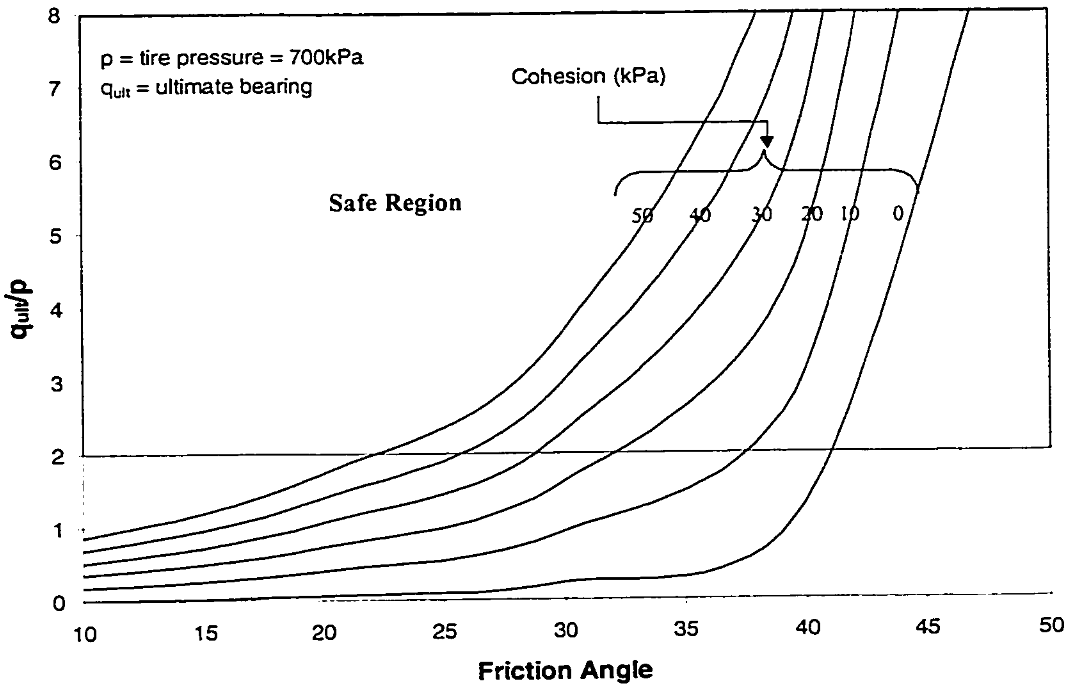

Figure 11 Factor of safety (q_{ult}/p) vs friction angle and cohesion.

4.3 Finite Element Strain Analyses

Finite element strain analyses were done using Phase^2, which is a two-dimensional finite element program for calculating stresses and displacements. Phase^2 can be used to solve a wide range of mining and civil engineering problems (Rocscience, 2000). The program can be used for elastic analyses, but also supports plasticity. Although the software is primarily designed for underground problems, it can be used to solve two-dimensional near-surface problems including those involving traction (or surface loads) such as wheel loads.

The axisymmetric option was selected as it allows a circular load, whereas the plane strain option simulates a strip load (of infinite length) A circular stress distribution on the road surface is better approximation of a tire than a strip load.

The assumptions used to generate the models are:

- Type of model used – axisymmetric
- Size of half model = 15w(width) x 7w(depth) , where w is the width of tire footprint
- Type of material = isotropic and elastic
- Mesh type – graded
- Element type – 4-noded quadrilaterals
- Number of elements = 1600
- Number of nodes = 1700
- Poisson's ratio = 0.4
- Loading = 1MPa stress over a circular area (diameter w)

Since the applied stress is 1MPa, the stresses or strains calculated by the model can be scaled by the actual stress exerted by the tire on the road (generally taken as the tire pressure). Given that 700kPa is a common tire pressure for haul trucks, the model output (stress or strain) shown in subsequent figures has been obtained by multiplying the model output by 0.7. Moreover, the model dimensions can also be scaled by the actual tire size. For example, the depth is shown in multiples of tire width (w).

Figure 12 shows a typical axisymmetric model used to generate vertical strain plots in the subsequent sections. The axis of rotation is at x = 0 (x and y are horizontal and vertical axes, respectively). The wheel load is applied between the points (0,0) and (0,0.5). The boundary of the model (at y = 0) represents the surface of the haul road and thus is a free boundary. The vertical boundaries of the model (at x = 0 and x = 15) are restrained in x direction, thus the material at the boundary is allowed to move in vertical (y) direction only. The lower boundary of the model (at y = -7) is restrained in y direction. The right and lower boundaries are chosen to be at a reasonable distance from the tire, so that the boundary conditions do not affect the stresses and strains beneath the tire. The top layer (between y = 0 and y = -0.5) represents the surface course. While the base course is between y = -0.5 and y = -1.5, the sub-base is between y = -1.5 and y = -3.0. The layer below y = -3.0 represents the sub-grade or in-situ material. The thickness, thus the boundaries of different layers vary for models in section 4.5, in order to analyze the effect of varying thickness on strain bulbs.

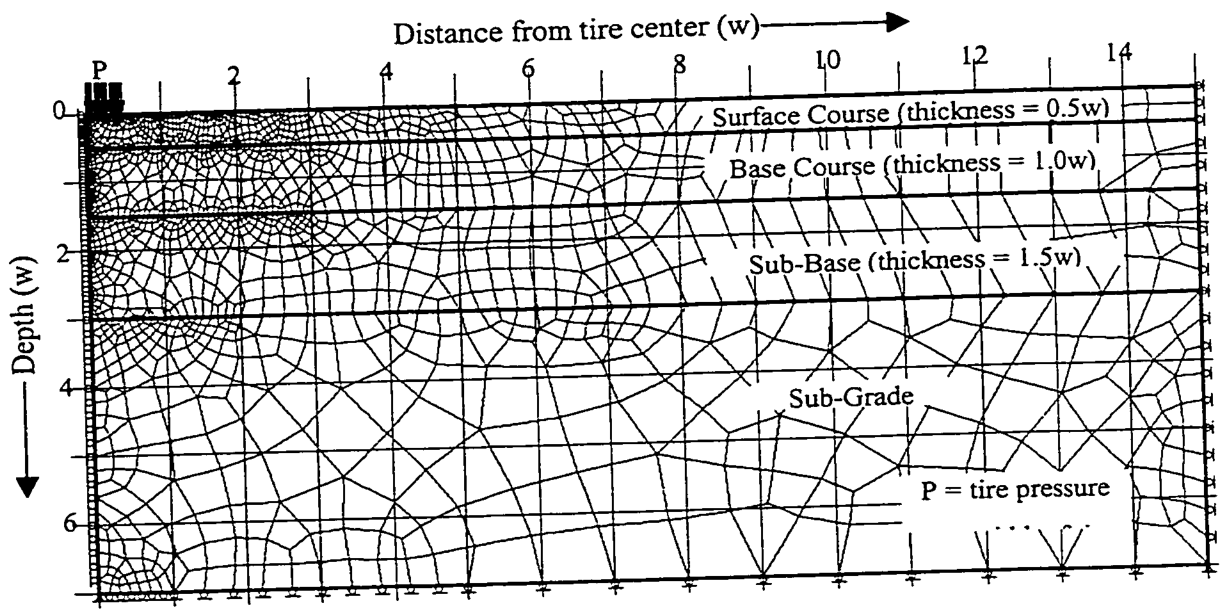

Figure 12 Axisymmetric model for case B study.

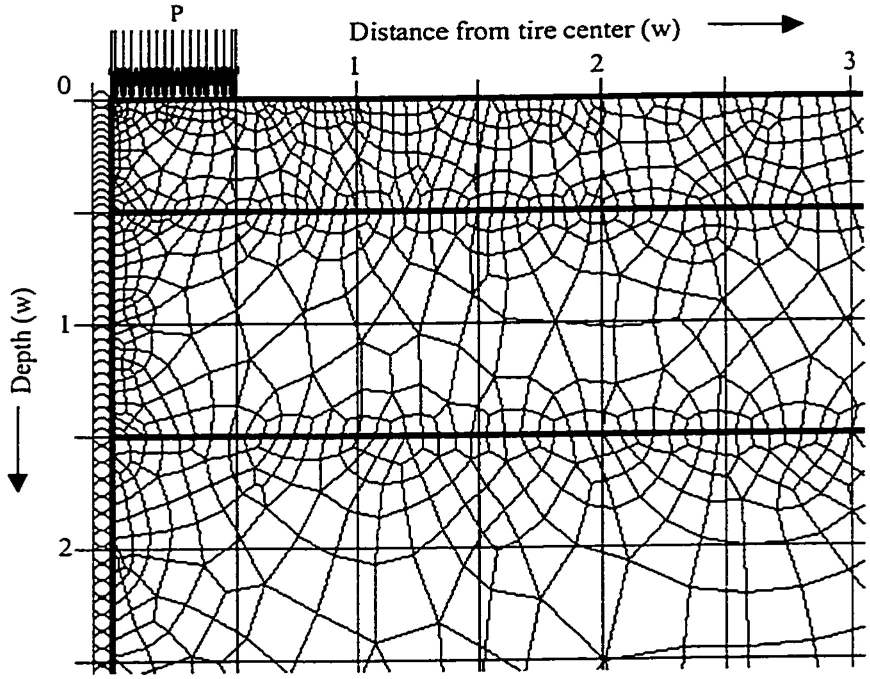

Figure 13 Meshing near the tire (zoomed view of Figure 12).

An axisymmetric model allows only one circular load (or tire) in a model. So, the effect of strain bulb interaction can not be studied directly in a Phase^2 model. However, the principle of elastic superposition allows superposition of elastic stresses or strains. Therefore, the axisymmetric model was used to generate the vertical strain distribution below a single circular tire load and the results were numerically superimposed, using Microsoft Excel, to simulate strains beneath two to four tires of the back axle of a loaded truck. The result thus obtained were be contoured using WINSURF.

4.4 Effect of Layer Stiffness on Vertical Strain

The axisymmetrical Phase2 model was generated to analyze vertical strain below a circular load for different combination of materials, including uniform stiffness across the layers, stiff surface course, stiff base course and stiff sub-base. The thickness of various layers for the analyses was:

- Surface course = 0.5w
- Base course = 1.0w
- Sub-base = 1.5w

Table 11 shows the Young's modulus assigned to various layers for the different cases studied in this section. The construction material should be well compacted achieve maximum Young's modulus.

Table 11 Young's modulus (MPa) of various materials for different cases.

Layer	Uniform Material (B1)	Stiff Surface (B2)	Stiff Base (B3)	Stiff Sub-Base (B4)
Surface Course	50	500	350	150
Base Course	50	350	500	350
Sub-Base	50	150	150	500
Sub-Grade	50	50	50	50

Figure 14 shows the effect of layer moduli on the strain bulbs below a tire. The shift in contours at the boundary of different layers (more evident in cases B2 through B4) is due to the difference in the layer moduli. In case B1 the contours should have been smooth through the boundaries of adjacent layers and the shift in the contours is the artifact of the model (due to meshing at the boundary). The stress level in the haul road cross-section decreases with depth. Thus if the Young's modulus is same for all layers then the strain will be highest at the top layer and decreases with the depth. Thus Case B1 gives extremely high vertical strain for surface course. Also, cases B2 and B3 result in very high strain in the surface course (more than 2000 micro-strain, which is unacceptable) because the stiffest material is not used for the surface course. Case B2 has material with highest Young's modulus as surface course and stiffness of each layer decreases with the depth. This moduli distribution results in the lowest vertical strain, which at all point is less than the critical strain limit (1500-2000micro-strains). Therefore, it can be concluded that a haul road should have the stiffest material at the top and the stiffness of various layers should decrease with depth. As shown in section 5.3.5, fly ash can be added to haul road construction materials to increase their stiffness. The greatest benefit comes from having the stiffest layer near the road surface. This means placing fly ash stabilized materials in the base course, since the use of fly ash in the running surface is not recommended. Case B2 will used to study the effect of layer thickness on the vertical strain bulbs.

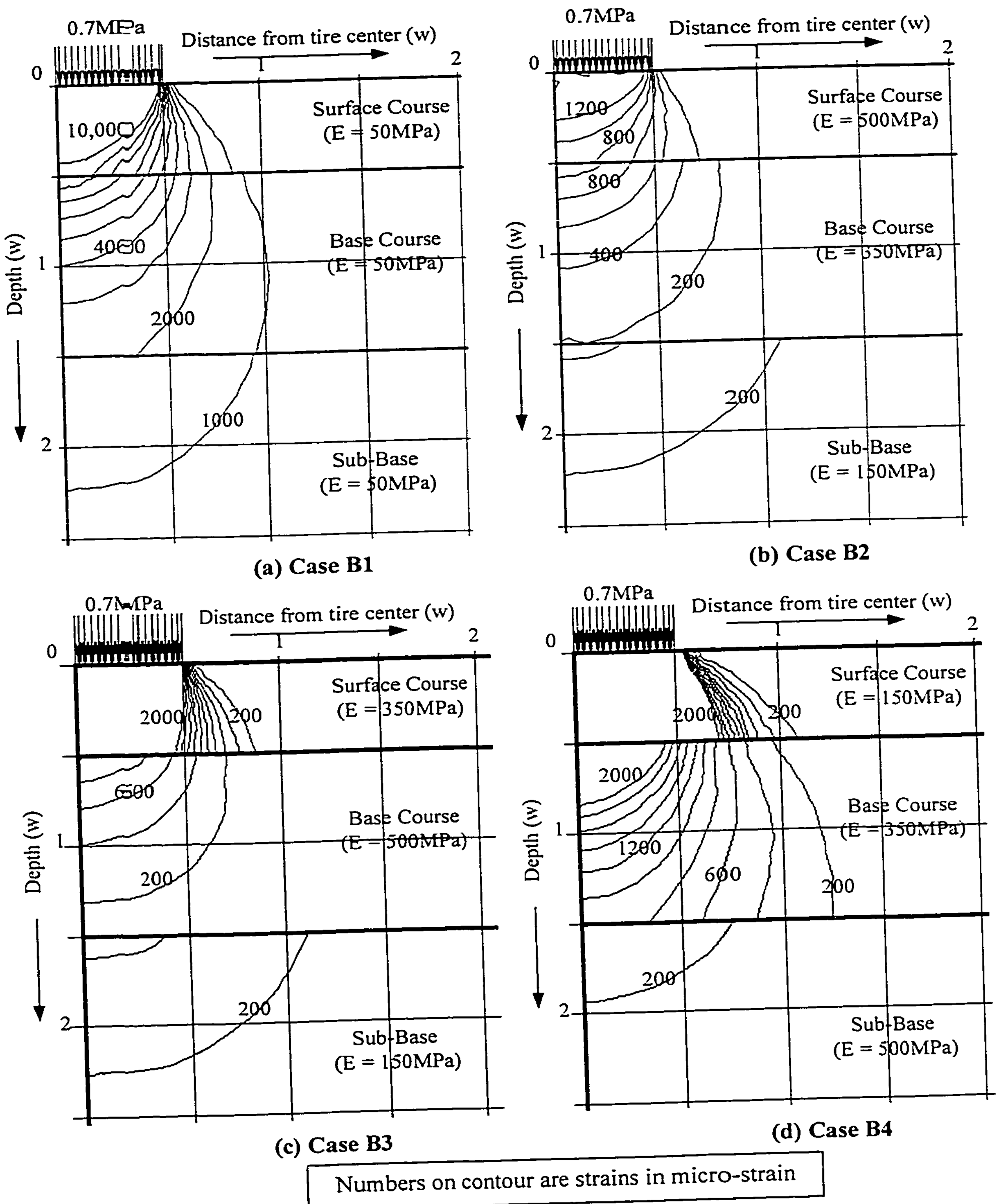

Figure 14 Vertical strain bulbs for different combinations of Young's moduli.

4.5 Effect of Layer Thickness on Vertical Strain

The axisymmetrical model similar to that used in section 4.3 was used to study the effect of varying layer thickness on strain bulbs. The thickness of the layers is given in Table 12.

Table 12 Thickness of layers for different cases (normalized to tire width).

Layer	Case Number				
	C1	C2	C3	C4	C5
Surface Course	0.5	0.3	0.5	0.3	0.3
Base Course	1.0	0.6	0.6	1.0	0.6
Sub-Base	1.5	1.0	1.0	1.0	1.5

Case C1 is the same as case B2 of Figure 14. Vertical strain bulbs for cases C2 through C5 are shown in Figure 15. As evident from the figure, the vertical strain in a layer increases as the cover thickness (total thickness of layers above) decreases. Thus, the base course in case C2 (0.3w cover thickness) has the highest strain (1400 micro-strain), whereas the base course in case C3 (0.5w cover thickness) has a maximum vertical strain of 1000micro-strain. The cost of road construction increases with increase in the cover thickness (because more construction material is used per kilometer of road). So, the case that has least cover thickness should be selected, provided that the maximum strain in any layer is below the critical strain limit (generally assumed to be between 1500-2000micro-strains) with some allowance for the fact that these strain bulbs are due to only one tire and interaction of the tires would increase the strain levels in each layer. So, case C3 can be safely selected for analyzing effect of tire interaction, as the vertical strain at any point is less than 1200micro-strains.

From the above discussion, it is evident that required thickness of various layers is primarily dependent on the load configuration and the material stiffness. For the tire pressures and material properties assumed in the section, 0.6m of surface course, 0.75m of base course and 1.25m of surface course would be adequate, assuming a critical strain limit of 1500micro-strain.

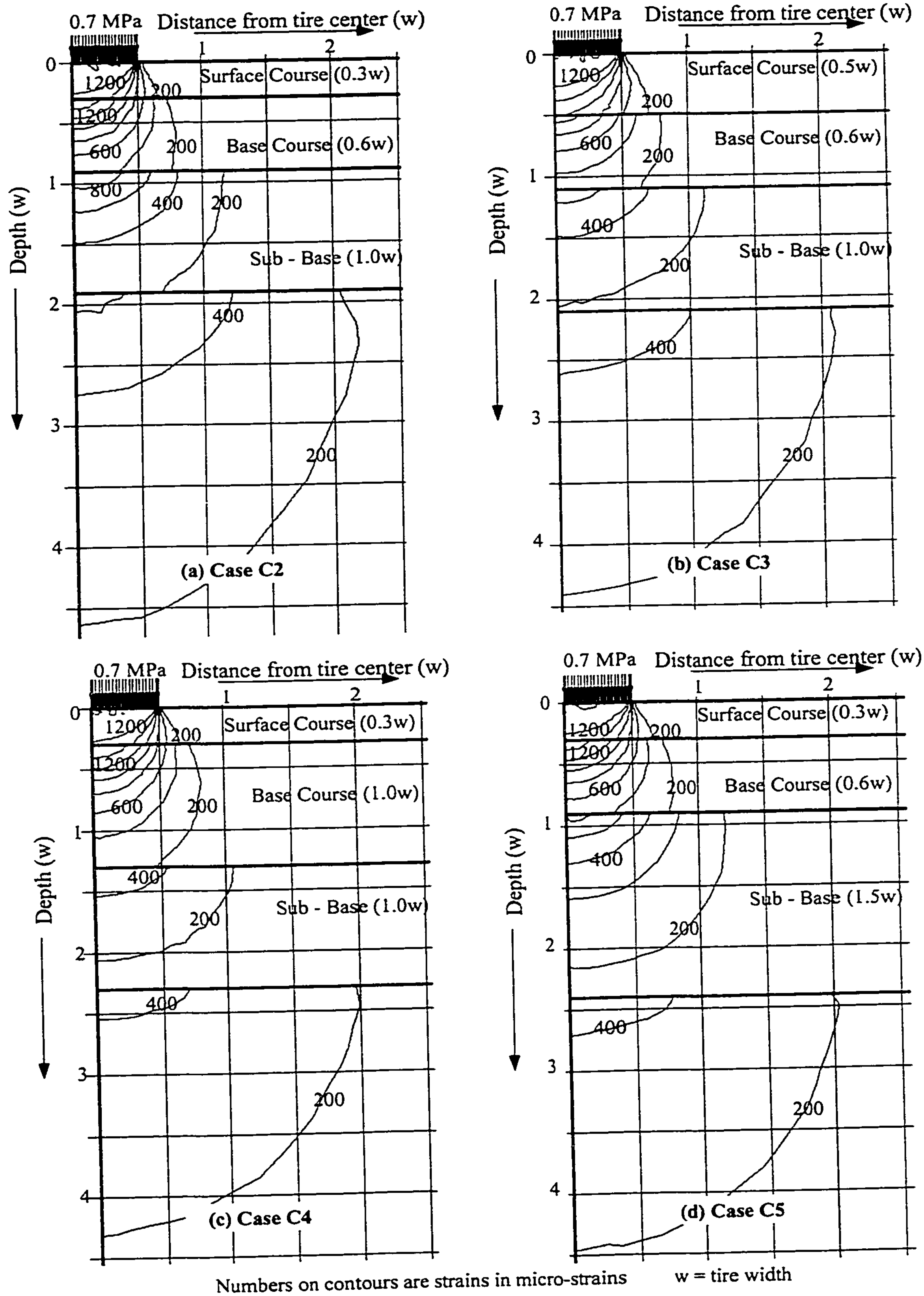

Figure 15 Vertical strain bulbs for different layer thickness.

4.6 Effect of Tire Interaction

As stated earlier, the axisymmetric model of Phase^2 allows only one circular load (tire), but in reality, the strain bulbs generated by different tires along a truck axle interact and the resultant vertical strain generated is greater than that by one tire. The effect of tire interaction was examined by superimposing the strain bulbs generated by one tire to represent multiple tires of a truck. The most critical case is the back axle of the truck, which has four tires, whereas the front one has only two. Moreover there is little interaction between front and back tires of a truck, as the vertical strain generated is insignificant at a horizontal distance of 2.5w from the tire center and the distance between the centers of the front and rear axles is 5.3w (Haulpak 930E), w being the width of the tire (≈ 1.2m).

Case C3 (section 4.5) was used to generate strain bulbs for one tire. Data were queried at a grid of 0.05w x 0.05w for horizontal distance of 2.5w and vertical distance of 0.7w. The data were mirrored to generate full strain bulbs for one tire, as an axisymmetrical model generates only half of the space. Then the strain values at grid points were staggered by a horizontal distance of 1.15w and added to generate strain values at various grid points to represent vertical strain generated by two adjacent tires (Figure 16). The result obtained by the above procedure was staggered again by a horizontal distance of 4.1w to get values of vertical strain at grid points representing strains generated by four tires along the back axle of a truck.

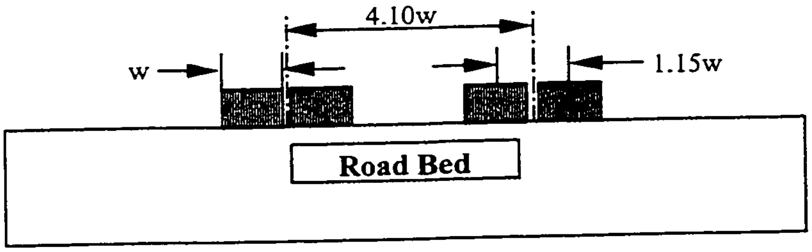

Figure 16 Schematic diagram for position of tires on back axle of a truck (Haulpak 930E).

The data thus generated for the three cases (one tire, two tires and four tires) were plotted using WINSURF software, which is a grid-based contouring program. Linear krigging was used as the gridding method. The data were then contoured using a 200micro-strains contour interval. The result thus obtained for each case is shown in Figure 17 through Figure 19. The approximate maximum vertical strains estimated from the figures for the various layers are summarized in Table 13.

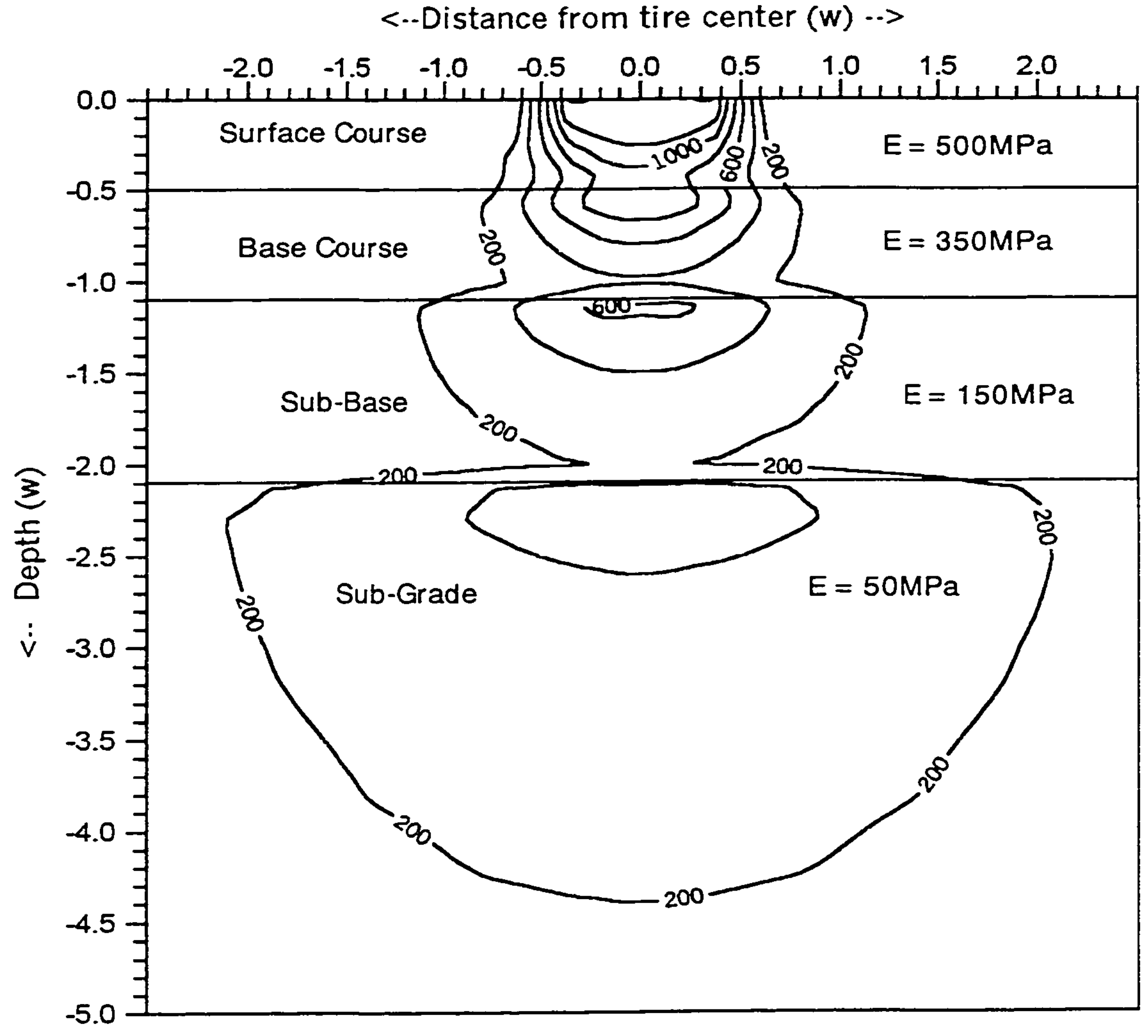

Figure 17 Vertical strain (in micro-strain) for one tire (load = 0.7MPa).

Table 13 Maximum vertical strain for various layers.

Layer	One Tire	Two Tires	Four Tires
Surface course	1400	1400	1400
Base Course	900	1100	1100
Sub-Base	700	900	900
Sub-Grade	500	900	900

Study of the figures and the table reveals that interaction between adjacent tires affects the vertical strain levels in the base course and below. The effect of tire interaction is not significant in surface course because the strain bulbs in that layer are not wide enough to interact. In the base course the maximum strain level increased from 900 to 1100micro-strain, when more than one tire was considered. The increases for sub-base and sub-grade were from 700 to 900micro-strains and from 500 to 900micro-strains respectively. The interaction between the pairs of tires at the opposite end of the rear axle of the truck does not affect the maximum strain level in any course but the strain bulbs extends deeper in the sub-grade (400 and 600micro-strain contours). Thus it can be concluded that interaction of strain bulbs generated by the tires along the back axle of a truck significantly increases the vertical strain level in the base course and below.

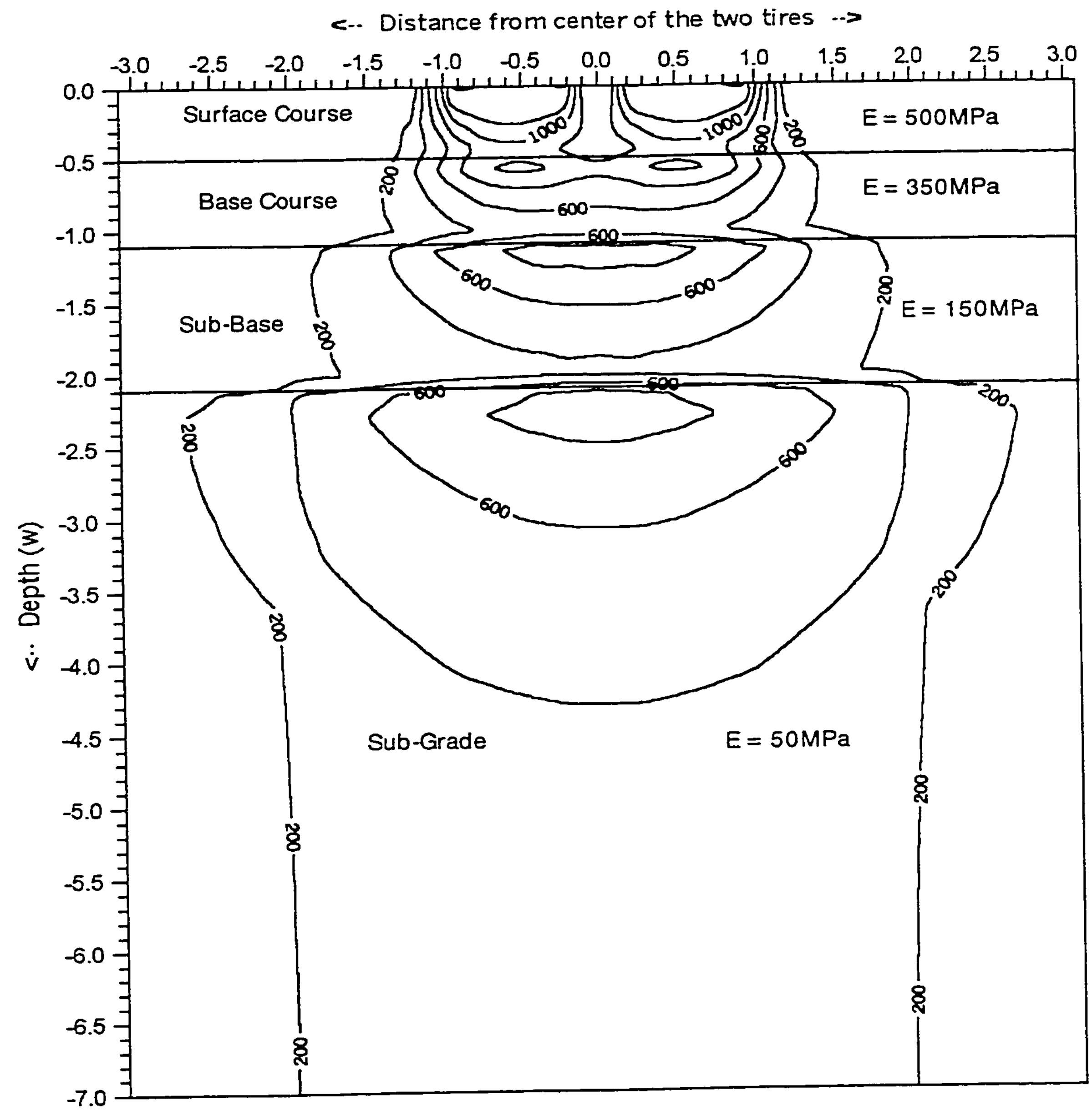

Figure 18 Vertical strain (in micro-strain) for two tires (load = 0.7MPa).

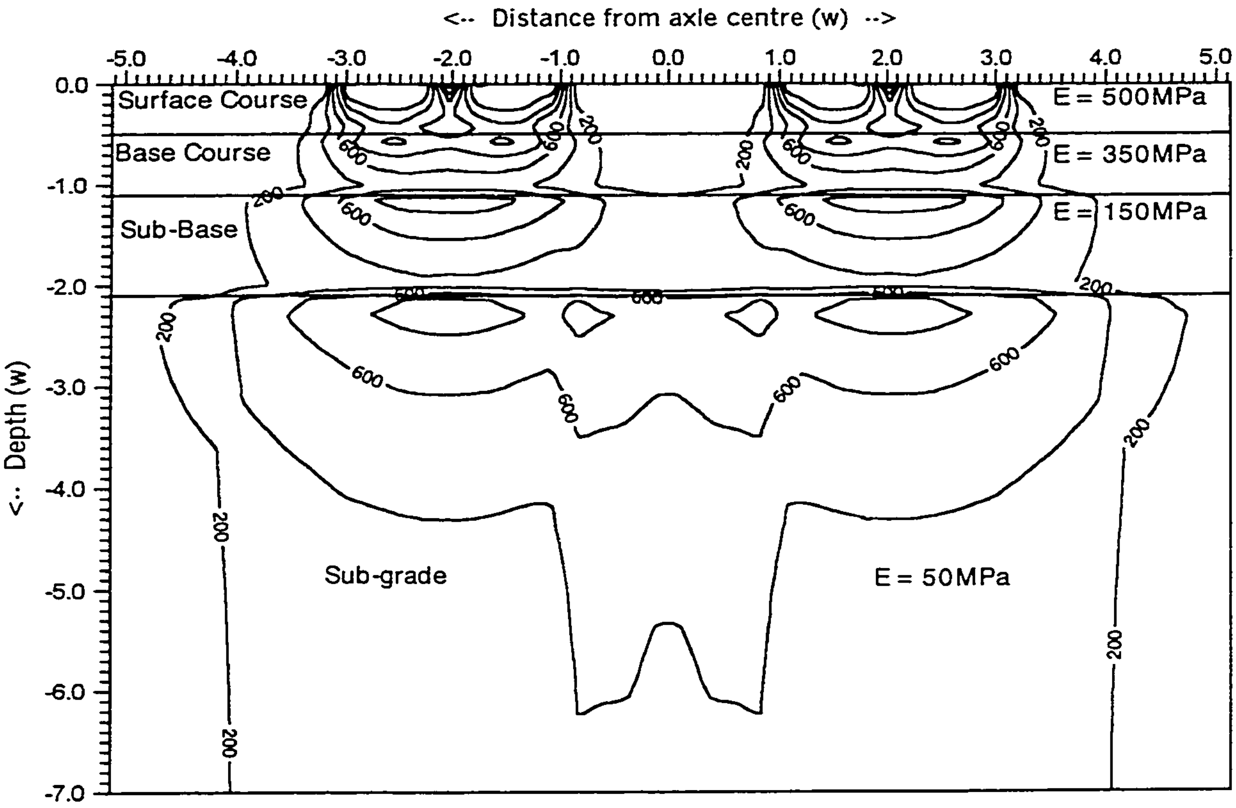

Figure 19 Vertical strain (in micro-strain) for four tires (load = 0.7MPa).

4.7 Summary and Recommendations

Although it is important that bearing capacity of the haul road construction material be greater than the stress generated by the load (tires), bearing capacity is seldom a limiting factor in most practical cases where crushed rock is used to construct the surface course.

The most critical criterion for haul road design is the vertical strain. Apart from load geometry, vertical strain primarily depends on modulus of elasticity (strictly speaking modulus of rigidity, but modulus of elasticity gives a conservative estimate of modulus of rigidity as discussed in Section 3.3) and the thickness of various layers.

Once available construction materials have been analyzed for their properties, there can be many combinations of the materials. Laying the stiffest material on top and next stiffest material below it and so on gives best result in terms of least vertical strain.

Various possible layer thickness should be analyzed and the least thickness that gives vertical strain below the critical strain limit at all points, with some allowance for increase in strain due to tire interaction, should be chosen for road design.

The interaction of strain bulbs produced by adjacent tires on the rear axle of a truck resulted in a 20% to 80% increase in the maximum vertical strain in the base course and below (the effect increased with depth) but had near zero effect on the maximum vertical strain in the surface course. The interaction of stress bulbs generated by two pairs of tires at opposite ends of the rear axle of the truck has minimal effect on the maximum strain level at any depth but it deepens the resultant strain bulbs generated in the sub-grade. Strain bulbs generated by the front and the rear tires of a truck have little interaction.

If the maximum vertical strain in any course in a road is much less than the critical strain limit (1500 - 2000micro-strains), then the cover thickness above that course can be decreased or less stiff material can be used. A strain analysis should be performed on the final road cross-section to confirm that the vertical strain at all points is still less than the critical strain limit with the new course thickness and/or less stiff construction material(s).

5 FLY ASH STABILIZED HAUL ROAD CONSTRUCTION MATERIALS

5.1 Introduction

Alberta obtains more than 90% of its electrical power from coal burning power plants situated next to coal strip mines. Approximately 26Mt of coal (Coal Association of Canada 1999) are burned each year in Alberta, generating about 2.4 million metric tonne (Mt) of fly ash and 0.6Mt of bottom ash (Joshi 1999). Most of the ash is hauled from the power plants back into the mined-out areas for disposal in landfills. While efforts are underway to establish markets and other end uses for ash, the disposal of millions of metric tons (mt) of ash each year remains a problem.

Heavy, large capacity trucks are used to haul coal from the mine to the power plants. These trucks can achieve gross vehicle weights of 4000kN. The tire pressures used to support the weight of the truck and the coal are typically in the range of 600kPa to 690kPa. The haul roads must be constructed from materials with sufficient bearing capacity and stiffness to maintain road serviceability. Haul roads that are in poor condition can detrimentally influence mining by (1) reducing productivity by increasing rolling resistance, (2) increasing costs due to more road and truck maintenance.

The focus of this chapter is to evaluate whether the addition of fly ash to mine spoil or coal seam partings can improve the physical properties of these materials and thus improve their performance as construction materials for a haul road. The successful use of fly ash to stabilize soils elsewhere (Hobeda 1984) suggests that their use in haul roads should have multiple benefits, including diverting some ash from landfills to road construction and improving mining productivity.

5.2 Literature Review on Properties of Fly Ash Stabilized Haul Road Construction Materials

5.2.1 Fly Ash Properties

Properties of fly ash depend on many factors. The type of coal burned is the single most important factor influencing the type of fly ash generated. The type of collector used also affects the fly ash quality. The lime (CaO) content of fly ash dictates the cementing properties of fly ash as it is essential for a pozzolanic reaction to form cementitious compounds with the soil particles.

Type of coal – Cementing capability of fly ash decreases with increase in the rank of coal from which ash is produced. So, fly ash produced from bituminous coals generally has lower cementing capability (due to insufficient free lime) than ash from sub-bituminous coal (DiGioia et al. 1979). Fly ash from lignite shows good cementing properties without addition of lime, whereas fly ash from bituminous and sub-bituminous coals (types of coal present in Alberta) may require additional lime.

Collection system – Torrey (1978) reports that fly ash collected by electrostatic precipitators (ESP) has 38% more CaO and 58% less carbon than ash collected by mechanical collectors. Moreover the former is finer than the latter. Thus, fly ash collected by ESP is more reactive and consequentially, more suitable as haul road construction material than fly ash collected by mechanical collectors.

5.2.2 Lime-Fly Ash-Aggregate Mix (LFA) for Road Construction

Lime-Fly ash-Aggregate mix (LFA) has been widely used for road construction. Torrey (1978) reports use of fly ash, lime, cement, sand and aggregate mixes in ratios of 30:9:1:57:40 to surface a road with heavy traffic. Torrey (1978) also reports use of LFA for base and sub-base layers of roads. Vaeg (1984) discusses successful use of LFA as a road construction material in Sweden. Fly ash and LFA have various desirable properties as a haul road construction material.

Low cost and high availability - Fly ash, a major component in a LFA mix is a low cost material that is abundant near prairie coal mines. In fact, it is a liability for the utility companies because they must incur costs for environmentally sound disposal of fly ash. Fly ash disposable costs offset part of the costs incurred in transporting fly ash from a power plant to a road construction site. Moreover, rail wagon or haul trucks transporting coal from a mine to a power plant can carry ash on their return trip.

Cementing properties – Siliceous or alumino siliceous materials, present in fly ash, when in finely divided form, react with alkali or alkaline earth products such as CaO, to produce cementitious products, in presence of water. The alkali or alkaline earth products, if not present in the fly ash, can be added. The cementing reaction, which is time dependent, increases strength and decreases compressibility, permeability and frost susceptibility. Thus suitability of fly ash or LFA for road construction improves with the age of curing.

Low density – Compacted LFA has a low density (1800-2000kg/m^3) and can be used as a low density fill.

Compressive strength – LFA can have fairly high compressive strength compared to most soils used alone (Table 14 and Table 15). The strength of the LFA depends on the amount of fly ash that is used. Thus, LFA may be used to build roads designed for large haul trucks.

Table 14 Compressive strength of fly ash-lime-aggregate mixes (after Meyers et al. 1976).

Curing period	Compressive strength (MPa)
7 Days	2.76 – 3.10
28 Days	3.79 – 4.13
2 Years	≈ 10

Table 15 Compressive strength (MPa) of hydrated fly ash (after Meyers et al. 1976).

	Moisture content		
Curing period	20%	40%	60%
3 Days	9.49	3.46	1.36
7 Days	11.24	4.18	1.71
14 Days	14.72	4.94	2.06

Low compressibility - One desirable property of a haul road construction material is that it should not settle on repeated loading. The compressibility of fly ash is very low compared to other construction materials. The compression index and recompression index for fly ash varies from 0.10 to 0.25 and from 0.02 to 0.04, respectively (DiGioia et al. 1979).

Environmentally safe - Various studies done by the DiGioia et al. (1979) and the Kennedy et al. (1981) on the leaching properties of fly ash, demonstrate that there is little danger of leaching toxins from fly ash fill into water bodies in particular and the environment on the whole. Bituminous coal has an average of 0.3% free lime and 0.5% soluble sulfate. Rohrman (1971) reports that fly ash leachate is alkaline (pH 6.2 to 11.5), whereas Theis and Marley (1976) reports acidic nature of fly ash leachate. An acidic leachate can be expected to have higher concentration of trace elements. Fortunately, Pluth et al. (1981), after testing fly ash from five different Alberta coal mines, reports that the leachate of the fly ash is alkaline. Nevertheless, accurate prediction of leachate quality needs assessment of site-specific soil attenuation parameters.

5.3 Unconfined Strength and Modulus of Fly Ash-Soil Mixtures

Unconfined compression tests were performed on various combinations of fly ash, kiln dust and road building aggregates at different ages of curing to measure compressive strength and modulus.

Previous studies (DiGioia et al. 1979 and Hobeda 1984) have evaluated fly ash and fly ash mixed with cement and aggregates for use in commercial roads. The fly ash used in these tests was usually refined and the test objectives were to prove applicability in commercial roads. The objective of the this testing program is to find suitable combinations of fly ash, cementing material and aggregates for use in mine haul roads. Thus unclassified (unrefined) fly ash was used and the aggregates selected for the tests were the typical road building materials used for mine haul roads. The choice of materials was such that the test results have direct application for mine haul roads in central Alberta.

Careful mixing and proportioning of ingredients and water is a precondition to achieve desirable mix properties. Deviation of mix ratios from optimum may significantly degrade strength and other properties.

5.3.1 Component Properties

The first batch of fly ash, mine spoil and coal seam partings were obtained from the Sundance power plant and adjoining Highvale Mine on 20th of May 1999. Sundance delivered a second batch of fly ash on 20th of August 1999. The first batch of kiln dust was picked up from the Lafarge facility in Edmonton on 4th of June 1999 and Lafarge delivered a second batch on 29th of July 1999.

The unclassified fly ash from the Sundance power plant contains about 10% CaO (Ketcheson 1999). The unclassified fly ash differs from the fly ash that is sold by Lafarge. The commercial fly ash is cleaned (via a cyclone) to remove ash particles and larger particles, creating a Class Ci fly ash.

Cement kiln dust was obtained from the Lafarge Exshaw plant near Canmore. This material is currently a waste byproduct from cement production. The two batches of kiln dust differed in their ability to activate cementing capabilities of fly ash as discussed later.

Partings between seam 3 and seam 4 of Highvale Mine was used as an aggregate. It is a dark gray siltstone. Its liquid and plastic limits were determined to be 51% and 33%, respectively. Particle size analysis was done on dried partings that passed through 1" (25.4mm) sieve according to ASTM D422–63 (Figure 20). More than 90% of the particles passed through ¾" (19mm) sieve and more than 50% passed through 3/8" (9.5mm) sieve. Less than 5% of the material had particle diameter less than 0.85mm.

Mine spoil is the material found between seam 1 and the topsoil. It is a yellow to light brown silt. It is a non-plastic material so determination of Atterberg limits was not possible. Particle size analysis was done on the dried portion of the material that passed through a 1" (25.4mm) sieve according to ASTM D422–63 (Figure 20). More than 95% of the particles passed through a ¾" (19mm) sieve and slightly less than 50% passed through a 4.25mm sieve but approximately 25% of the particles had diameter smaller than 0.85mm. The mine spoil had a specific gravity of 2.62 (ASTM D854).

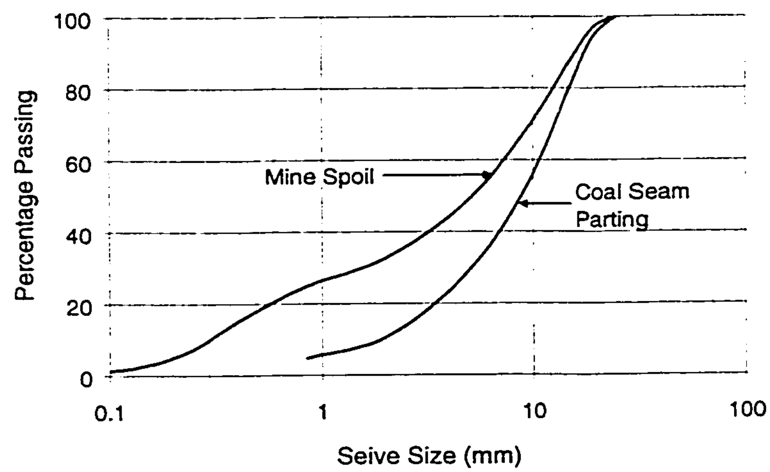

Figure 20 Particle size distributions.

5.3.2 Moisture-Density Relationships

Optimum moisture content is required for maximum compaction, which is essential for proper strength generation in a LFA mix. Moreover, moisture present in the mixture is essential for the pozzolanic reaction, which creates cementing action. Water contents were determined by conducting moisture-density tests following ASTM D558. A series of standard proctor compaction tests were performed and the measured moisture content was plotted against density. For subsequent strength testing, the water content corresponding to maximum density was chosen for the sample preparation. Figure 21 shows the moisture-density relationship for LFA mixes with mine spoil. All mixes (mine spoil or mine partings) had optimum moisture contents close to 14%.

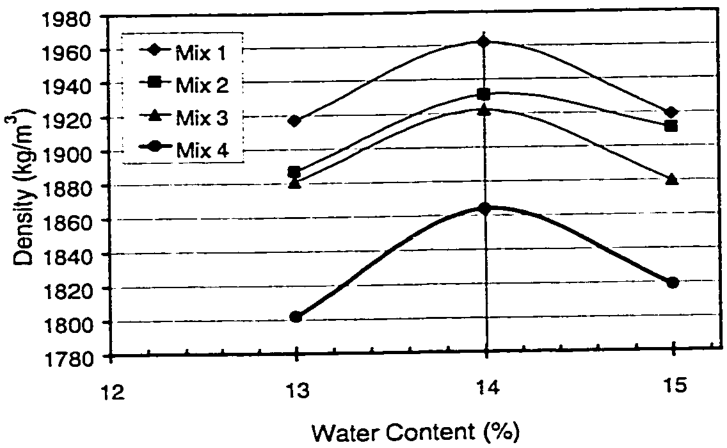

Figure 21 Moisture-density relationship for LFA mixes with mine spoil.

The optimum moisture contents for maximum compaction density of the coal seam parting and of the mine spoil were also measured and were found to be 0.5% to 1% lower than that for LFA. This may be attributed to presence of fly ash in LFA mixes.

Haul road construction materials are typically mixed at moisture contents slightly lower than optimum because it is easier to place and spread drier material.

5.3.3 Sample Preparation

The relative proportions of the different ingredients used for the tests were based on a literature review, suggestions by Lafarge, and results from previous tests. Fly ash and kiln dust were dry and fine grained, so no pretreatment was required.

This study was not designed to determine the amount of kiln dust needed to fully mobilize the cementing capacity of the fly ash. The goal was to focus on utilization of fly ash while minimizing the use of potentially more expensive additives containing CaO (kiln dust or lime). The choice of percent kiln dust was somewhat arbitrary in these tests and further research is needed in order to determine the optimal amount of kiln dust needed to achieve the desired material properties.

The parting material was air-dried for 5 days, then sieved and crushed. Material passing through a ¾" (19mm) sieve was used for testing. The mine spoil was cohesive and moist. It was air dried for 15 days. Dried lumps were broken to bring the grading below ¾" (19mm).

The materials were weighed according to the desired proportions (Table 16) and kept in separate containers. The ingredients were poured in a concrete mixer (adding water last) and mixed until a homogenous mixture was obtained (Figure 22). Approximate mixing times were around 20 to 25 minutes. The mixer was stopped frequently to carve sticking material behind blades and at the bottom the mixer.

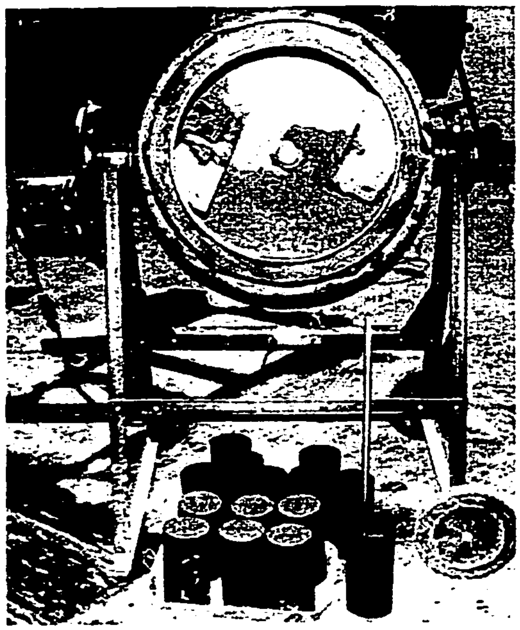

Figure 22 Concrete mixer and compacted samples.

Table 16 Composition of specimens.

Mix	Mix No.	Ingredients (%)				
		Fly* Ash	Kiln* Dust	Seam* Parting	Mine* Spoil	Water
Fly Ash Only		100	-	-	-	17
Fly Ash + Kiln Dust	1	90	10	-	-	18
Fly Ash + Kiln Dust	2	80	20	-	-	17
FA + KD + Parting	1	12.5	3.5	84	-	11
FA + KD + Parting	2	16	4	80	-	13
FA + KD + Parting	3	20	4	76	-	13

Mix	Mix No.	Ingredients (%)				
		Fly* Ash	Kiln* Dust	Seam* Parting	Mine* Spoil	Water
FA + KD + Parting	4	25	5	70	-	14
FA + KD + Spoil	1	12.5	3.5	-	84	14
FA + KD + Spoil	2	16	4	-	80	14
FA + KD + Spoil	3	20	4	-	76	14
FA + KD + Spoil	4	25	5	-	70	14

* dry percentage.

Cylindrical forms of diameter 101.6mm (4") and height 203.2mm (8") were cleaned and interior walls were oiled. Then the mixture was placed in the forms and compacted in three layers by rodding following the procedures given in ASTM D698. The densities achieved by this compaction are summarized in the Table 17.

Table 17 Density achieved during sample preparation.

Mix	Density (kg/m^3)	No. of Samples
Fly Ash Only	1530	12
Fly Ash + Kiln Dust (mix 1)	1650	9
Fly Ash + Kiln Dust (mix 2)	1635	14
Fly Ash + Kiln Dust + Parting (mix 1)	1825	12
Fly Ash + Kiln Dust + Parting (mix 2)	1850	14
Fly Ash + Kiln Dust + Parting (mix 3)	1850	14
Fly Ash + Kiln Dust + Parting (mix 4)	1760	14
Fly Ash + Kiln Dust + Spoil (mix 1)	1960	14
Fly Ash + Kiln Dust + Spoil (mix 2)	1930	14
Fly Ash + Kiln Dust + Spoil (mix 3)	1920	14
Fly Ash + Kiln Dust + Spoil (mix 4)	1870	14

The samples were kept in a moist room with 100% humidity and allowed to cure. The samples were taken out of the forms after 2 days using compressed air injected through a small hole in the bottom of the forms. The samples were then returned to the moist room until the day of testing.

The samples were either capped with sulfur or the sample ends were dressed to make them flat (the choice was dictated by the strength of the sample; the weak samples could not be capped because the samples broke while being taken out of the capping mould).

5.3.4 Test Procedure

Uniaxial compression tests were performed following ASTM D5102. The tests were initially planned to be taken after 3, 7, 14, and 28 (if required) days of curing. But the sample with 100% fly ash was found to be very weak so the 14-day test was cancelled and a test after 56 days of curing was done instead. The compression test were done with an automatic data acquisition system (data logger) except one set of tests (7-day test of fly ash and kiln dust (mix 1)) in which readings were observed manually. Compression rates ranging from 0.1 to 0.5mm/min were used but changing compression rates within this range did not seem to have any effect on the results. Changes in compression rates were made to keep the total loading time below 15 minutes so as to minimize creep effects.

Higher reading rates for data were used for higher compression rates to get a relatively consistent rate of reading with respect to strain. Data reading rates ranged between 2 and 15 readings per minute, with 10 readings per minute being the most common value. The lower limit on reading rate was guided by the fact that there should be enough data points to capture the complete nature of stress-strain curve and at the same time record the maximum stress.

5.3.5 Results

A series of tests were conducted to evaluate, in a general manner, the cementing action of the fly ash. Test specimens were made from fly ash with and without addition of kiln dust. The fly ash compacts well and can achieve minor strength simply by mechanical interlock between the compacted particles.

Compressive strengths and Young's modulus obtained from the tests are shown in Figure 23 and Figure 24 respectively. These figures show that the addition of kiln dust is needed in order to achieve significant strengths (>1MPa) from the fly ash. With kiln dust, the fly ash shows time-depend strength and stiffness improvements. These results confirmed expectations that fly ash alone from central Alberta coals does not possess sufficient CaO to be self-cementing.

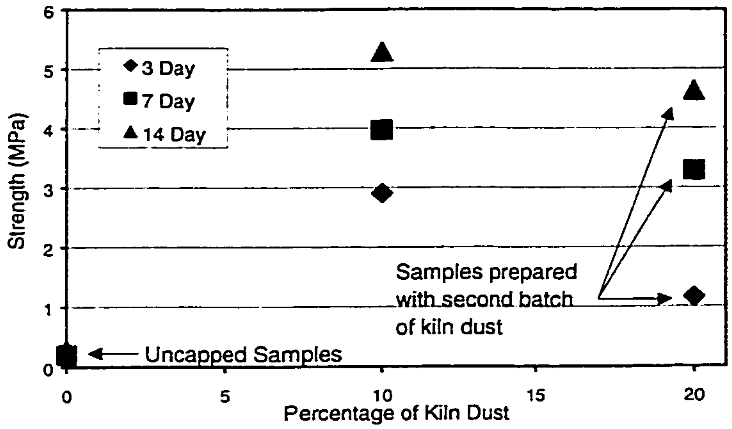

Figure 23 Unconfined compressive strength of fly ash - kiln dust samples

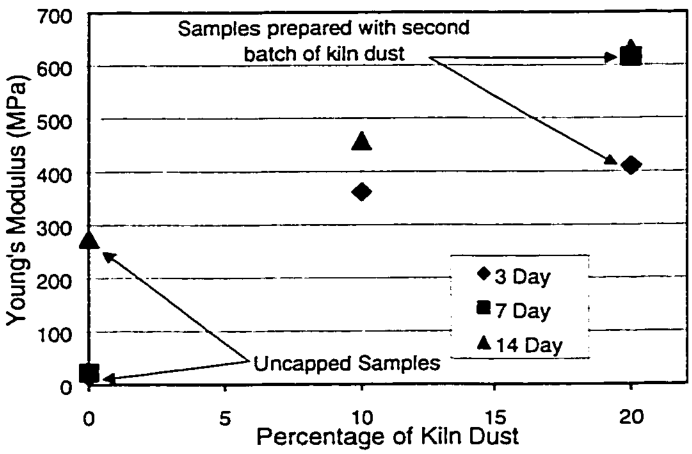

Figure 24 Young's modulus of fly ash - kiln dust samples.

Because only a few tests were performed, it is not possible to state the optimal kiln dust/fly ash ratio that creates the best "binder" for soil improvement. For subsequent tests where the binder was mixed with the soils, the kiln dust/fly ash ratio was selected between 0.20:1 and 0.28:1 by dry weight.

Figure 25 through Figure 28 show the compressive strengths and Young's modulus obtained from the tests involving mixtures of mine spoil or partings and binder (fly ash plus kiln dust). Most points shown on these figures are averages of three separate tests.

Given the variability in the test results, it appears the specimens made with crushed coal seam partings (siltstone) had properties that were similar to those made from the mine spoil (silt).

The strengths achieved in the stabilized soils are less than those for the fly ash-kiln dust samples, but are sufficiently high after a period of curing to be useful for road construction. While not a comprehensive suite of test data, the results show that strength and stiffness increase over a 28-day period and that mixes with high binder content perform best. Strengths in the order of 0.6MPa are obtained after 7 days while 28-day strengths are about 0.8 to 1MPa depending on the binder content. Unconfined compression tests conducted on cylinders of compacted silt or crushed siltstone gave compressive strengths of about 0.2 MPa (Table 18). Therefore, the addition of the fly ash-kiln dust binder can significantly improve the strength (and stiffness) of these materials. The Young's modulus generally increased with longer curing period and higher percentage of binder.

Table 18 Typical stabilized silt or siltstone properties.

Age	Unconfined Compressive Strength (MPa)	Young's Modulus (MPa)
7 Day	0.4 to 0.6	150 to 250
28 Day	0.8 to 1	150 to 350
No binder	0.2	<50

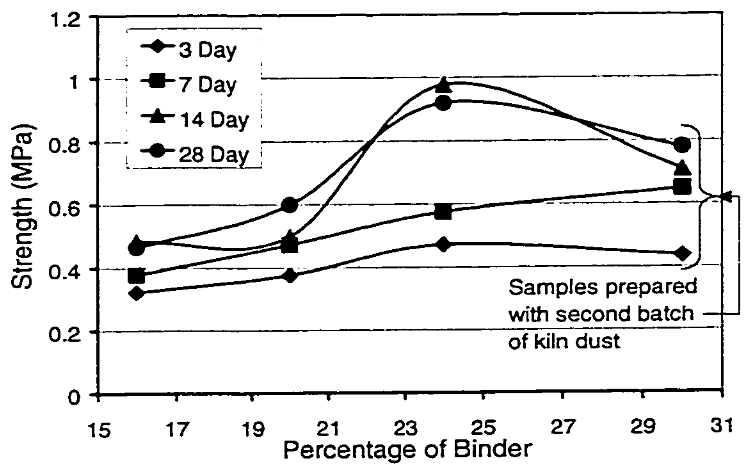

Figure 25 Unconfined compressive strength of samples made with crushed coal seam parting.

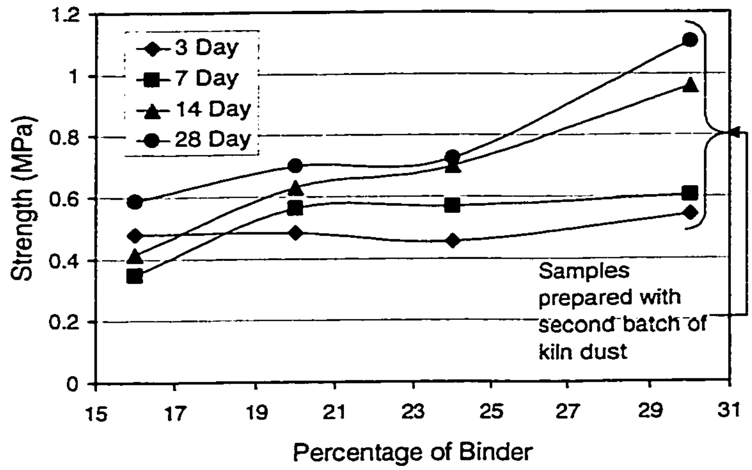

Figure 26 Unconfined compressive strength of samples made with crushed mine spoil.

The fly ash and the kiln dust were delivered in two batches. Both batches of fly ash seemed to have similar properties but the two batches of kiln dust appeared to differ. Samples with coal seam parting gave better results with the first batch of kiln dust, whereas mine spoil gave better results with second batch of kiln dust. The compressive strength should increase with percentage of fly ash but Figure 25 shows a decrease in compressive strength for the highest percentage of binder.

It should not be concluded that compressive strength peaks at 20% fly ash because the samples with parting (mix 4), spoil (mix 4) and kiln dust (mix 2), were prepared with the second batch of kiln dust. For specimens made with coal partings, mix 4 had compressive strengths lower than that of mix 3, which is reverse to the general trend (Figure 25). This may be attributed to a different type of kiln dust used to prepare mix 4 with parting. This may also be the reason for the lower strength of kiln dust-fly ash samples with 20% fly ash. But this anomaly was not observed in samples with spoil. Detailed test results are provided in the Appendix 8.4.

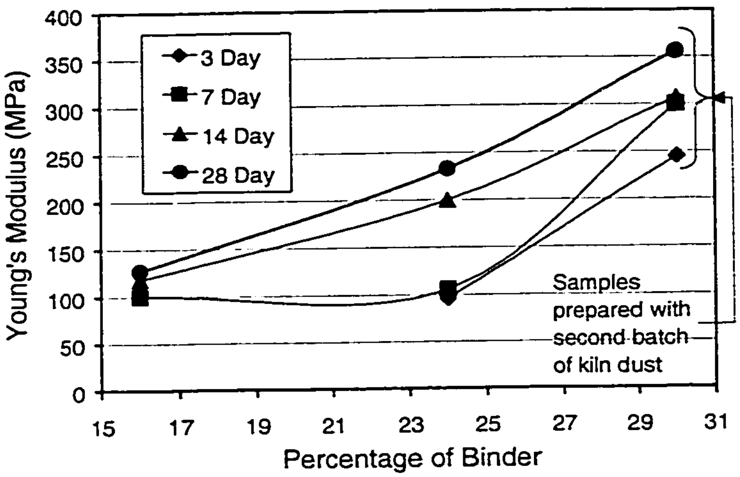

Figure 27 Young's modulus of samples made with crushed mine parting.

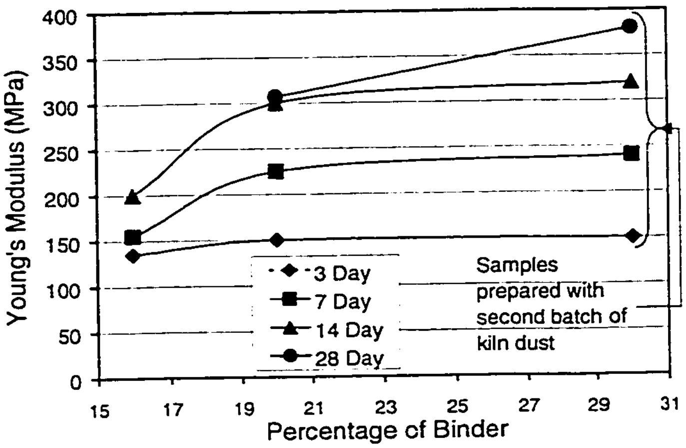

Figure 28 Young's modulus of samples made with crushed mine spoil.

5.4 Summary

Unconfined compressive strength tests conducted on various mixtures of fly ash, kiln dust, mine spoil, and coal seam partings showed that the cementing characteristics of unclassified fly ash from central Alberta coals was low. However, the addition of cement kiln dust, which is high in CaO, enabled the fly ash to exhibit significant cementing action.

Mixtures of fly ash, kiln dust, and mine spoil or coal seam partings had unconfined compressive strengths of about 0.4 to 0.6MPa after 7 days and 0.8 to 1MPa after 28 days. The elastic moduli of these materials were 150 to 350MPa after 14 to 28 days. This compares favorably with compacted mine spoil or coal seam partings which have estimated unconfined compressive strengths of less than 0.4MPa. Thus fly ash stabilized mine spoil or coal seam partings were found to have potential for use in constructing haul road base and sub-base layers since stresses induced in the base layer will be less than about 0.3 to 0.65MPa. Furthermore, the compacted fly ash stabilized soils had Young's moduli that were high enough to meet strain criteria for haul road construction.

More work is needed to better define the amount of CaO needed to fully activate the cementing characteristics of fly ash from Alberta's prairie coals. Alternatives to kiln dust as a source for CaO can also be tested. Once a cheap, yet effective binder is developed, it has good potential for use as an additive in road construction near coal-fired power plants in Alberta.

One problem with binder use in road construction is that the strength and stiffness of the stabilized soils are time-dependent. Road construction procedures and the length of time that the road must wait before being placed into service are important considerations. However, where opportunities occur, construction of haul roads using fly ash is recommended.

6 CONCLUSIONS AND RECOMMENDATIONS

The research addressed a variety of inter-related topics about haul road design and construction. This chapter summarizes the results and findings all the chapters. It also recommends a method for haul road design and future work.

6.1 Summary of Results/Findings

1. Due to the introduction of larger haul trucks over the last decade, geometrical elements of haul roads, such as width, have increased. Larger trucks also place greater load on the road but little design work has been done by Canadian mines (except Syncrude) to take care of this factor. Haul road construction and maintenance procedures followed by various mines are based on past experience and trial and error methods.

2. Developing tires suitable for large trucks is a challenge. Michelin has developed a 'low pressure, low profile' tire that can satisfactorily carry high loads at higher speed while also imposing lower stress to the haul road.

3. There are many methods of road design, out of which the CBR and resilient modulus methods are particularly applicable to the design of haul roads. Although the CBR method is a commonly accepted and applied method of haul road design in surface mines, it has many inherited shortcomings, which may lead to under or over design. In case of mines that use ultra-large trucks (GVW > 400 mt), it becomes imperative to use a haul road design method based on the resilient modulus of the construction materials, which warrants more complex analysis than the CBR method.

4. Bearing capacity is seldom a limiting factor in most practical cases where crushed rock is used for the surface or running course. The most critical criterion for haul road design is the vertical strain. Apart from load geometry, vertical strain primarily depends on modulus of elasticity and the thickness of various layers. Laying the stiffest material on top and next stiffest material below it, and so on, results in the lowest vertical strain.

5. The interaction of strain bulbs produced by adjacent tires on the rear axle of a truck results in a 20% to 80% increase in the maximum vertical strain in the base course and below (the interaction effect increases with depth) but has near zero effect on the maximum vertical strain in the surface course. Interaction of stress bulbs generated by two pairs of tires at

opposite ends of the rear axle of the truck has minimal effect on the maximum strain level at any depth but it deepens the strain bulbs generated in the sub-grade. Strain bulbs generated by the front and the rear tires of a truck have little interaction.

6. Unconfined compressive strength tests conducted on various mixtures of fly ash, kiln dust, mine spoil, and coal seam partings showed that the cementing characteristics of unclassified fly ash from central Alberta coals was low. However, the addition of cement kiln dust, which is high in CaO, enabled the fly ash to exhibit significant cementing action. Mixtures of fly ash, kiln dust, and mine spoil or coal seam partings had unconfined compressive strengths of about 0.4 to 0.6MPa after 7 days and 0.8 to 1MPa after 28 days. The elastic moduli of these materials were 150 to 350MPa after 14 to 28 days. This compares favorably with compacted mine spoil or coal seam partings which have estimated unconfined compressive strengths of less than 0.4MPa elastic modulus of less than 50MPa. Thus, the addition of binder increased the compressive strength by 100% and increased the elastic modulus by 500%. Therefore, fly ash stabilized mine spoil or coal seam partings were found to have potential for use in constructing haul road base and sub-base layers since stresses induced in the base layer will be less than about 0.3 to 0.65MPa. Furthermore, the compacted fly ash stabilized soils had Young's moduli that were high enough to meet the strain criteria for haul road construction.

6.2 Recommended Haul Road Design Method

As discussed in Chapter 3, two methods of road design are applicable to haul roads of surface mines. The first method is based on the CBR of the material and the second one is based on the resilient modulus. The CBR method is very simple and is widely understood and followed. But recently some authors have argued against its use as discussed in the Section 3.3 and they report that the resilient modulus based method is better. This was further confirmed by the author's personal communication with practicing engineers.

The resilient modulus method is explained in detail in Chapter 3. Major steps of the method are given in Figure 29. The method is based on the criteria that the vertical strain at any point in haul road should be less than a critical strain limit. The critical strain limit is dependent on the traffic density and design life of the haul road, which gives the number of load repetitions during the design life of the road. Generally, this limit falls between 1500 and 2000 micro-strain.

Resilient modulus is the major input for modeling vertical strain. It can be determined either by a resilient modulus test (AASHTO 1993[b], T294) or by a falling weight deflectometer test. The Young's modulus gives a conservative estimate of the resilient modulus. The resilient modulus of a material is highly sensitivity to compaction effort and water content during compaction. These factors must be considered when determining values for use in numerical models.

Initially, the thickness of each layer should be estimated based on past experience or designs at mines with similar conditions. For least vertical strain, the stiffest material should be put at the top and next stiffest underneath it and so on. For modeling strain other material properties such as Poisson's ratio is also required. The increase in strain due to interaction of tires should also be considered. If the strain any layer is more than the critical strain limit then the thickness and/or the stiffness of the layer above that material should be increased. On the other hand, if the strain in any layer is much less than the critical strain limit then the thickness of the layer above that layer can be decreased. The amount by which the thickness should be increased or decreased depends on the difference between the vertical strain and the critical strain limit. Initially, 0.1m is a good increment. In both cases the modeling should be repeated to ensure that the strain at all points is less than the critical strain limit.

The layer thickness determined by this method depends on the resilient (Young's) modulus of the haul road construction material. A low modulus construction material may result in a very thick layer, which may be unacceptable for economic or operational reasons. Then it becomes essential to investigate the use improved compaction methods and/or the addition of cementing agents such as fly ash to improve the rigidity of the construction material and consequentially to lower the fill height (volume) requirement. Strain modeling should be performed again to ensure that the vertical strain at all points is less than the critical strain limit.

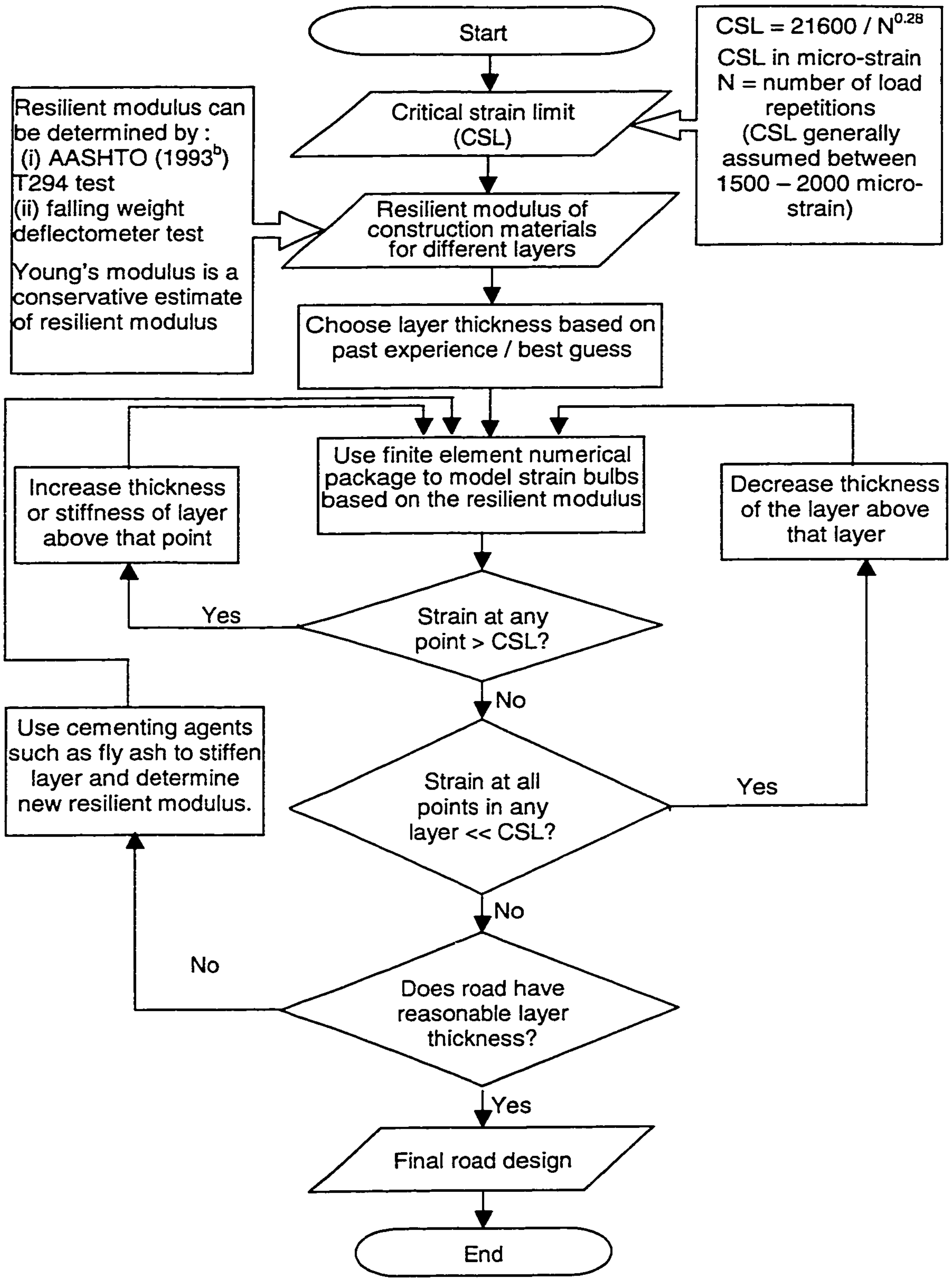

Figure 29 Major steps of the resilient modulus haul road design method.

6.3 Future Work

The laboratory work was limited to studying the effect of varying only the major component mixes. Moreover, the recommended method of design was not field-tested. Thus, recommendations for future work are:

- Monitor deflection and rut depth on a test strip built with fly ash stabilized construction material to demonstrate that fly ash can used for haul road construction.
- The effect of other locally available binder materials such as sulfur or coke for stabilizing haul road construction materials should be studied in the laboratory.
- To justify use of binders, the cost of adding binders should compared with savings generated in terms of reduced travel time, reduced truck maintenance, reduced road maintenance and increased road life. The effect of binders on reduced rolling resistance should also be measured either directly or as an increase in truck speed and/or reduction in fuel consumption.
- A test strip should be built following the recommended method and monitored to test the merits of the method.

7 REFERENCES

AASHTO. 1993[a]. *Standard Specifications for Transportation Materials and Methods of Sampling and Testing*. Part I - Specifications. Sixteenth Edition. American Association of State Highway and Transportation Officials. Washington D.C. USA.

AASHTO. 1993[b]. *Standard Specifications for Transportation Materials and Methods of Sampling and Testing*. Part II - Tests. Sixteenth Edition. American Association of State Highway and Transportation Officials. Washington D.C. USA.

Ahlvin, R.G., Ulery, H.H., Hutchinson, R.L. & Rice, J.L. 1971. Multiple wheel heavy gear load pavement test. *Basic Report, USA Waterways Experiment Station Report.* Vol. 1. AFWL – TR – 70-113.

American Society of Civil Engineers. 1950. Development of the CBR flexible pavement design methods for airfields. *Symposium, Transactions, ASCE.* Vol 115.

Atkinson, Thomas. 1992. Design and layout of haul roads. *SME Mining Engineering Handbook.* 2nd edition. Society of Mining, Metallurgy, and Exploration, Inc. Littleton, Colorado: 1334 – 1342.

Australian Asphalt Pavement Association. 1983. *Structural Design of Pavement Flexible Pavements.* Manual No. 1 (M1). Victoria, Australia.

Bowles, J.E. 1984. *Physical and Geotechnical Properties of Soils.* Second edition. McGraw-Hill Book Company. New York, USA.

Boyd, W.K. & Foster, C.R. 1949. Design curves for very heavy multiple wheel assemblies. *Proceedings, American Society of Civil Engineers.* Vol. 75.

Cameron, R. 1999. Personal communication. Syncrude Canada Limited.

Canadian Mining Journal, 2000. Ed. Wernuik, M.J. February, 2000. Vol. 121 – No.2.

Coal Association of Canada, 1999. Web Page: http://www.coal.ca/stats.htm#domesticconsumption.

DiGioia, A.M., McLaren, R. J. & Taylor, L.R. 1979. *Fly Ash Structural Fill Handbook.* EA-1281. Research Project 1156-1. Monroeville, GAI Consultants.

Doyle, M. 1999. Personal communication. Michelin Tire.

Foster, C.R. & Ahlvin, R.G. 1954. Stress and deflections induced by a uniform non-circular load. Proceedings: Highway Research Board. Vol. 33. Washington, DC, USA.

Good Year. 1998. Tire Maintenance Manual.

Hobeda, P. 1984. *Use of Waste Material from Coal Combustion in Road Construction.* NTIS.

Joshi R.C. 1999. Personal communication.

Kaufman, W. W. and Ault, J. C. 1977. Design of surface mining haulage roads – a Manual. U.S. *Department of Interior, Bureau of Mines, Information Circular* 8758.

Kennedy, F. M., Schroeder, A. C. & Veitch, J. D. 1981. *Economics of Ash Disposal at Coal-fired Power Plants.* PB82-192535. NTIS.

Ketcheson R 1999. Lafarge Canada Inc. Personal communication.

Knapton, J. 1988. *The Structural Design of Heavy Duty Pavements for Ports and Other Industries.* British Ports Federation. London, England.

Meyers, J. F., Pichumani, R. & Kapples, B. S. 1976. *Fly Ash as a Highway Construction Material – A Manual.* 76-16 Implementation Package. U.S. Department of Transportation, Federal Highway Administration.

Mohammad, L. N., Titi, H. H. & Herath, A. 1998. Intrusion technology: An innovative approach to evaluate resilient modulus of sub-grade soils. *Application of Geotechnical Principles in Pavement engineering.* American Society of Civil Engineers. Geotechnical Special Publication Number 85: 39-58.

Morgan, J. R., Tucker, J. S. & McInnes, D.B. 1994. A mechanistic design approach for unsealed mine haul roads. *Pavement Design and Performance in Road Construction* 1412: 69-81.

Pluth, D. J., Gwyer, B. D. & Robertson, J. A. 1981. Physical characteristics and chemistry of fly ash. *Proceedings: Coal Ash and Reclamation. Alberta Land Conservation and Reclamation Council* RRTAC 81-3: 68-80.

Porter, O.J. (1938). The preparation of sub-grades. *Proc. Highw. Res. Bd.* Washington 18 (2): 324-331.

Porter, O.J. (1949). Development of CBR flexible pavement design for airfields. Development of the original method for highway design. *Proceedings: American Society of Civil Engineers.* Vol. 75: 11-17.

Rohrman, F.A. 1971 (August). Analyzing the effect of fly Ash on water pollution. *Power*: 76-77

Terzaghi, K. 1943. *Fundamentals of Soil Mechanics*. John Wiley and Sons Inc. New York, USA.

Theis, T. L. & Marley, J.J. 1976. *The Contamination of Groundwater by Heavy Metals from Land Disposal of Fly Ash*. US Energy Research and Development Administration. Contract No. E (11-1) – 2727. NTIS

Thompson, R. J. and Visser, A. T. 1997. A mechanistic structural design procedure for surface mine haul roads. *International Journal of Surface Mining, Reclamation and Environment* 11 (1997): 121-128.

Thompson, R. J. 1996. *The Design and Management of Surface Mine Haul Roads*. Ph.D. thesis. Faculty of Engineering. University of Pretoria.

Torrey, S. 1978. *Coal Ash Utilization – Fly Ash, Bottom Ash and Slag*. Pollution Technology Review No. 48. New Jersey: NDC.

Wade, N. H. 1989. Design Manual for Surface Mine Haul Roads. Monenco Consultant Limited, Calgary, Alberta.

Whitlow, R. 1990. *Basic Soil Mechanics*. 2nd Edition. J. Wiley & Sons. New York.

Wieren, L. W. V. and Anderson, H. M. 1990. *An overview of haul roads at Syncrude Canada Limited*. Course notes for Mine Planning and Equipment Selection.

Yodder, E.J. & Witczak, M.W. 1975. *Principals of Pavement Design*, 2nd edition. Wiley. New York.

8 APPENDICES

8.1 Tables Summarizing Questionnaire Responses

Table 19 Mines to which questionnaire was sent

Name and Address of Mine	Response
Manager, Baymag Mines, C/o 10655 Southport Rd SW, Street 800, Calgary, AB T2W 4Y1	No Response
Doug Bainstable, Manager, Bienfait mine, P.O. Box 399, Bienfait, SK S0C 0M0	No Response
Joe Agostino, Manager, Boundary Dam Mine, P.O. Box 908, Estevan, SK S4A 2A7	No Response
R. James Lipkewich, G.P.S. Drilling Coordinator, Bullmoose Mine, P.O. Box 500, Tumbler Ridge, BC V0C 2W0	Responded
Bob McCarthy, Cardinal River Coals Ltd., P.O. Bag 2570, Hinton, AB T7V 1V5	Responded
Doug Stokes, GM, Coal Mountain Mine, P.O. Box3000, Sparwood, BC V0B 2G0	No Response
Chuck Williams, Manager, Coal Valley Mine, P.O. Bag 5000, Edson, AB T7E 1W1	No Response
George Warnock, Elkview Mine, R.R. #1, Hwy 3, Sparwood, BC V0B 2G0	Responded
Bill Foster, GM, Fording River Operations, P.O. Box 100, Elkford, BC V0B 1H0	No Response
Joe Loring, Manager, Garson Mine, Copper Cliff, ON P0M 1NO	No Response
Brad Johnston, GM, Gennesee Coal Mine, P.O. Box 460, Warburg, AB T0C 2T0	No Response
Pat Koski, GM, Greenhills Operations, P.O. Box 5000, Elkford, BC V0B 1H0	Responded
Ray Reipas, GM, Gregg River Mine, Bag Service 5000, Hinton, AB T7V 1V6	No Response
Mark Richards, Highland Valley Copper, P.O. Box 1500, Logan Lake, BC V0K 1W0	Responded
Vince Miller, GM, Highvale Mine, P.O. Box 30, Seba beach, AB T0E 2B0	No Response
Kevin Foley, Iron Ore Company of Canada, P.O. Box 1000, Labrador City, NF A2V 2L8	Responded
Martin Bergeron, Manager, Jeffrey Mine, P.O. Box 1500, Asbestos, QC J1T 3N2	No Response
Ernie Marcotte, GM, Lac Des Iles Mine, P.O. Box 3386, Thunder Bay, ON P7B 5J9	No Response
Louis Wentzel, GM, Les Mines Selbaie, P.O. Box 370, Joutel, QC J0Y 1N0	No Response
Chris Senior Mines Engineer, Line Creek Mine, P.O. Box2003, Sparwood, BC V0B 2G0	Responded
Serge A. Michaud, Manager, Mount Wright Mine, Fermont, QC G0G 1J0	No Response
Tom Strawson, C.E.T., Mine Technician, Obed Mine, P.O. Bag Service 4000, Hinton, AB T7V 1V8	Responded
Walter Klassen, Manager, Paintearth Mine, P.O. Box 730, Forestburg, AB T0B 1N0	No Response
Doug Rolfe, Intermediate Engineer, Poplar River Mine, P.O. Box 599, Coronach, SK S0H 0Z0	Responded
Simon Houle, GM, Qit-Fer Et Titane Inc (Mine), C.P. 160, 951 de l'Escale, Harve Saint-Pierre,QC G0G 1P0	No Response

Sue Bonham-Carter, Quintette Mine, P.O. Box 1500, Tumbler Ridge, BC V0C 2W0	Responded
J. Agostino, Manager, Shand Mine, P.O. Box 908, Estevan, SK S4A 2A7	No Response
Biu Dzus, Manager, Sheerness Mine, P.O. Box 2020, Hanna, AB T0J 1P0	No Response
Harold Beebe, Smoky River Coal Limited, P.O. Box 2000, Grande Cache, AB T0E 0Y0	No Response
N. Chouinard, Mine Superintendent, Stratmin Graphite Inc., 585 chemin du Graphite, Lac-des-iles, QC J0W 1J0	Responded
Mario De Crescentis, Mine Manager, Suncor Energy, Oil Sands, P.O. Box 4001, Fort McMurray, AB T9H 3E3	No Response
Jack Jodrey, Mining, Syncrude Canada Ltd., P.O. Bag 4009, Fort McMurray, AB T9H 3L1	Responded
Neil Johnson, Manager, Wabush Mines (Scully Mine), P.O. Box 3000, Wabush, NF A0R 1B0	No Response
Al Brown, Manager, Whitewood Mine, P.O. Box 88, Wabamun, AB T0E 2K0	No Response
Erin Tough, Mount Polley Mines, P.O. Box 12, BC V0L 1N0	Responded
Buan Robertson, General Manager, Kemess Salt Lake Mine, Royal Oak Mines, P.O. Box –3519, Smithies, BC V0J 2N0	No Response
C. Patel, Project Manager, Kemess South Project, c/o 5501 Lakeview Drive, Kirkland, WA 98033	No Response

Table 20 Mines canvassed in the study

No.	Mine	Operator	Owner	Product	Average Stripping Ratio (tonnes /tonnes)	Production (M Tonnes)	
						Ore	Waste
1	Bullmoose Mine	Bullmoose Operating Corporation	Teck Corporation	Metallurgical Coal	18.9 : 1	3.145	35.074
2	Elkview Coal Corporation	Teck Corporation	Teck Corporation	Metallurgical Coal (mostly)	8.1 : 1[!]	3.0*	24.456**
3	Highland Valley Copper	Highland Valley Copper	Cominco-50%, Rio Algom-33.6%, Teck-13.9%, Highmont-2.5%	Copper and Molybdenum	0.87 : 1	47.5	41.3
4	Line Creek Mine	Luscar Ltd.	Luscar Ltd.	Coal	6.52 : 1[!!]	4.20	27.5**
5	Luscar Mine	Cardinal River Coals Ltd.	Luscar Ltd. + Consol Ltd.	Coal	10 : 1[!]	2.8	29**
6	Mount Polley	Imperial Metals Corporations (IMC)	IMC and Sumitomo Corporation	Gold and Copper	1 : 1	7	7
7	Obed Mountain Mine	Luscar Ltd.	Luscar Ltd.	Thermal Coal	7.29 : 1	1.5	19[**]
8	Poplar River Mine	Luscar Ltd.	Luscar Ltd.	Lignite Coal	5.5 : 1	3.6	20[**]
9	Quintette Operating Corporation	Teck Corporation	Teck Corporation	Metallurgical Coal	8.4 : 1	3.04*	25.8[**]
10	Carol Lake Project	Iron Ore Company of Canada	North Limited	Iron Ore Pellets & Concentrates	5.88:1[!]	39	19
11	Stratmine Graphite Corporation	Stratmine Graphite Corporation	I Metal Group (France)	Graphite	2.7 : 1	0.363	0.907
12	Syncrude	Syncrude	Several Oil Companies	Oil Sand	0.8 : 1	160	100[**]
13	Greenhills Operation	Fording Coal Ltd.	Fording Coal Ltd.	Metallurgical Coal	10.08	4.48[**]	45.2[**]

*clean coal

**in million Bank cubic meter

! in bcm/cmt (bank cubic meter/ clean metric ton)

!! in bcm/rmt (bank cubic meter/ raw metric ton)

Table 21 Operating hour and materials handled by the mines

No.#	Mine	Time$ Worked (net operating hr./yr.)		Ore Handled (million tonnes-kms / yr)	Waste Handled (million tonnes-kms / yr)	Largest Truck Used (Payload) (tonnes)
		Trucks	Road Maintenance Equipment			
1	Bullmoose Mine	8520!	As Required	375,400	10,320,000	180
2	Elkview Coal Corporation	121,800(at Mine) 4,000 (at Plant)	33,200	20.017	158.625	218
3	Highland Valley Copper	158,448	8245 – 10,615 graders - 25,407	95.68	256.760	172
4	Line Creek Mine	83,130	23,000	-	-	216
5	Luscar Mine	125,000	25,000	20	40.000	234
6	Mount Polley	26,600	5,750	5.843	5.020	80
7	Obed Mountain Mine	8713	4782	-	-	153
8	Poplar River Mine	17,000	10,000	12.3	No Waste Handled	150
9	Quintette Operating Corporation	6,200!	4,500!	0.38	-	216
10	Carol Lake Project	130,000	40,000	40	7.500	179
11	Stratmine Graphite Corporation	15,000 $\pm$ 1000	-	-	-	35
12	Syncrude	250,000	-	175	395.000	290
13	Greenhills Operation	273,216	-	-	-	216

mines referred by this number in other tables.
! hours per piece of equipment.
$ cumulative hours (sum of hours worked for each piece of machine.

Table 22 Type of loading and haul road maintenance equipment

Equipment	Mines Using
Haul Road Maintenance Equipment	
Scraper	7
Dozer	11
Grader	13
Water Truck	13
Wheel Tractor	7
Sand Truck	1
Loading Equipment	
Cable Shovel	11
Hydraulic Shovel:	
Front Shovel	4
Backhoe	6
Dragline	2
Front End Loader	12

Table 23 Haulage equipment

Model No.	Make	No. of Trucks	GVW (tonnes)	Payload (tonnes)
CAT 769 C	Caterpillar	4		32
DJB 25 C	Caterpillar	1		23
CAT 777 B	Caterpillar	6	161	80
CAT 776 A	Caterpillar	1	250	120
CAT 776 D	Caterpillar	4	250	150
CAT 785	Caterpillar	8		136
CAT 789	Caterpillar	11, 43*	317.5	180, 172*
CAT 793	Caterpillar	34	415	218
630 E	Dresser Haulpak	11	286	170
830 E	Dresser Haulpak	53	399	231
930 E	Haulpak	8	480	290
R 170	Euclid	12		
3315(B/C)	Titan	33	285	170
MT 4400	Unit Rig	5	392.3	236
M 36	Unit Rig	7		
120	Wabco	8	204	109
170	Wabco	27	268	154
630 E	Wabco	3		

*different mines used the same models with different pay loads, number used and payloads are given in order

Table 24 Haul road length and life

Material	Cumulative Length (km)	Average* Expected Road Life (years)
In-Pit		
Product Haul	17.3	1.6
Waste Haul	12.8	1.1
Common Haul	20.6	1.7
Total In-Pit =	50.7	1.4
Ex-Pit		
Product Haul	74.8	10
Waste Haul	13.2	7
Common Haul	11.7	5
Total Ex-Pit =	99.7	8.0

* average weighted for number of mines reporting

Table 25 Materials used for road construction (except surface coarse)

Construction Material	No. of Mines Using	Percentage
Run of Mine (waste)	8	67
Sandstone	4	33
Glacial Till	1	8
Sand	1	8
Pit Run Gravel	1	8
Shale	2	17
Siltstone	1	8
Crushed Stone	1	8
Rut & Roll Fill	1	8

One of the mine did not reported this information.

Table 26 Haul road geometry

Item	Mine Number 1	2	3	4	5	6	7	8	9	10	11	12	13
Max. Grade (%)	10	10	10	10	8 – 12	10	10	5[A8]	7.5	8	10	8-10	6-8
Max. Curve Super Elevation (%)	3 – 4	3	-	4	3[A5]	-	A7	B8	4	5	-	2-3	5
Maximum Road Cross-Slopes (%)	3.25	1.5	-	2	3	-	B7	-	4	0	3	2	5
Min. Running Width (m)	31	30	24	25	30	30	30	20	28	25	15	25	28[A13]
Ditch Sizing (total width X depth) (m)	3.5x0.9	3x1	A3	3x1.5	-	3x1	C7	4x1	3.5x0.9	2x2	-	1x1	-
Avg. Height of Safety Berms (m)	2.55[A1]	2.7	3	3.5	1.5	2	2	1.6	2.6	3	1.2	2.0	2[A1]
Maximum Breaking Distance Limitation (m)	-	-	-	-	B5	33.5	-	-	84[A9]	-	-	50	-
Number of Lanes	2	2	2	2	2	2	2	2	2	2	2	2	2
Runaway Lanes:					C5								
- Max. Gradient (%)	25	20	15	30	-	-	-	-	20	15	-	-	12-14
- Avg. Length (m)	B1	150	100	150	-	-	-	-	62	-	-	-	70-80
- Spacing (m)	C1	30[A2]	1000	-	-	-	-	-	240	-	-	-	30[A2]

A1 - 3/4 of largest tire application
B1 - function of entry velocity, acceleration due to gravity, road grade, and rolling resistance
C1 - function of final velocity, road grade, acceleration due to gravity, and rolling resistance
A2 - 30m vertical spacing on 8% ramp; shorter ramp with 7.5m vertical spacing has also been used
A3 - drainage ditch were of depth 0.5m-1.5m
A5 - not generally used
B5 - not considered
C5 - no longer incorporated
A7 - not many curves, they are generally flat
B7 - very slight grade to facilitate runoff
C7 - 1m deep and 2m wide at base
A8 - 3% loaded, 5%empty
B8 - 200/Radius of curvature(m)
A9 - @ 10% grade - 84m ; section 4.36 Art. 4921 H,S,R code for mine in British Columbia
A13 – 3 times the width of largest haul truck

Table 27 Haul road construction materials and provisions for water crossing

Mine	Base Coarse	Surface Coarse	Water Crossing	Use of Imported Materials
1	80% passing -0.5m of run of mine rip rap of thickness as required.	80% passing -0.3m of same material as base coarse.	"U key" ditches to catch surface drainage for treatment, two culverts for stream crossing	Pit run and contracted crush
2	Pit run (free of mud) in variable thickness.	Crushed or fine pit run, thickness of application 25mm to 50mm	Culverts for small drainage path, natural drainage paths are crossed by course free drainage material.	No imported materials used
3	Run of mine, 2m thick	Crushed waste rock (-50mm), 0.5m thick	Data not available	No imported materials used
4	Pit run material consisting of a mix of siltstone, sandstone and shale	Fine pit run using as much sandstone as possible, 2m thick	Rock drains	Geotextile - Used to stabilize road fill in very wet area, it is covered by 2m of pit run material.
5	Run of mine rock of size -2m, thickness of application 3m minimum	Run of Mine rock of size -0.3m, thickness of application 0.5m	0.61m (2feet) culverts or where permitted, rock drains	No imported materials used
6	Naturally segregated pit waste of size - 0.61m of variable thickness ranging from 1m to 10m.	Blasted waste rock from pit of size – 19mm, thickness of application less than 0.3m.	Culverts and coarse rock drains	No imported materials used
7	Sandstone, 10m thick	Pit run gravel, 0.5m thick	Data not available	No imported materials used
8	Glacial till - in 0.15m(max.) lifts, watered, bladed and packed, thickness - 1m (min.)	Gravel – crushed to -50mm, thickness – 50mm (min.)	600mm (min.) diameter culverts	No imported materials used
9	Run of mine - shale and sandstone of size -1.5m, thickness of application - more than 3m.	Combination of run of mine shale (of size -80mm), plant coarse reject (of size –40mm), crushed run of mine (of size –30mm). Thickness of application - less than 0.5m	Culverts – accommodate 200 year return flow fill – run of mine (free of organic materials)	No imported materials used
10	Bed Rock – Quarzite (sub grade)	Run of mine–waste rock, treat rock	All drainage culverts – where applicable	No imported materials used
11	Sub Base – waste rock (size -1m), thickness of application: 1m	Crushed stone of size -19mm, thickness – less than 0.3m	Data not available	Calcium solution for dust suppression in summer time

Mine	Base Coarse	Surface Coarse	Water Crossing	Use of Imported Materials
	Base – Crushed stone (size -63.5mm), thickness 0.3m to 0.61m.			
12*	Subgrade : 50mm of rut and roll fill Subbase : 1m of Pf sand in 350mm thick (loose) lifts. Base : 0.8 m of pit run gravel in 500 mm (max.) thick (loose) lifts.	0.8m of crushed gravel in 250mm thick (loose) lifts.	Crossings over ditches using 0.61m pipe, multiple pipe in high flow ditches.	A test pad of sulfur, tailing sand and lean oil sand.
13	sandstone (blasted or in-situ)	-30 mm crushed sandstone	ditches, sumps	-

*recommended design criteria for 320 mt haul trucks.

Table 28 Materials used for surface coarse

Construction Materials	No. of Mines Using	Percentage
Crushed Run of Mine (waste)	10	77
Crushed Pit Run Gravel	4	31
Shale	1	8
Plant Coarse Reject	1	8
Crushed Sandstone	2	15

Table 29 Symptoms of haul road deterioration

Symptoms	No. of Mines Experiencing	Percentage
Potholes	12	92
Soft Ground – Rutting	10	77
Settlement	9	69
Washboarding	8	61
Slippery when Wet	7	54
Frost Heave	5	38
Loose Surface Coarse	3	23
Water Drainage Problem	1	8
Coal Seam Crossing, Back Break	1	8
Rolling (large shear plane)	1	8

Table 30 Causes of haul road deterioration

Number of Mines Reporting (%)

Causes	Sub Grade	Sub Base	Base Course	Surface Course
Dust /Binder Deficiency	0 (0)	0 (0)	1 (8)	5 (38)
Gravel Deficiency	0 (0)	0 (0)	1 (8)	8 (61)
Heavy Traffic Volume	1 (8)	1 (8)	6 (46)	8 (61)
High Ground Water Level	1 (8)	1 (8)	3 (3)	5 (38)
Ice and Snow	0 (0)	0 (0)	1 (8)	6 (46)
Operator's Driving Technique	0 (0)	0 (0)	0 (0)	1 (8)
Poor Coarse Compaction	3 (23)	3 (23)	3 (23)	2 (15)
Precipitation / Runoff	3 (23)	4 (31)	6 (46)	12 (92)
Spring Breakup	2 (15)	3 (23)	7 (54)	9 (69)
Vehicle Spillage	0 (0)	0 (0)	1 (9)	7 (54)
Truck too Heavy for Road	0 (0)	0 (0)	3 (23)	4 (31)
Poor Maintenance	1 (8)	1 (8)	1 (8)	1 (8)
Base Settlement	0 (0)	0 (0)	1 (8)	0 (0)

Table 31 Measures to improve trafficability

Measures	No. of Mines taking the Measure	Percentage
Grading	13	100
Resurfacing	12	92
Road Realignment	9	69
Plowing-Scarifying-Sanding	12	92
Excavate / Backfill Soft Spots up to:		
Sub Grade	3	23
Sub Base	5	38
Base Course	5	38
Surface Course	9	69
Raising Grade	10	77
Ditch / Culvert Maintenance	1	8

Table 32 Methods used for dust suppression

Methods	No. of Using	Percentage
Water Sprinkling	13	100
Oil Sprinkling	1	8
Calcium Chloride	4	31

Table 33 Road maintenance frequency

		Mine Number												
		1	2	3	4	5	6	7	8	9	10	11	12	13
Clean / Regrade	Ex-Pit	NA	AR	C	D	D	AR	D	D	AS	D	BW	C	AR
	In-Pit	NA	AR	C	H	C	AR	D	D	AS	D	BW	C	AR
Repair	Ex-Pit	NA	AR	AR	W	BA	NR	AR	A	AS	D	NA	A	AR
	In-Pit	NA	AR	AR	BW	AS	NR	D	A	AS	D	NA	AS	AR
Dust Suppression	Ex-Pit	NA	DS	AR	BA	OS	OS	AR	DS	DW	DS	FW	DS	AR
	In-Pit	NA	DS	AR	C	TS	OS	AR	DS	DW	DS	FW	DS	AR

NA - Data not available
D – Daily
BA - BI-Annual
A – Annual
AR – As required
H – Hourly
OS – Once per Shift
DW – Depends upon weather (every 2hr in summer)
DS – Daily during summer
W – Weekly
TS –Twice or Thrice per Shift
FW – Four times a week in summer
C – Continuously
BW - BI-Weekly
NR - Not Required

Table 34 Other haulage information

Mine No.	Truck Dispatch System	Automated Fleet Condition Monitoring	Runaway Lanes	Speed Limits
1	Not Used	Cat TPMS /VIMS	Every 30m elevation @20-25%	Main access - 15kmph, service area - 20kmph, In pit – 50kmph
2	Modular	Used	Used	Used
3	Modular	Not Used	Used	50 kmph
4	Not Used	Not Used	Used	Variable
5	Modular	Modular	Used on older long ramps	35 kmph
6	Not Used	Not Used	Not Used	30 kmph (8 kmph downhill loaded)
7	Not Used	Not Used	Used	At ramps speed limit controlled by truck electrics - 40kmph
8	Not Used	Not Used	Not Used	80 kmph
9	Not Used	Not Used	Used	30 kmph for heavy vehicles
10	Modular	VSM	Used	30 kmph
11	Not Used	Not Used	Not Used	50 kmph
12	Not Used	Not Used	Not Used	at intersections and congested areas
13	Modular	DDEC*	Used	45 kmph

Real time engine telemetry on three trucks.

8.2 Structural Components of Tires

The components of a typical tire are described in detail in the Tire Maintenance Manual, Good Year, 1998.

Tread is the outermost part of the tire, which is in contact with the ground, thus providing traction. It should have cut and wear resistance required by the site and application needs.

The strength of the **carcass** determines the extent of inflation pressure that a tire can withstand.

Breakers (Belts) are placed between the tread and the carcass. Their function is to distribute road shock to protect the carcass. They also control the tire diameter, and give it better impact and penetration resistance.

The **bead** is bundles of high tensile steel wire, which anchors the tires to the rim.

Side walls are the protective rubber covers of the carcass on the sides of a tire.

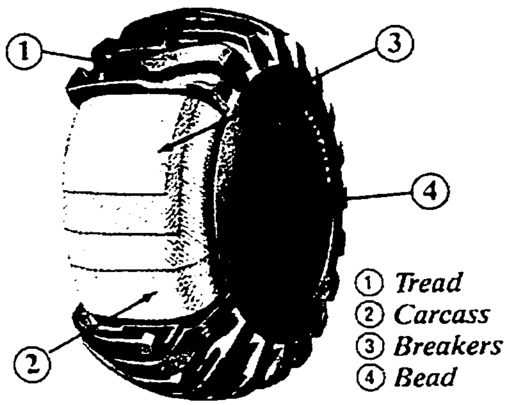

Figure 30 Components of a radial tire

8.3 Calculation of Layer Thickness Using Resilient Modulus

Assumptions:

Foot print area of the tire = $\pi (w/2)^2 = \pi (1.2/2)^2 = 1.13 \text{ m}^2$

Stress exerted by the tire (q) = load/area = 80*9.81/1.13 = 690kPa

The stress can be estimated from Table 35 using the tire width (w or 2a) and the surface pressure (q).

The thickness of various layers should be such that the maximum stress level faced by any layer should be less than the compressive strength of that layer and the strain induced should be less than 200micro-strains.

For sub-grade:

Compressive strength of the material = 80kPa

Resilient modulus of the material (E) = 40Mpa

$\therefore$Stress it can bear = 40*strain limit ($2000*10^{-6}$) = 80kPa

Maximum stress the sub-grade can bear (σ) = 80kPa

$\therefore \sigma/p = 80/690 = 0.12 = A + B$

where A and B are influence factors given in Table 35

$\therefore$From Table 35, cover thickness required = z = 3.4a = 2.04m

For sub-base:

Compressive strength of the material = 150kPa

Resilient modulus of the material (E) = 80Mpa

$\therefore$Stress it can bear = 80*strain limit ($2000*10^{-6}$) = 160kPa

Maximum stress the sub-grade can bear (σ) = 150kPa

$\therefore \sigma/p = 150/690 = 0.22 = A + B$

where A and B are influence factors given in Table 35

$\therefore$From Table 35, cover thickness required = z =2.4a = 1.44m

For base course:

Compressive strength of the material = 400kPa

Resilient modulus of the material (E) = 200Mpa

$\therefore$Stress it can bear = 200*strain limit ($2000*10^{-6}$) = 400kPa

Maximum stress the sub-grade can bear (σ) = 400kPa

$\therefore$ σ/p = 400/690 = 0.58 = A + B

where A and B are influence factors given in Table 35

$\therefore$From Table 35, cover thickness required = z = 0.96a = 0.58m

The material for the surface course has compressive strength higher than the maximum stress (690kPa) and the strain caused (690kPa/350Mpa = 1970micro-strains) is less than the strain limit of 2000micro-strains. Thus the material can be used as the surface course.

<u>Thickness of various layers for the method:</u>

Sub-base = Cover thickness required for sub-grade – cover thickness required for sub-base
= 0.60m

Base course = Cover thickness required for sub-base – cover thickness required for base course
= 0.86m

Surface Course = Cover thickness required for base course = 0.58m

Table 36 shows stress calculated below a set of four circular tires representing back axle of a truck using the influence factor given in Table 35.

Table 35 Influence factor table for a circular load (after Whitlow, 1983)

z/a	r/a →	0	0.2	0.4	0.6	0.8	1.0	1.2	1.5	2.0	3.0
0	A	1.0	1.0	1.0	1.0	1.0	0.5	0.0	0.0	0.0	0.0
	B	0.0	0.0	0.0	0.0	0.0	0.0	0.0	0.0	0.0	0.0
0.2	A	0.804	0.798	0.779	0.735	0.630	0.383	0.154	0.053	0.017	0.004
	B	0.188	0.193	0.208	0.235	0.260	0.085	-0.078	-0.044	-0.016	-0.004
0.4	A	0.629	0.620	0.592	0.538	0.443	0.310	0.187	0.086	0.031	0.008
	B	0.320	0.323	0.327	0.323	0.269	0.124	-0.008	-0.045	-0.025	-0.008
0.6	A	0.486	0.477	0.451	0.404	0.337	0.256	0.180	0.100	0.041	0.011
	B	0.378	0.375	0.363	0.382	0.254	0.144	0.045	-0.021	-0.025	-0.010
0.8	A	0.375	0.368	0.347	0.312	0.266	0.213	0.162	0.102	0.048	0.014
	B	0.381	0.374	0.351	0.307	0.38	0.153	0.075	0.006	-0.018	-0.010
1.0	A	0.293	0.288	0.270	0.247	0.215	0.179	0.143	0.098	0.052	0.017
	B	0.353	0.346	0.321	0.278	0.220	0.154	0.092	0.028	-0.010	-0.011
1.2	A	0.232	0.228	0.217	0.199	0.176	0.151	0.126	0.092	0.053	0.019
	B	0.315	0.307	0.285	0.248	0.201	0.149	0.100	0.044	0.000	-0.010
1.5	A	0.168	0.166	0.159	0.148	0.134	0.119	0.103	0.80	0.051	0.021
	B	0.256	0.250	0.233	0.207	0.174	0.137	0.102	0.057	0.014	-0.007
2.0	A	0.106	0.104	0.101	0.096	0.090	0.083	0.075	0.063	0.045	0.022
	B	0.179	0.181	0.166	0.152	0.134	0.113	0.093	0.064	0.028	0.000
3.0	A	0.051	0.051	0.050	0.049	0.047	0.045	0.042	0.038	0.032	0.020
	B	0.095	0.094	0.091	0.086	0.080	0.073	0.066	0.054	0.035	0.011
4.0	A	0.30	0.030	0.029	0.028	0.028	0.027	0.026	0.025	0.022	0.016
	B	0.057	0.057	0.056	0.054	0.051	0.048	0.045	0.040	0.031	0.015
5.0	A	0.019	0.019	0.019	0.019	0.019	0.018	0.018	0.018	0.016	0.012
	B	0.038	0.038	0.037	0.036	0.035	0.034	0.031	0.028	0.025	0.015
10.0	A	0.005	0.005	0.005	0.005	0.005	0.005	0.005	0.005	0.004	0.004
	B	0.010	0.009	0.009	0.009	0.009	0.009	0.009	0.009	0.008	0.008

$\sigma_z = q\,(A + B)$ and $e_z = q\,(1 + \nu)[\,(1 - 2\nu)\,A + B]$

Where: σ_z and e_z are vertical stress and strain, respectively.

q = stress applied — a = radius of the circular load

ν = Poisson's ratio — z = depth below the surface

r = horizontal distance the load applied — A & B obtained from the table

Table 36 Stress calculation below a rear axle of a haul truck

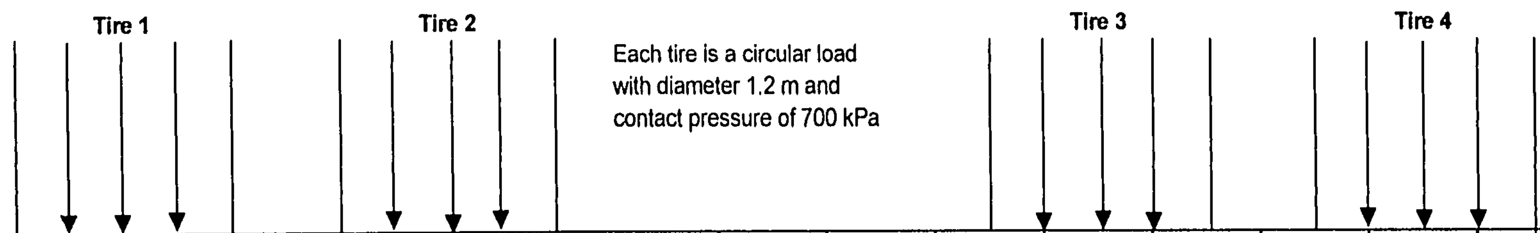

Horizontal distance from one end of axle (m) → / Depth (m)	0.0	0.6	1.2	1.8	2.4	3.6	4.2	4.8	5.4	6.0	6.6	7.2	7.8	8.4	9.0
0.00	350	700	350	350	700	350	0	0	0	350	700	350	350	700	350
0.12	328	694	328	328	694	328	1	0	1	328	694	328	328	694	328
0.24	304	664	308	308	664	304	4	0	4	304	664	308	308	664	304
0.36	280	606	291	291	606	280	11	2	11	280	606	291	291	606	280
0.48	256	532	278	278	532	256	21	6	21	256	532	278	278	532	256
0.60	233	456	262	262	456	233	30	8	30	233	456	262	262	456	233
0.72	210	389	247	247	389	210	37	13	37	210	389	247	247	389	210
0.90	179	306	225	225	306	179	46	19	46	179	306	225	225	306	179
1.20	137	215	188	188	215	137	51	30	51	137	215	188	188	215	137
1.80	83	124	130	130	124	83	47	43	47	83	124	130	130	124	83
2.40	52	74	90	90	74	52	37	43	37	52	74	90	90	74	52
3.00	36	58	65	65	58	36	29	37	29	36	58	65	65	58	36
6.00	10	19	19	19	19	10	8	17	8	10	19	19	19	19	10

8.4 Unconfined Compressive Strength Test Results

A series of compression tests were performed to measure Unconfined Compressive Strengths and Young's Moduli of various combination of fly ash, kiln dust and aggregates (coal seam parting and mine spoil). Moisture density tests were also performed determine optimum moisture content for each combination of ingredients tested. Results these tests are given in this section.

Table 37 Moisture density test result

	Dry Proportion of Ingredients (%)	Moisture Content (%)	Density (kg/m^3)
1	Fly Ash – 12.5 Kiln Dust – 3.5 Parting – 84	15	1783
		13	1823
		11	1840
		10	1825
2	Fly Ash – 16 Kiln Dust – 4 Parting – 80	11	1807
		12	1824
		13	1848
		14	1816
3	Fly Ash – 20 Kiln Dust – 4 Parting – 76	12	1833
		13	1864
		14	1821
		15	1805
4	Fly Ash – 25 Kiln Dust – 5 Parting – 70	13	1732
		14	1782
		15	1738
5	Fly Ash – 12.5 Kiln Dust – 3.5 Spoil – 84	13	1917
		14	1962
		15	1919
6	Fly Ash – 16 Kiln Dust – 4 Spoil – 80	13	1887
		14	1931
		15	1911
		16	1879
7	Fly Ash – 20 Kiln Dust – 4 Spoil – 76	13	1881
		14	1922
		15	1880
8	Fly Ash – 25 Kiln Dust – 5 Spoil – 70	13	1802
		14	1864
		15	1819
9	Fly Ash – 80 Kiln Dust – 20	16	1626
		17	1638
		18	1622

Table 38 Uniaxial compressive strength (kPa)

	Moisture (%)	Number of Curing Days			
Materials (proportion given in dry %)		3	7	14	28
Fly Ash (100)	17	254	200	626*	665**
Fly Ash (90) + Kiln Dust (10)	18	2906	3966	5289	-
Fly Ash (80) + Kiln Dust (80)	17	1162	3285	4635	-
Fly Ash (12.5) + Kiln Dust (3.5) + Parting (84)	11	322	378	484	465
Fly Ash (16) + Kiln Dust (4) + Parting (80)	13	376	473	499	600
Fly Ash (20) + Kiln Dust (4) + Parting (76)	13	472	576	978	920
Fly Ash (25) + Kiln Dust (5) + Parting (70)	14	437	648	710	780
Fly Ash (12.5) + Kiln Dust (3.5) + Spoil (84)	14	478	347	415	588
Fly Ash (16) + Kiln Dust (4) + Spoil (80)	14	485	565	630	700
Fly Ash (20) + Kiln Dust (4) + Spoil (76)	14	455	570	700	727
Fly Ash (25) + Kiln Dust (5) + Spoil (70)	14	544	700	960	1100

Table 39 Modulus of elasticity (MPa)

	Moisture (%)	Number of Curing Days			
Materials (proportion given in dry %)		3	7	14	28
Fly Ash (100)	17	16.3	21.9	275*	318**
Fly Ash (90) + Kiln Dust (10)	18	362.1	-	457.6	-
Fly Ash (80) + Kiln Dust (20)	17	410	615	630	-
Fly Ash (12.5) + Kiln Dust (3.5) + Parting (84)	11	184	100	118	127
Fly Ash (16) + Kiln Dust (4) + Parting (80)	13	160	231	164	164
Fly Ash (20) + Kiln Dust (4) + Parting (76)	13	96	106	200	233
Fly Ash (25) + Kiln Dust (5) + Parting (70)	14	245	300	307	356
Fly Ash (12.5) + Kiln Dust (3.5) + Spoil (84)	14	135	155	200	147
Fly Ash (16) + Kiln Dust (4) + Spoil (80)	14	150	225	300	307
Fly Ash (20) + Kiln Dust (4) + Spoil (76)	14	220	157	250	272
Fly Ash (25) + Kiln Dust (5) + Spoil (70)	14	150	240	320	380

*30 day result

**60 day result

8.4.1 Stress Vs Strain Curves

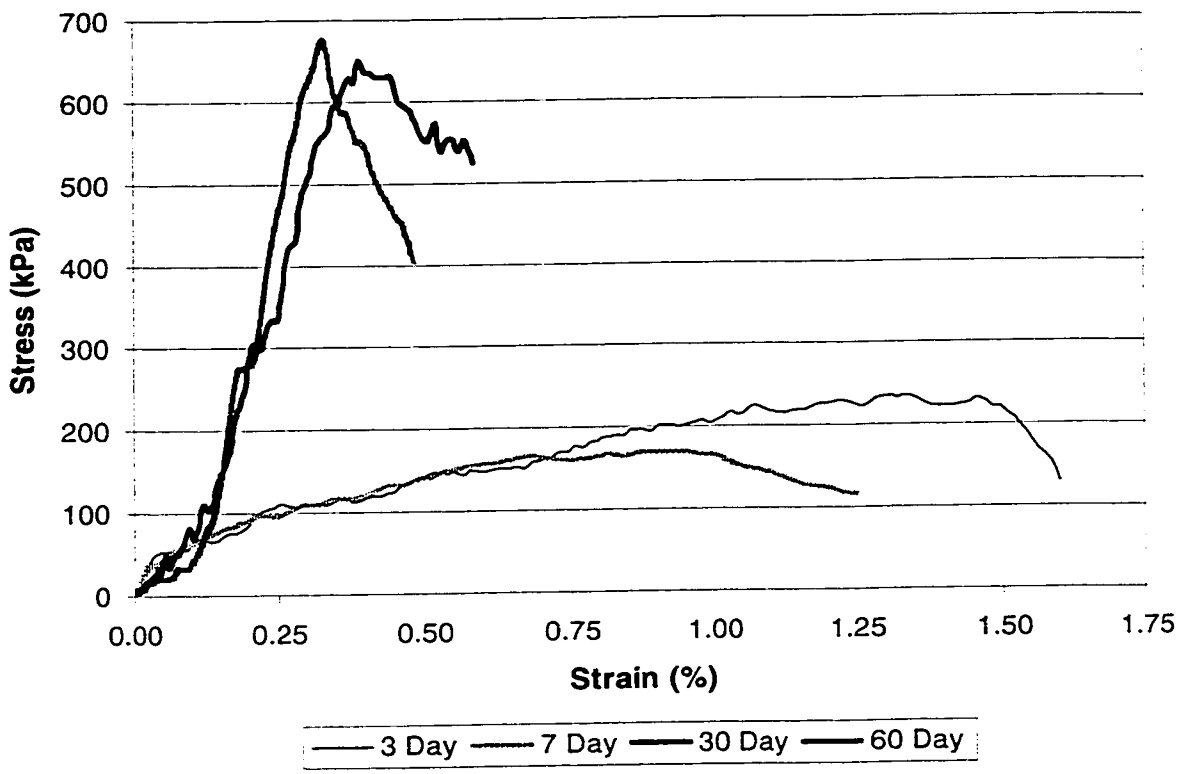

Figure 31 Stress vs Strain (fly ash only)

- Composition: Fly Ash – 100%.
- 3 day and 7 day test were done with uncapped samples while the other two test were done with sulfur capped samples. This may be one of the significant reasons of difference between compressive strengths of samples at 7 day and 30 day.
- Compressive strength of sample at 3 day of curing is more than that at 7 day of curing. It may result at imperfection in sample preparation. This also indicates that fly ash by itself has little cementing property.
- 3 day and 7 day test curves are smoothed by averaging 7 stress values around the data point.

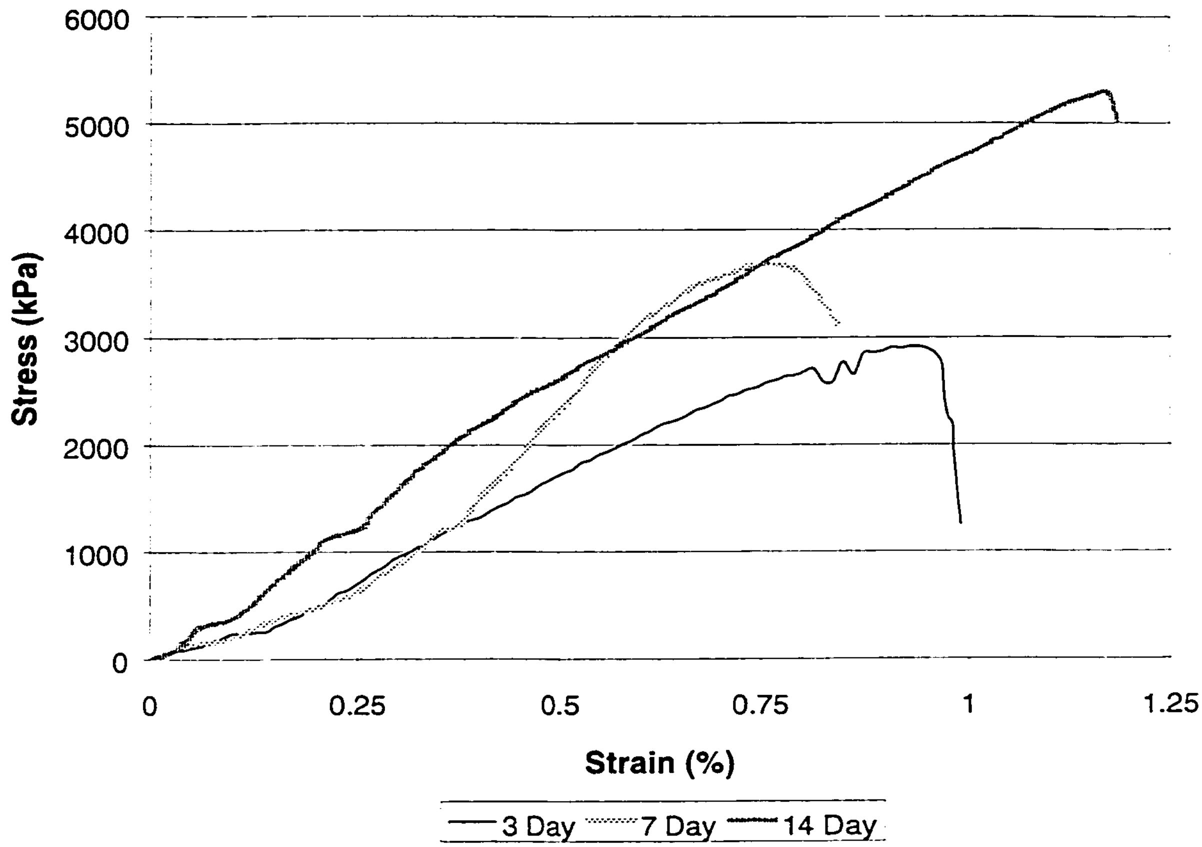

Figure 32 Stress vs Strain (fly ash and kiln dust, mix1)

- Composition: Fly Ash – 90% and Kiln Dust – 10%.
- These samples showed considerable strengths and failed abruptly unlike all other test performed which showed gradual decrease of strength after failure. So, very little post-failure characteristic could be recorded.
- Compressive strength increased steadily with time of curing whereas modulus of elasticity increased marginally.

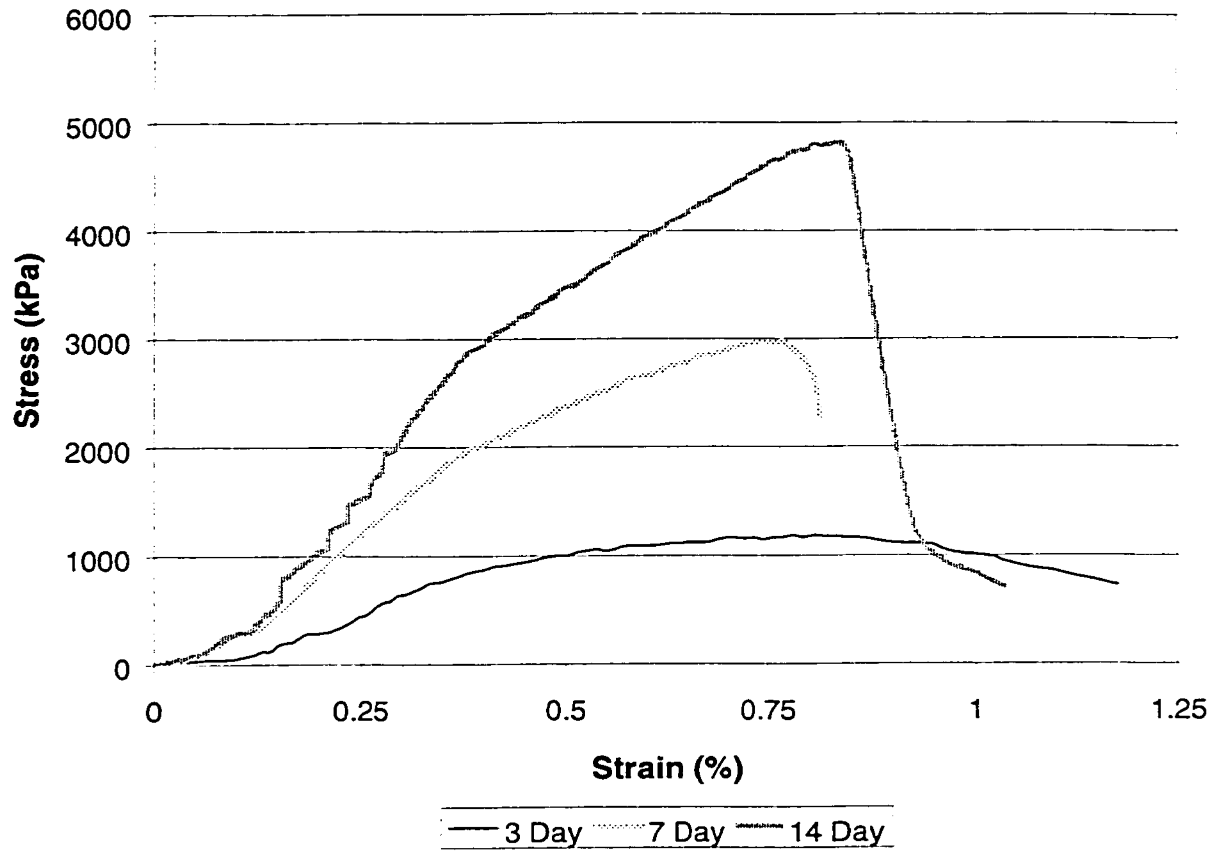

Figure 33 Stress vs Strain (fly ash and kiln dust, mix2)

- Composition: Fly Ash – 80% and Kiln Dust – 20%.
- Samples cured for 3 days failed gradually but other sample failed abruptly as indicated sudden drop of the curve after maximum stress.
- Compressive Strength as well as modulus of elasticity increased steadily with period of curing.

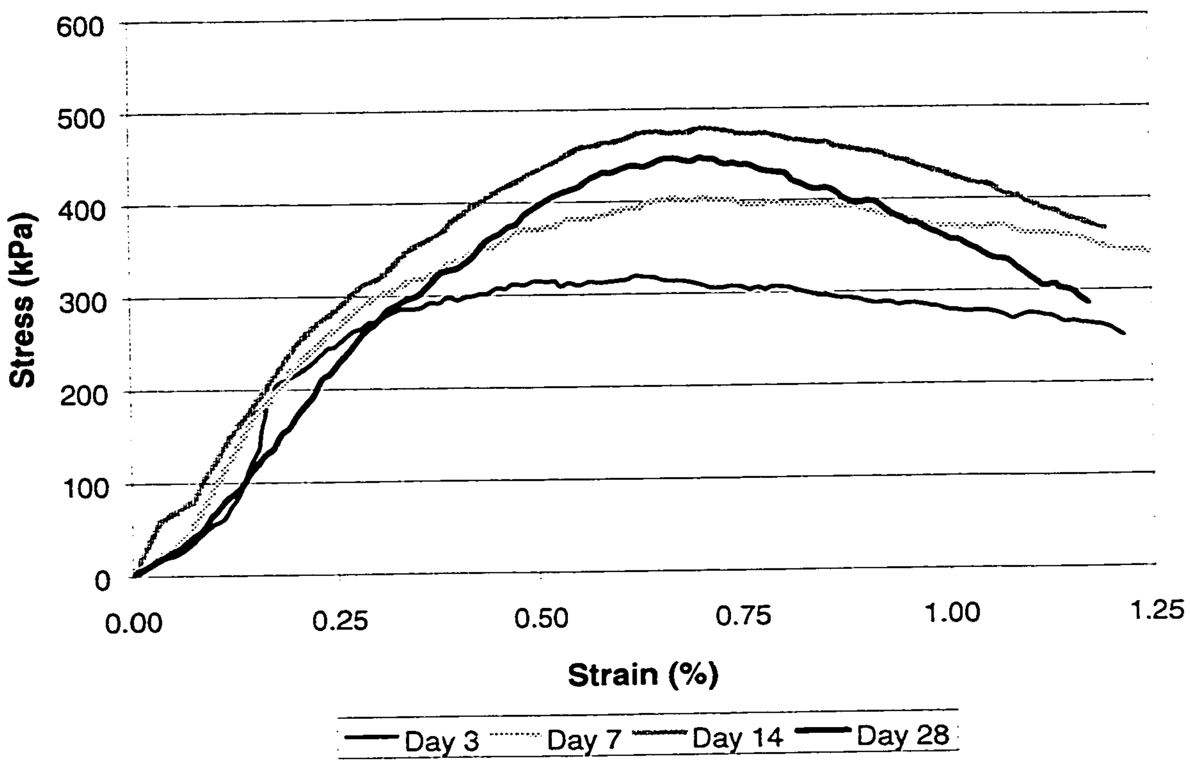

Figure 34 Stress vs Strain (fly ash with kiln dust and parting, mix 1)

- Composition: Fly Ash – 12.5%, Kiln Dust – 3.5% and Mine Parting – 84%.
- Compressive strength increased marginally with time of curing except for 28 days of curing which may be attributed to poor compaction during sample preparation or human error in sample preparation.
- Modulus of elasticity remained nearly constant over the period of curing.
- The stress decreased gradually after failure.
- All the curves are smoothened to overshadow noise of recording instrument.

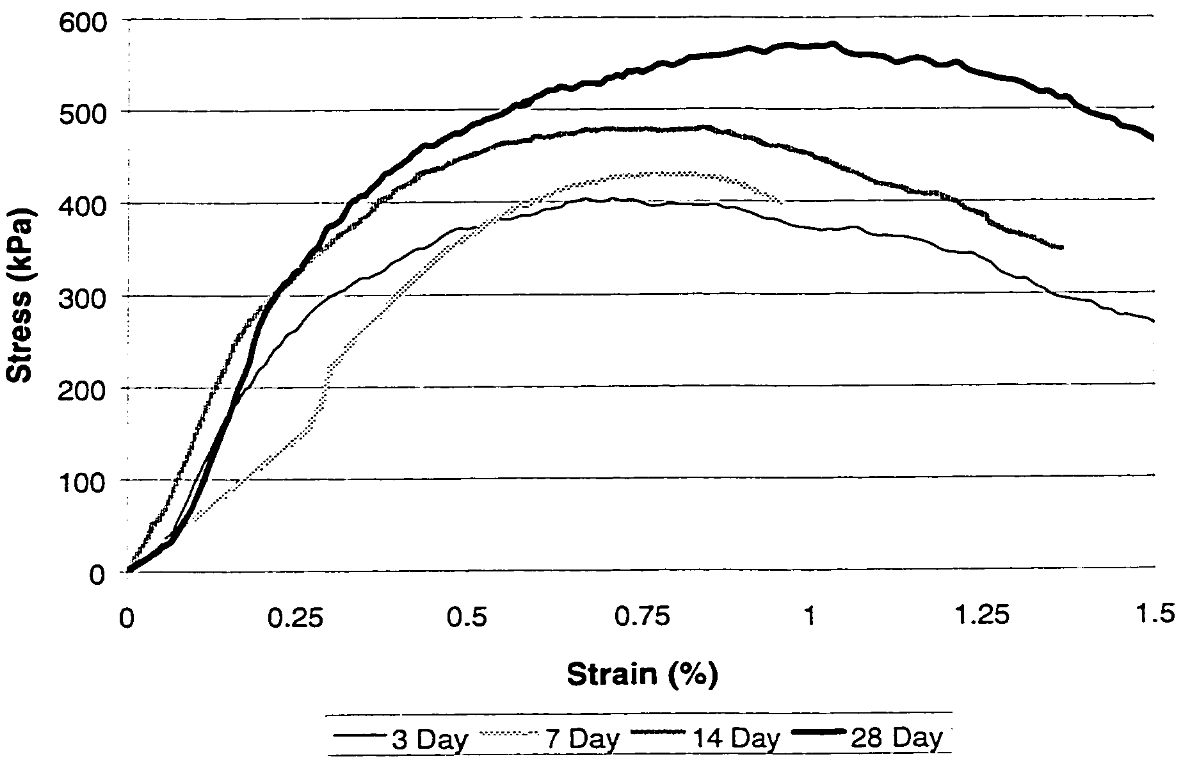

Figure 35 Stress vs Strain (fly ash with kiln dust and parting, mix 2)

- Composition: Fly Ash - 16%, Kiln Dust - 4% and Mine Parting - 80%.
- As expected, compressive strength increased with the curing period and there is a slight modulus of elasticity over the period.
- All the curves are smoothened to overshadow noise of recording instrument.

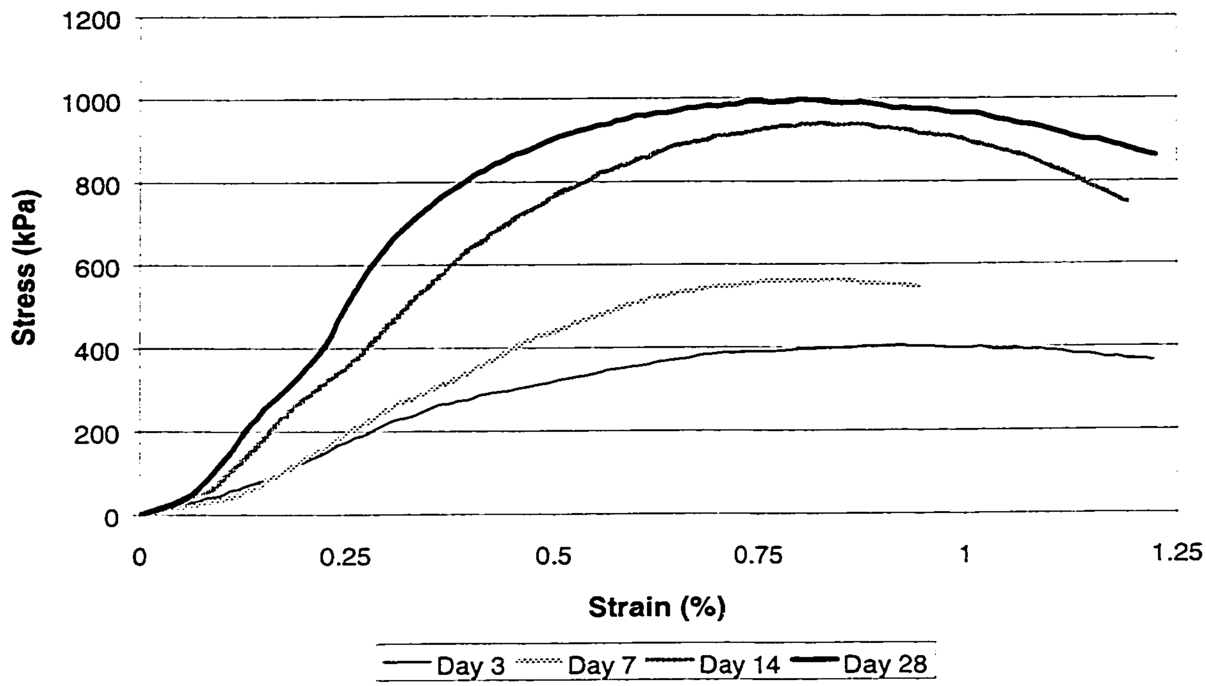

Figure 36 Stress vs Strain (fly ash with kiln dust and parting, mix 3)

- Composition: Fly Ash - 20%, Kiln Dust - 4% and Mine Parting - 76%.
- Significant increase in compressive strength with the period of curing can be observed. This indicates effectiveness of binders in the mix. Moreover, modulus elasticity also shows increasing trend with the period.
- 14 days of curing gives nearly full strength, as there is only slight increase in strength from 14 days to 30 days of curing.
- All the curves are smoothened to overshadow noise of recording instrument.

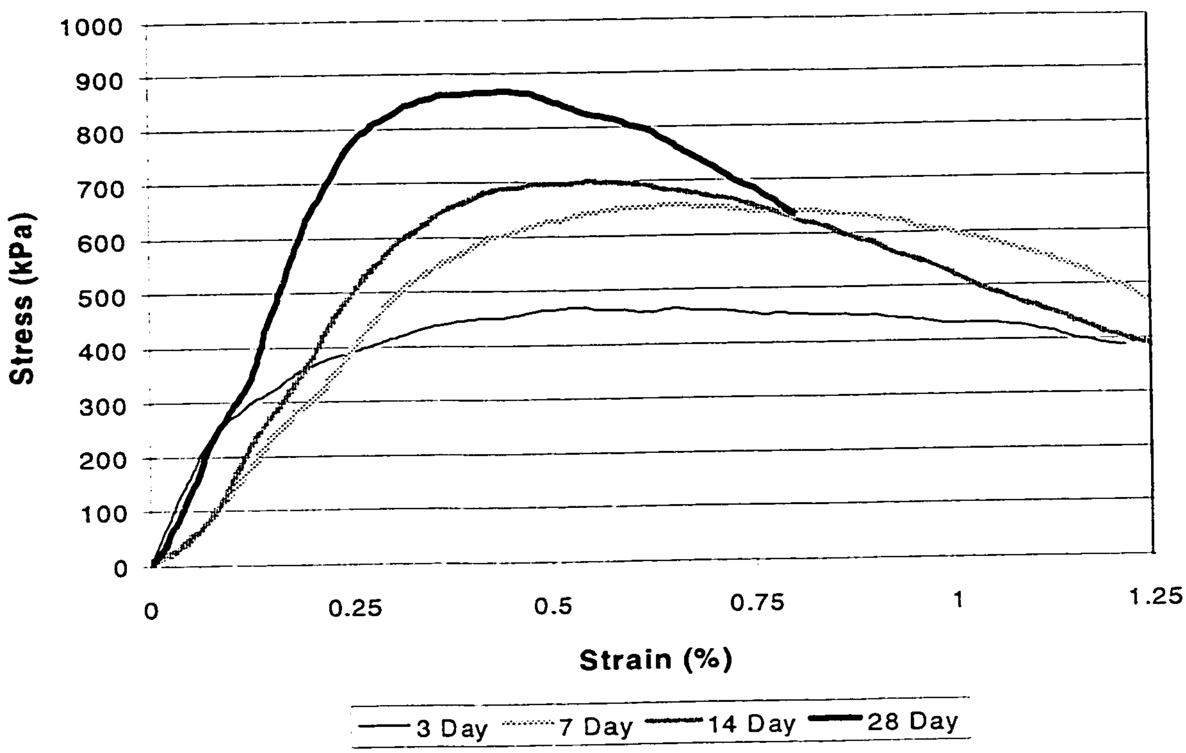

Figure 37 Stress vs Strain (fly ash with kiln dust and parting, mix 4)

- Composition: Fly Ash - 25%, Kiln Dust 5 % and Mine Parting - 70%.
- Compressive strength increased steadily with period of curing but increase in modulus of elasticity was marginal.
- All the curves are smoothened to overshadow noise of recording instrument.

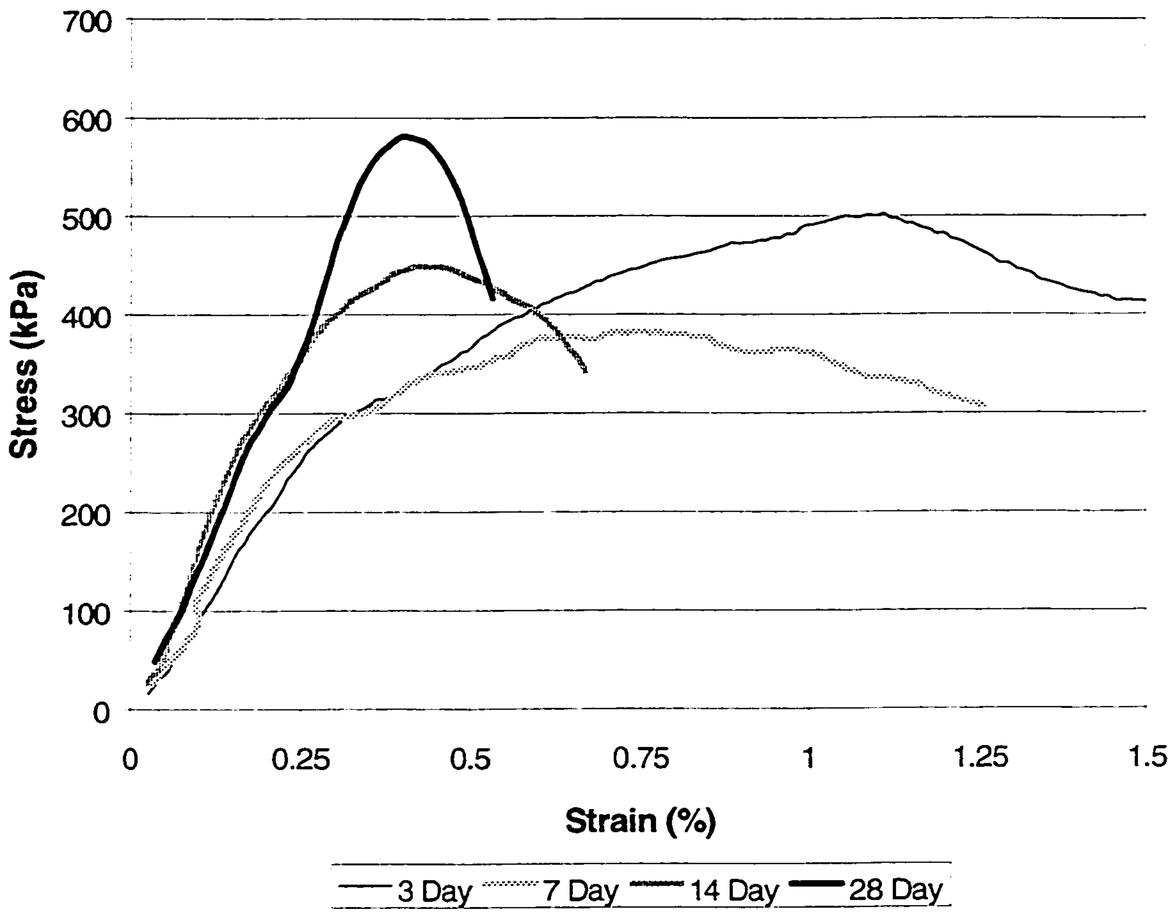

Figure 38 Stress vs Strain (fly ash with kiln dust and mine spoil, mix 1)

- Composition: Fly Ash – 12.5%, Kiln Dust – 3.5% and Mine Spoil - 84%.
- No trends of compressive strength increase over days of curing can be observed, indicating that the binding materials (fly ash and kiln dust) are highly deficient in the mix thus have little effect on the strength of the samples. This also supported by overall low strength shown at all ages.
- The difference in the characteristic at different ages of curing can be attributed to difference in compaction levels and individual difference in samples.
- All the curves the smoothened to overshadow noise of recording instrument.

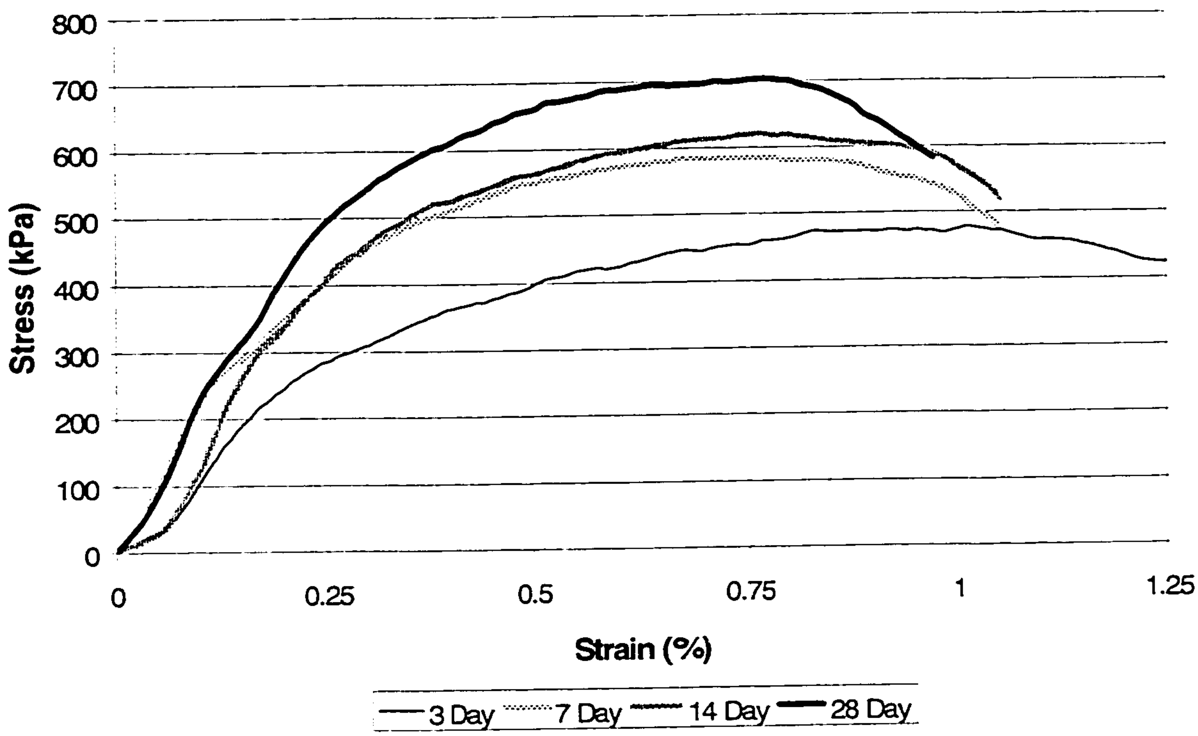

Figure 39 Stress vs Strain (fly ash with kiln dust and mine spoil, mix 2)

- Composition: Fly Ash - 16%, Kiln Dust - 4% and Mine Spoil - 80%.
- Compressive strength increased steadily over the period of curing and overall compressive strength is higher than mix 1 of same components. Thus it can concluded that percentage of cementing material in this mix has some effect over the strength of samples.
- Modulus of Elasticity also increased marginally with the time of curing.
- All the curves are smoothened to overshadow noise of recording instrument.

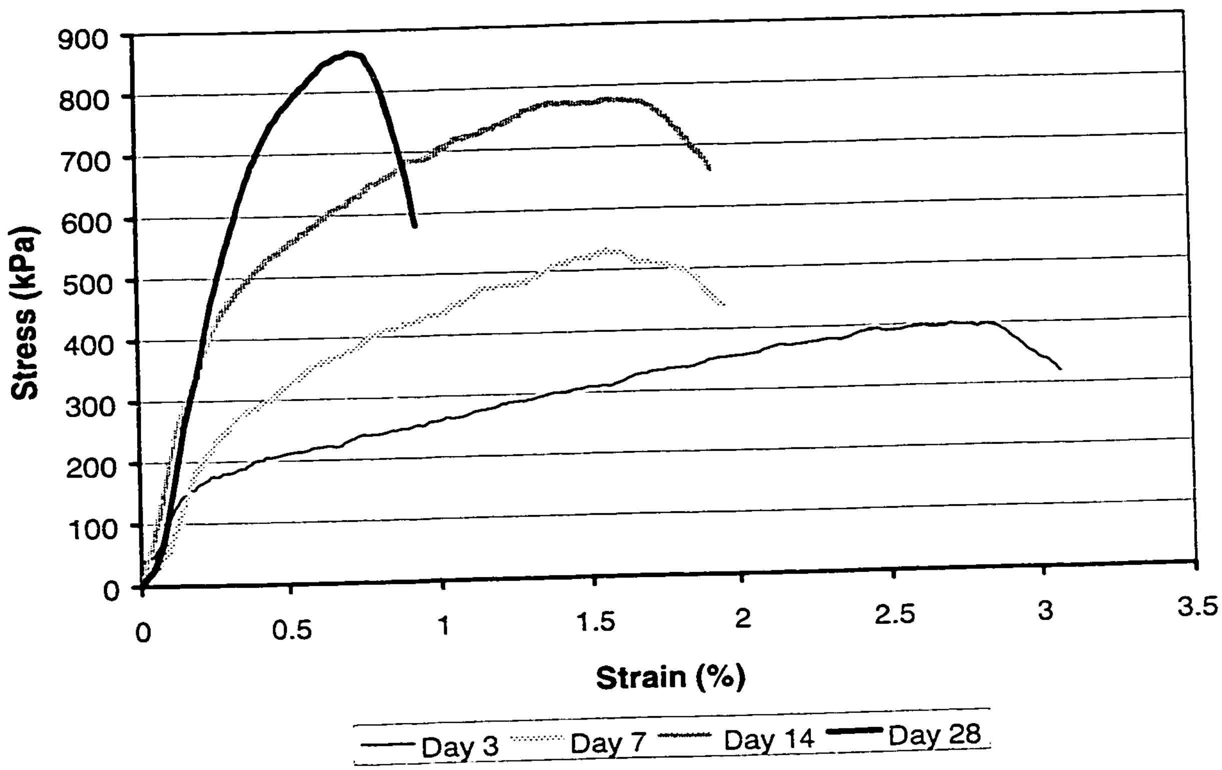

Figure 40 Stress vs Strain (fly ash with kiln dust and mine spoil, mix 3)

- Composition: Fly Ash - 20%, Kiln Dust - 4% and Mine Spoil - 76%.
- Compressive strength increases significantly and consistently with period of curing showing that cementing components have significant effect on the strength of the material.
- Modulus of elasticity also increases with period of curing and the sample fails at much lower strain after curing for a longer period.
- All the curves are smoothened to overshadow noise of recording instrument.

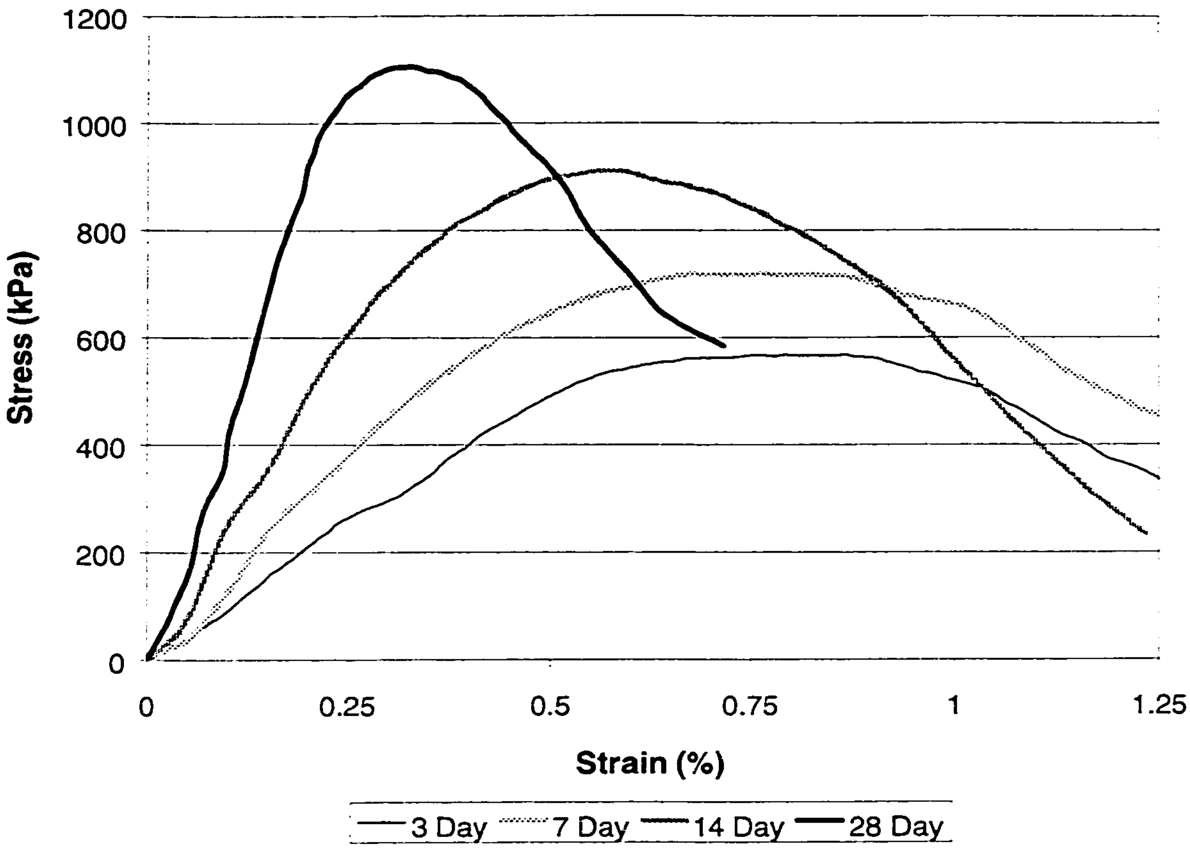

Figure 41 Stress vs Strain (fly ash with kiln dust and mine spoil, mix 4)

- Composition: Fly Ash - 25%, Kiln Dust - 5% and Mine Spoil - 70%.
- Compressive strength increases significantly and consistently with period of curing showing that cementing components have significant effect on the strength of the material.
- Modulus of elasticity also increases with period of curing and the sample fails at much lower strain after curing for a longer period.
- All the curves are smoothened to overshadow noise of recording instrument.